Risk and Environmental Modelling
Delft Institute of Applied Mathematics

Simulating inspections on corroded surfaces

Master Thesis

Author: Agnieszka Ostrowska

Delft University of Technology
July, 2006

To my parents and to my brother

Delft University of Technology

ABSTRACT

SIMULATING INSPECTIONS ON CORRODED SURFACES

by Agnieszka Ostrowska

Corrosion is a common problem in oil industry that often affects plant reliability. Therefore, control and monitoring of corrosion is of significant importance to maintain the reliability on the desired level and to prevent failure. Where and when to inspect are the crucial questions when planning the inspection process.

The thesis covers two main issues. Firstly, it describes two models that allow simulating the corrosion process. These models are then used to generate corroded surfaces and to realize the second goal of the project, which focuses on simulation of inspections. For the purpose of the second task three sampling inspection schemes are designed and their performance is investigated in the simulation experiments. The study is restricted to the spatial aspect of the inspection procedure.

Key words: corrosion, sampling inspection, simulation.

Members of the Committee:

Chairperson of Graduate Committee:	Prof. Dr. Ir. Jan M. van Noortwijk

Graduate Committee:

Prof. Dr. Ir. Jan M. Van Noortwijk	Delft University of Technology, Faculty of Electrical Engineering, Mathematics and Computer Science
Dr. Hans van der Weide	Delft University of Technology, Faculty of Electrical Engineering, Mathematics and Computer Science
Prof. Dr. Jolanta K. Misiewicz	University of Zielona Góra, Faculty of Mathematics, Informatics and Econometrics
Ir. Sieger Terpstra	Shell Global Solution, Amsterdam, Inspection Technology department
Ir. Sebastian Kuniewski	Delft University of Technology, Faculty of Electrical Engineering, Mathematics and Computer Science

Acknowledgments

The two years at Delft University of Technology, The Netherlands, have been a valuable and unforgettable experience. I would like to thank Prof. Roger M. Cooke for giving me the opportunity to take part in the MSc program "Risk and Environmental Modelling". I am also thankful to Prof. Jolanta Misiewicz and Dr. Marek Malinowski for encouraging me to take a part in this program.

I am very grateful to Prof. Jan van Noortwijk, for supervising my work and providing me with very helpful comments and corrections. I also would like to thank Sebastian Kuniewski for the time and help that he granted to this project.

I wish to express my sincere appreciation to Sieger Terpstra and Fred Hoeve of Shell for giving me the possibility to work on a project that proved both challenging and interesting.

I would like to thank my professors, friends and colleagues here in Delft who were close to me when I needed help.

I am grateful to my parents and brother for their love, support and belief in me.

Contents

i. List of figures

ii. List of tables

1. Introduction

Together with a wider use of steel and other metals subject to corrosion, knowledge of a corrosion mechanism becomes a very important and relevant issue. Such knowledge may allow predicting the lifetime of metal systems and planning eventual maintenance actions (e.g. inspection, repair or replacement), which are important for safety and economic reasons.

Usually, when planning the inspection process the following questions arise:

- When the inspection procedure should be carried out?
- What kind of inspection technique should be applied?
- What parts of the system should be inspected?
- What inspection coverage should be chosen?

Over the last decades, mathematical models have been developed that allow determining a cost-optimal inspection frequency (or interval) (see, for example, [4] [14], [26]). Studies to develop and improve tools detecting the degradation were and are conducted as well. The issue concerning the choice of the areas that should be inspected is also of big interest for many engineers employed in the planning inspection process. In this field, the so-called sampling inspection approach is more and more considered and appreciated. Some studies regarding the derivation of the optimal sample size (in several industry fields) were performed [27], [28]. However, the general formula that would be applied for any inspection process is not yet found, and seems to be rather unlikely to find.

In the oil industry, hundreds of kilometers of pipework and vessels of a large size are operated. Since a large majority of them is made of the carbon steel, corrosion is a major cause of its degradation. Their failure may lead to release of the product they contain such as oil or gas, which represents a risk to the safety of people, it may harm the environment, and is a significant cause of economic loss. Therefore, a lot of attention is paid to monitor the reliability of pressure containing components. For various reasons, 100% inspection of such huge systems (plants) is not carried out, as many components are not prone to degradation or have a low failure probability. But if degradation is possible, and/or the consequence of failure is high, there is an obligation to demonstrate integrity of the components. For this purpose, sampling inspection is a widely used approach within industry.

1.1. Goal of the thesis

The objective of this project is to design and investigate the performance of the sampling inspection plans in simulation experiments. In order to fulfill this task two models simulating the corrosion process are introduced. They are further incorporated as a tool to generate corroded surfaces on which inspection schemes are simulated. The analysis of the reliability of three inspection schemes applied to surfaces with a different distribution of defects is performed.

1.2. Outline of the thesis

The report is organized as follows. Chapter 2 contains the description of two models that are designed to simulate the corrosion process. These are: the multivariate gamma model and the Poisson model, described in section 2.1 and 2.2, respectively. These two corrosion generating techniques are used for the purpose of a reliability (performance) analysis of the inspection schemes conducted in Chapter 3. This chapter introduces three sampling inspection schemes: regular, adaptive, and sequential inspection. The framework and simulation results of these three schemes are presented there.

The conclusions of the analysis and recommendations for future research are presented in Chapter 4.

2. Methods to simulate corrosion

In this chapter we introduce two methods designed for generating a corrosion surface. The surface S is considered as a discrete squared domain where each point (location) may be affected by the corrosion mechanism. The extension of corrosion in all three dimensions, i.e. length, width and depth, is regarded as a stochastic process. However, in order to assure that this process reflects the real behavior of the degradation corrosion mechanism, one assumes that this process is non-decreasing in time.

Independently of the dimension of the surface S, the corrosion process is assumed to proceed in the same way. However, in further simulation experiments we will restrict ourselves to the dimension of at most 100x100 units. The latter limitation was made for the presentation purpose. However, it has to be pointed out that the possible surface sizes depend on the corrosion generating method used as they require different computational effort. This issue will be further explained in the subsequent paragraphs.

In the following two subsections the two corrosion simulation techniques are described. The first approach (see section 2.1) is based on the joint normal transform method that allows obtaining any multivariate distribution with a pre-specified dependence structure and fixed marginals. In our considerations, this dependence structure will be given by the correlation matrix of exponential form. This assumption is necessary to assure its positive definiteness. In the proposed model we will use a gamma marginal distribution as the gamma process is frequently and commonly used to govern the corrosion process mechanism (see, for example [4], [5], [6] or [18]). For other examples of the implementation of the joint normal transform method the reader is referred to [1] and [2]. The second section, 2.2, presents the so-called Poisson corrosion method in which the Poisson stochastic process is used as a driving force when modeling the corrosion initiation and further extension. Within this model we assume that when corrosion is initiated at some location, its extension will affect all the neighboring points in a certain number of years. Such assumption introduces the dependence between possible degradations on particular locations and together with the chosen surface size has an influence on the structure of generated corroded surface.

Together with a detailed description of both techniques, some examples are presented as well. The Poisson and the multivariate gamma-process model will be further applied when performing simulations of corrosion behavior.

2.1. Multivariate gamma-process model

In this paragraph we introduce and describe one of the techniques for generating corrosion on a surface being a subset of $\mathbf{R}^2$, that is, the so-called multivariate gamma-process model. This method uses the multivariate normal distribution (see Definition 2.1, below) which is a common way of generating a realization from any multivariate distribution with given marginal distributions. When simulating a corroded surface, we assume dependence between surface locations. Therefore, the multivariate normal distribution will be used to generate the designed surface with its spatial variability.

Definition 2.1

A n-dimensional vector of normal random variables $\overline{X} = (X_1, X_2, ..., X_n)$ where $X_i \in R$, $i=1,...,n$ is said to have a **multivariate normal distribution** if its probability density function $f(\overline{x})$ is of the form

$$f(\overline{x}) = f(x_1, x_2, ..., x_n) = \left(\frac{1}{2\pi}\right)^{\frac{n}{2}} |\Sigma|^{\frac{-1}{2}} \exp\left\{-\frac{1}{2}\left(\overline{x} - \underline{\mu}\right)^T \Sigma^{-1}\left(\overline{x} - \underline{\mu}\right)\right\}$$

where $\underline{\mu} = (\mu_1, ..., \mu_n)$ is the vector of means and Σ is the variance-covariance matrix of the multivariate normal distribution. The elements of matrix Σ are of the following form:

$$\Sigma_{ij} = Cov(X_i, X_j) = E(X_i X_j) - E(X_i)E(X_j).$$

The relation of the covariance matrix to the product moment correlation matrix ρ is expressed by the formula:

$$\rho(X_i, X_j) = \frac{Cov(X_i, X_j)}{\sigma_i \sigma_j} = \frac{\Sigma_{ij}}{\sigma_i \sigma_j},$$

where the formal definition of the product moment correlation between two random variables reads:

Definition 2.2

The **product moment correlation** (called also linear or Pearson correlation) of two random variables X and Y having finite expectations $E(X)$, $E(Y)$ and finite variances σ_X^2, σ_Y^2 is defined as:

$$\rho(X,Y) = \frac{E(XY) - E(X)E(Y)}{\sigma_X \sigma_Y}.$$

Note, that in Definition 2.1, if random variables X_i, $i=1,\ldots,n$, follow a standard normal distribution, i.e. $X_i \sim N(\mu_i, \sigma_i)$ where $\mu_i = 0$ and $\sigma_i = 1$ for $i=1,\ldots,n$, then the covariance matrix Σ is equal to the product moment correlation matrix ρ.

Since in the joint normal transform method the rank correlation is used as the measure of the dependency between random variables, its definition is presented as well.

Definition 2.3

The **rank correlation** (also called Spearman rank correlation) of random variables X, Y with cumulative distribution functions F_X and F_Y is given by

$$\rho_r(X,Y) = \frac{E\left[F_X(X)F_Y(Y)\right] - E\left[F_X(X)\right]E\left[F_Y(Y)\right]}{\sqrt{Var(F_X(X))Var(F_Y(Y))}}.$$

It is worth to emphasize that the rank correlation always exists, can take any value in the interval [-1, 1] and is independent of the marginal distributions. Moreover, the Spearman correlation is invariant under non-linear strictly increasing transformations (see Propositions 3.8 and 3.9 in [3]). On the other hand, the product moment correlation is invariant only under linear strictly increasing transformations (see Propositions 3.4 in [3])

Looking at Definitions 2.2 and 2.3 one can observe the direct link between the rank and product moment correlation, which is expressed by

$$\rho_r(X,Y) = \rho\left(F_X(X), F_Y(Y)\right).$$

Based on [3], the subsequent steps of the joint normal transform method can be summarized as follows:

(i) Variables $X_1, X_2, \ldots, X_n$ are assumed to have the invertible univariate distribution functions $F_1, F_2, \ldots, F_n$, respectively. The dependency between considered variables is expressed by the rank correlation matrix ρ_r.

(ii) A sample $(y_1, y_2, \ldots, y_n)$ is taken from a joint normal distribution with standard normal marginals and the rank correlation matrix ρ_r as above.

(iii) In order to calculate a sample from a distribution with marginal distributions $F_1, F_2 \ldots, F_n$ and rank correlation ρ_r the following transformation is made:

$$\left(F_1^{-1}(\Phi(y_1)), F_2^{-1}(\Phi(y_2)), \ldots, F_n^{-1}(\Phi(y_n))\right),$$

where Φ denotes the standard normal cumulative distribution function.

Now, since the transformations $F_i^{-1}(\Phi(y_i))$ are monotone and strictly increasing, the multivariate distribution of $(X_1, X_2, \ldots, X_n)$ has the rank correlation matrix ρ_r.

However, in the gamma model, instead of the rank correlation the product moment correlation - ρ (Definition 2.2) is used as a dependency measure. The main reason for this is that using the normal distribution, one can find a joint normal distribution that realizes a given product moment correlation matrix ρ, while in case of the rank correlation matrix such joint normal distribution may not exist [3]. As a consequence, the assumed (desired) product moment correlation matrix of the multivariate distribution with gamma marginals could be different (due to the non-linear transformation) from the imposed matrix ρ of the multivariate normal distribution. However since these differences appeared to be not so significant (see Appendix A, section 4) we will ignore them in our model.

Because the wall loss due to the corrosion process is non-decreasing in time (the amount of degradation always accumulates) and has nonnegative values, a gamma distribution is chosen as the marginal distribution when applying the multivariate model. This distribution is defined on the positive domain and as a result it is frequently used for modeling the degradation processes. The formal definition of a gamma distributed random variable is presented below.

Definition 2.4

A random variable X is said to be **gamma distributed** with a shape parameter $a > 0$ and a scale parameter $b > 0$ (with the notation $X \sim Gamma(x \mid a, b)$) if its probability density function is given by:

$$gamma(x \mid a, b) = \frac{1}{b^a \cdot \Gamma(a)} x^{a-1} \exp(-\frac{x}{b}) I_{[0, +\infty]}(x),$$

where $\Gamma(a)$ is a complete gamma function defined as

$$\Gamma(a) = \int_0^\infty x^{a-1} \exp(-x) dx.$$

Since in our study, the analysis of the corroded surfaces will be performed at one particular time point, the gamma distribution with given shape and scale parameter will be used to represent the corrosion depths for all surface points. It is worth to note, that in order to perform the analysis of the corrosion mechanism in time, the gamma process (Definition 2.5) with shape function, say $a(t)$, and scale parameter, say b, can be used. Hereafter, when referring to the multivariate gamma-process model, the gamma model name will be used equivalently.

Definition 2.5

Let $a(t)$ be a non-decreasing, left continuous, real-valued function for $t \geq 0$, with $a(0) \equiv 0$. The **gamma process** with shape function $a(t) > 0$ and scale parameter $b > 0$ is a continuous-time stochastic process $\{X(t): t \geq 0\}$ with the following properties:

(i) $X(0) = 0$ with probability one;

(ii) $X(s) - X(t) \sim Gamma(x \mid a(s) - a(t), b)$ for all $s > t \geq 0$;

(iii) $X(t)$ has independent increments.

For more properties of the gamma process, see [31].

As it was mentioned above, the corrosion generating methods presented here are designed to work on squared surfaces. Therefore, let us consider a surface S of size $k \times k$, resulting in $n = k \times k$ locations. Further, let $\bar{X} = (X_1, ..., X_n)$ denotes a gamma random vector representing the corrosion depths on the considered surface (at a given inspection time). With this setup each random variable X_i is uniquely associated with a location on S. More precisely, X_i stands for a corrosion depth at a location $(x(i), y(i))$ with x and y being the Cartesian coordinates of S.

For generating the corrosion surface with the multivariate technique, an assumption about dependency between corrosion depths at each location is made. Concretely, we assume the following product moment correlation between elements of $\bar{X}$:

$$\rho(X_k, X_l) = \exp\left\{ -d\left(\sum_{i=1}^{2} | dist_i |^p \right)^q \right\} \qquad (2.1)$$

where $dist_1$ denotes the distance between the X_k and X_l with respect to their first coordinates on the surface S (i.e. $dist_1 = |x(k) - x(l)|$). Similarly, $dist_2$ is the distance between the X_k and X_l (i.e. $dist_2 = |y(k) - y(l)|$) with respect to their second coordinates. The parameter d is constant and determines the amount of correlation, while the parameters p and q are associated with the vector norm.

The correlation function given by the formula (2.1) introduces a special kind of distance dependency. It means that the locations which are close to each other have a bigger correlation than those which are more separated (share greater distance). Moreover, it has to be mentioned that due to the computational effort required for calculation of such correlation matrix, the size of the corroded surfaces generated by the gamma model is limited to at most 50×50 units.

The corrosion generating method described here is a one-step procedure in the sense that the generated surface with particular defect depths represents the current (cumulative) state of the corroded surface as a result of a long-lasting degradation process. However, it is worth to note that this model can be extended and used also for modeling corrosion in time. That is, the defects depths generated in a one-step procedure can be regarded as the corrosion increments created in a unit time. Then, the cumulative (actual) corrosion level at each location will be obtained by summing up the corresponding increments of wall loss generated in each time step.

It has to be mentioned that the surfaces generated by the gamma model have a characteristic feature that all their locations are affected by corrosion immediately. Thus, it can be advised to use the multivariate model for modeling a general corrosion process as shown in Example 2.1. However, the same example shows that changing the parameters of the model, one can generate surfaces where some locations are highly corroded while others are in their initial stage.

Example 2.1

Remind that when generating the corroded surfaces using the gamma method, together with a specification of the shape and scale parameters of the gamma distribution, the values of the correlation parameter, d, and norm parameters, p and q, must be assessed as well. Choosing particular values of these quantities several classes of corroded surfaces can be obtained. For example, one can model smooth surfaces that correspond to a general (uniform) corrosion mechanism, which causes a relatively uniform reduction of thickness over the surface of a corroding material. On the other hand, it is also possible to generate corroded areas which reflect the behavior of the localized (pitting) degradation process characterized by the formation of holes or pits on the metal surface. Some illustrations

showing characteristic properties of already mentioned corrosion types are presented in the next two figures (Figure 2.1 and 2.2).

Figure 2.1 *Example of uniform (general) corrosion.*

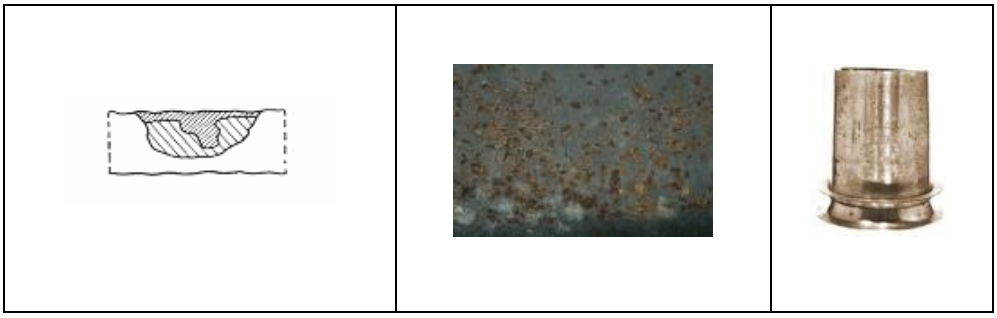

Figure 2.2 *Example of localized (pitting) corrosion.*

Within the gamma generating technique, the parameter d has the biggest influence on the surface smoothness and therefore it is called the correlation parameter. When fixing (and keeping unchanged) the values of the vector norm parameters, one can perform a sensitivity analysis with respect to the variable d. Looking at the formula (2.1) one can conclude that with a smaller value of this parameter a bigger correlation between surface locations is introduced. This will cause more smoothness of the generated corrosion areas and simultaneously will reflect uniform corrosion. On the other hand, high values of the correlation parameter are equivalent to a bigger variability of the pitting degradation process. The latter inferences are confirmed in Figure 2.3 where some characteristic plots of generated surfaces are presented for different values of d. Moreover, the accompanied Figure 2.4 shows the dependence between locations' distance and their correlations. It is worth to note that in the example presented here, the norm parameters p and q were equal to 2 and 0.5, respectively. The latter setup gives the simple Euclidean norm on the Cartesian grid.

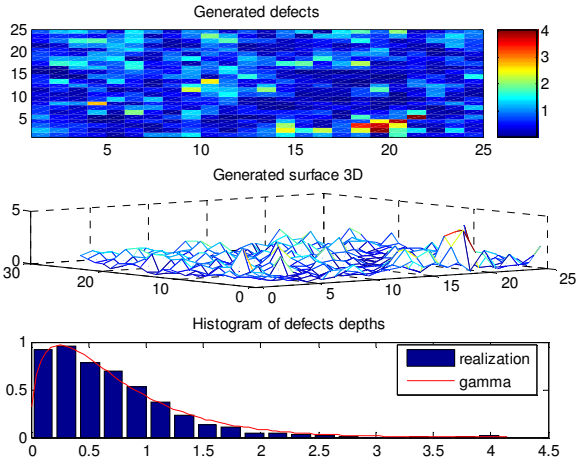

the correlation parameter d = 1

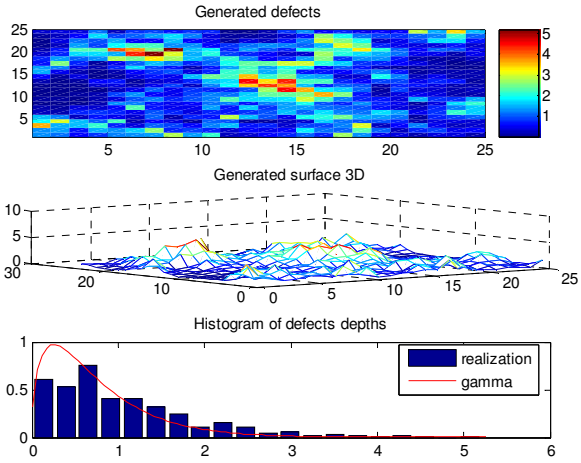

the correlation parameter d = 0.5

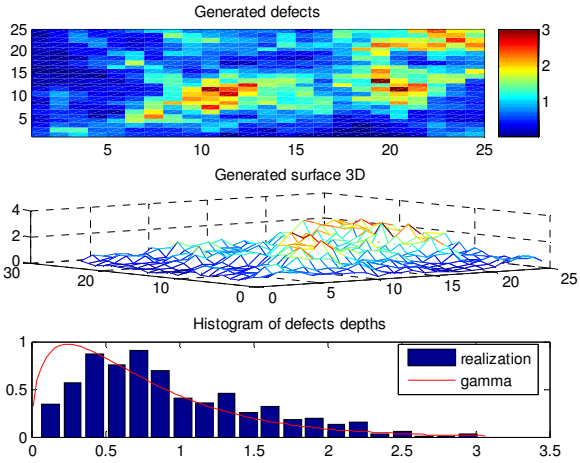

the correlation parameter d = 0.15

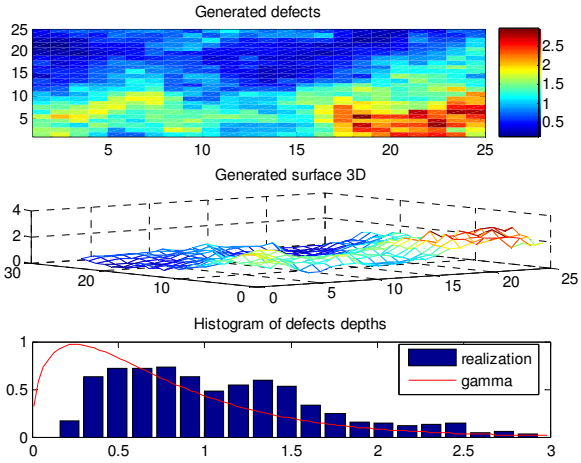

the correlation parameter d = 0.05

Figure 2.3 *Examples of corroded surfaces generated by the gamma technique.*

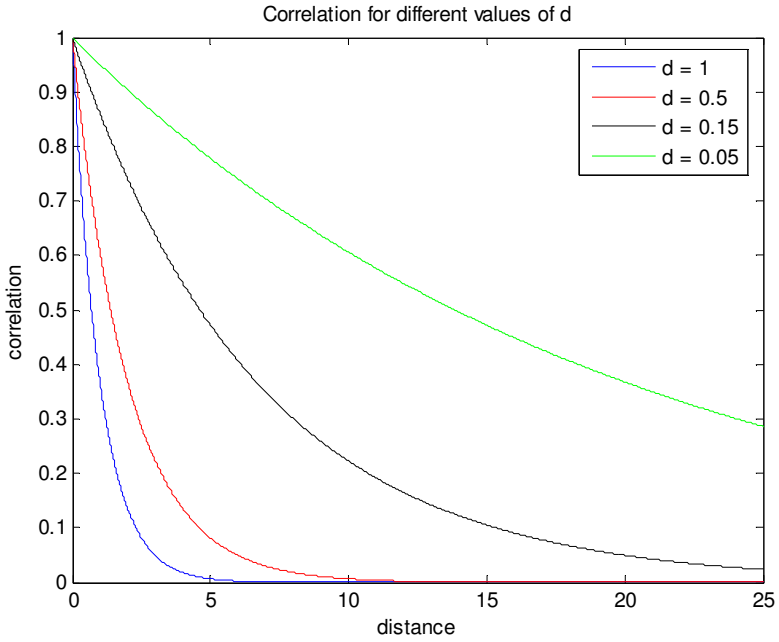

Figure 2.4 *Correlation functions for different values of d.*

2.2. Poisson model

The Poisson technique is designed to model a three-dimensional corrosion process. That is, it allows a corrosion extension in the depth, length and width dimensions. An important property of this model, that makes it different from the gamma model, is that it is a time-step model. In other words, in opposite to the gamma method, where the generated surface represents the actual state of the corrosion depths with all locations affected; the Poisson model allows modeling the corrosion in time. That is, it can be seen how the defects appear, extend and grow in course of time. As a result, one can simulate the surfaces where only some locations are affected and the rest of the surface is free of defects. Thus, the Poisson model seems to be more general and universal, as it can be used to generate more variable corrosion surfaces (see Figure 2.10). It can be especially useful to model the pitting corrosion mechanism.

The Poisson process (see Definition 2.6) is frequently used in diverse fields of science such as physics, astronomy, transportation or telecommunication, to model counting-type events [19], [20] and [21]. For example, the number of telephone calls arriving at a switchboard during any specified time interval, or the number of traffic accident at certain place up to particular time t, may follow the Poisson distribution. In our model, this distribution will be used to model the stochastic processes of the corrosion initiation and

extension. In mathematical terms, $\{X(t), t \geq 0\}$ is a stochastic process if $X(t)$ is a random quantity for all $t \geq 0$.

Definition 2.6

A stochastic process $N(t)$ is a **time-homogeneous**, one-dimensional **Poisson process** if:

- the numbers of events occurring in two disjoint (non-overlapping) subintervals are independent random variables;
- the probability of the number of events in some subinterval $[t\ ,\ t + h]$ is given by

$$P\big([N(t+h) - N(t)] = k\big) = \frac{\exp(-\lambda h) \cdot (\lambda h)^k}{k!},\ k = 0, 1. \ldots$$

where the positive number λ is a fixed parameter, known as the rate parameter. In words, this means that the random variable $N(t + h) - N(t)$, being the number of occurrences in the time interval $[t\ ,\ t + h]$, has a Poisson distribution [1] with parameter $\lambda \cdot h$.

On the other hand, a **non-homogeneous Poisson process** is a Poisson process with rate parameter $m(t)$ such that the rate parameter of the process is a function of time. In this case, the probability of the number of events in the subinterval $[t\ ,\ t + h]$ is given by

$$P\big([N(t+h) - N(t)] = k\big) = \frac{\exp\left\{-\int_t^{t+h} m(s)ds\right\} \cdot \left(\int_t^{t+h} m(s)ds\right)^k}{k!},\ \text{for } k = 0, 1, 2, \ldots$$

Modeling the corrosion initiation

Let us start the description of the Poisson simulating corrosion method, from modeling the corrosion initiation. Here, a non-homogenous Poisson process $N_1(t)$ with time-dependent rate $m(t) = q \cdot \lambda \cdot t^q$ is used. In other words, this process generates 'the arrivals' of the corrosion spots and $m(t)$ represents the intensity of the spot appearances (rate of

[1] For the definition of a Poisson distribution reader is referred to [7], [8] or [16].

appearances). The expected number of such arrivals is a function dependent on time t, and is equal to:

$$E\left(N_1(t)\right) = \int_0^t m(s)ds = \lambda \cdot t^{\,q}\,.$$

Note that for q = 1 the number of corrosion initiations will be linear in time with constant intensity rate equal to λ, what results in the homogenous Poisson process. Moreover, it is worth to point out that higher values of the parameters q and λ result in more arrivals.

In order to model the preferential locations for the occurrences of the initial corrosion spots, a special function defined on the surface S is introduced. This function is given in the matrix form (SpT), which takes values on the interval [0, 1] and expresses a probability that a particular location will be affected by the Poisson initiation process.

In the next figure (Figure 2.5) one can see an example of the initiation function. Such particular model can be used to describe the initiation of the corrosion mechanism within the oil-pipes. It is because the bottom of the pipe is usually more probable to be affected by the degradation process (a higher value of the corrosion initiation function will reflect this phenomenon) than the remaining parts of the pipe. As another example, one can imagine a complex system, which consists of several components that are joined by welds. Then, the welded parts are considered as the preferential locations for being subject to corrosion.

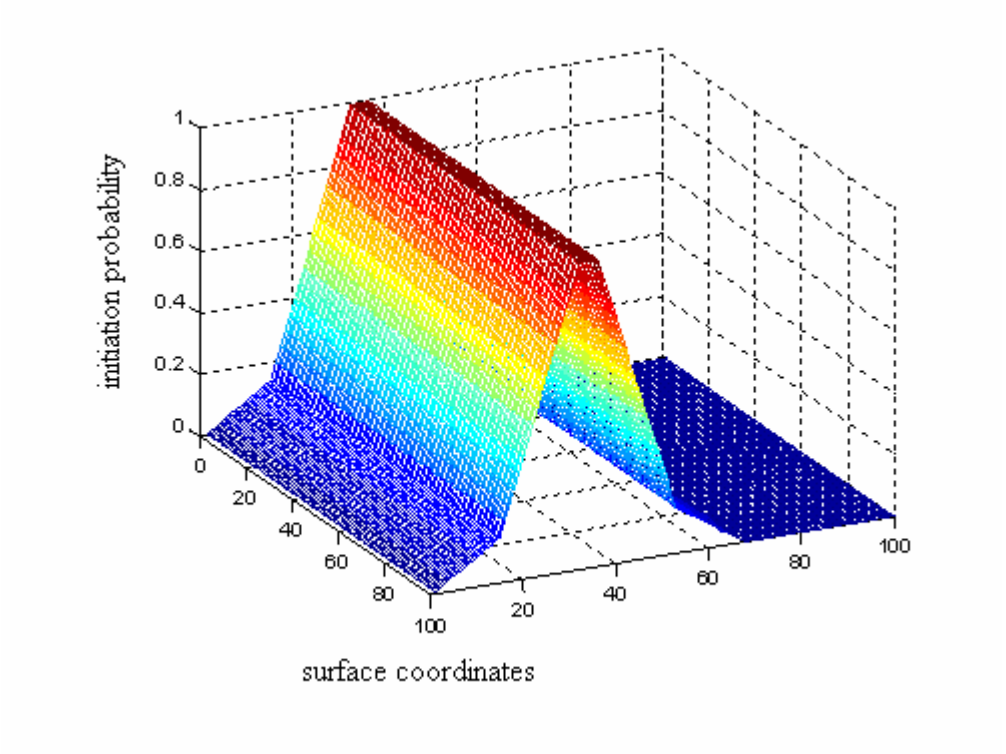

Figure 2.5 *Example of a probability function of the corrosion initiation locations.*

The SpT function is used when determining the set of possible initial corrosion locations. This set is created in the following way. Firstly, the matrix RnU corresponding to the considered surface and consisting of uniform numbers independently drawn from the interval [0, 1] is generated. In the next step, the values of the initiation function, SpT, and the generated random numbers are compared for each location. As a result, if for a given location, the drawn random number is less than or equal to the corresponding value of the initiation function, this surface location is accepted and included to the initial location set. It is worth to point out that the initiation set is determined once and the number of its elements strongly depends on the initiation function. A graphical example of the initial location set can be seen in Figure 2.6.

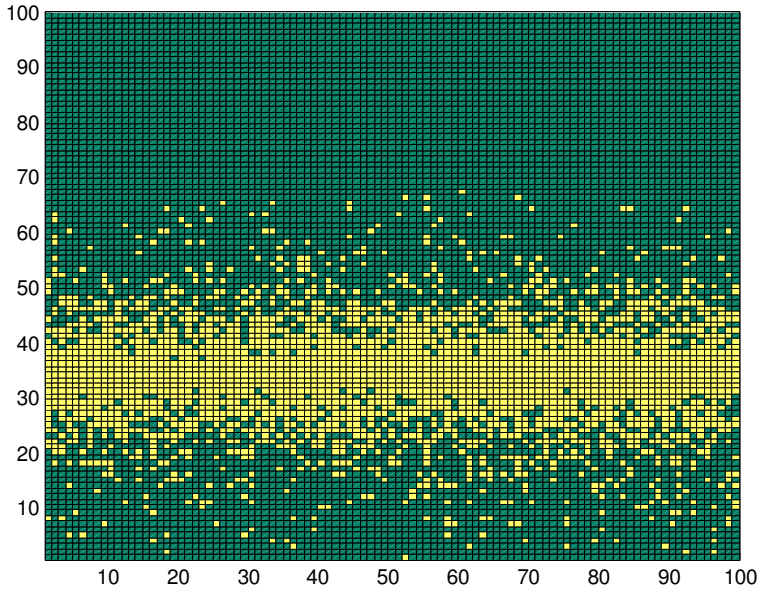

Figure 2.6 *Example of the initial locations set.*

Having defined the set of initial (preferential) corrosion locations, at each time point *t*, t =1, 2, …, $Tmax$, the $N_1(\Delta t)$ initial corrosion locations are selected randomly from this set and simultaneously are removed (excluded) from this set. More precisely, the $N_1(\Delta t)$ with Δt =1 is given by

$$N_1(\Delta t) = N_1(t) - N_1(t-1)$$

and in consequence has a Poisson distribution with parameter $\lambda\left(t^q - (t-1)^q\right)$.

It has to be mentioned that the elements of the initiation set which were affected by the corrosion process during its extension phase (described below) at some time *t*, are also excluded from this set.

In Figure 2.7 an example of the realization for $N_1(\Delta t)$ = 100 is presented while Figure 2.8 shows the updated location set (without already selected points).

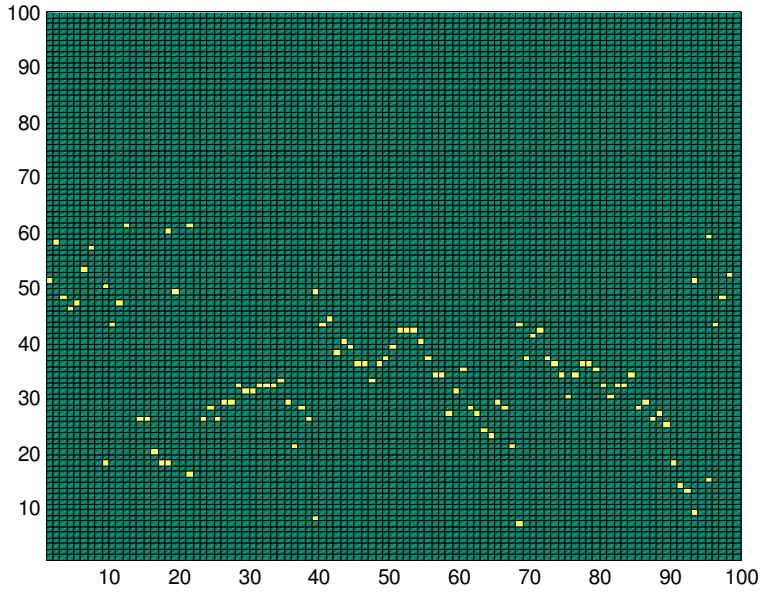

Figure 2.7 *Realization of 100 initiations from the initiation set.*

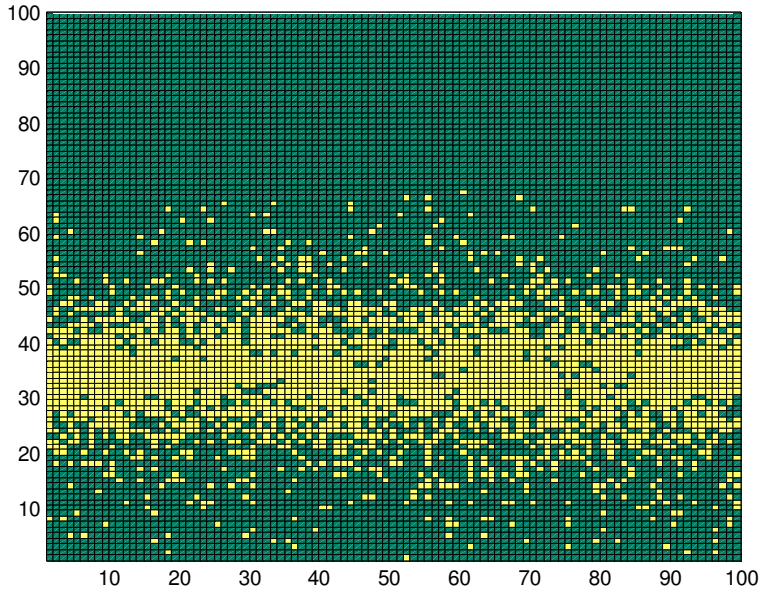

Figure 2.8 *Updated initiation set.*

The process of corrosion initiation described above, works as long as the initiation set is not empty. Once its last element is affected by the corrosion and it is removed from this set, the initiation process is terminated. As a result, only the extension process progresses.

Modeling the corrosion extension

As soon as the corrosion spot appears, its extension process is governed by Poisson distributions defined on the locations of the surface S. Let us denote these random variables by $N_2(i, j)$, where i and j denote the Cartesian coordinates on the surface S. Note that $N_1(t)$ is a Poisson process in time and $N_2(i, j)$ a Poisson process in space. The intensity of the Poisson process $N_2(i, j)$, denoted by $\lambda_{i,j}$, is defined in terms of the extension intensity function $\nu(i, j)$. This function, $\nu(i, j)$, takes values on [0, ∞) and determines the corrosion extension at the particular location.

The extension mechanism consists of the following steps:

1) Firstly, a set of potential locations subject to extension is established. In other words, the information about the points affected by the corrosion and all their neighbors is gathered. All of them belong to the mentioned set. It has to be pointed out that for the discrete surface considered here each location has at most eight neighbors.
2) For a given point from the potential location set, say (i,j), its possible corrosion growth (in the depth dimension) depends on two conditions. Briefly speaking, these conditions determine whether the considered point can be affected by the extension process and if yes, how much the corrosion level will increase; see condition a) and b), respectively.

   a) In order to allow a corrosion growth at the location (i,j), a constraint regarding the maximum allowable difference in corrosion level between neighboring locations has to be satisfied. It should be explained that the maximum allowable difference level taking positive natural values is the driving parameter of the Poisson technique and strongly influences the surface structure. In other words, depending on the value of this parameter one can generate more or less smooth surfaces. (When referring to this parameter the *steps* name will be also used equivalently.)

   The mentioned level constraint requires that all neighbors of the point (i,j) have to have a corrosion level that does not differ more than $steps$ -1. In mathematical terms: all neighbors of the point (i,j) have to have a corrosion level at least equal to

$$level(i,j) - steps + 1. \qquad (2.2)$$

In other words, the cardinality of the set $D_{i,j}$ defined below has to be equal to the number of neighbors of the location (i,j).

$$D_{i,j} := \{(k,l) : (k,l) \text{ is neighbor of } (i,j) \text{ and } level(k,l) \geq level(i,j) - steps + 1\}$$

If some neighboring location of the point (i,j) has a corrosion depth smaller than (2.2), then the corrosion extension at the point (i,j) is not allowed. Otherwise its corrosion level will increase according to the rules defined in b).

b) To decide how much the corrosion depth of the location (i,j) will change, the number of its surrounding locations with corrosion level bigger than $level(i,j)$ is checked. More precisely, the so called intensity set $I_{i,j}$ is created, where

$$I_{i,j} := \{(k,l) : (k,l) \text{ is neighbor of } (i,j) \text{ and } level(k,l) > level(i,j)\} \cup \{(i,j)\}.$$

Due to the extension process, the new depth of the location (i,j) is equal to:

$$level(i,j)' = \min\{N_2(i,j), b\}.$$

The minimum operator assures the consistency with the pre-specified maximum allowable difference level ($steps$) and $N_2(i,j)$ and b are defined as follows:

- $N_2(i,j)$ is a Poisson number drawn from the Poisson distribution with the parameter $\lambda_{i,j}$ given by

$$\lambda_{i,j} := \sum_{(x,y) \in I_{i,j}} \nu(x,y)$$

- b stands for the so-called upper bound and is defined as:

$$b := steps + \min\{level(k,l) : (k,l) \text{ all neighbors of } (i,j)\} - level(i,j).$$

When all the potential locations have been visited by the extension process the considered surface is updated by recording new corrosion levels, $level(i,j)'$. This surface together with new arrivals caused by the Poisson initiation process is considered as the current state of the surface S. Thanks to the consistency between level's extension at each

location and the previous state of the surface, the maximum allowable difference between neighboring locations (parameter $steps$) is preserved after the performed update.

It is worth to point out that because the update of the corrosion levels is made after the extension process visited all the possible locations , the order of visitation is not relevant and has no influence on surface properties. Moreover, such defined corrosion process implies that the increase in the corrosion levels at one run of the extension process is independent among locations.

For a better understanding and for the purpose of illustration of the Poisson generating corrosion technique, an example is presented. Moreover, Figure 2.10 shows some types of corrosion surfaces that can be generated by this method.

Example 2.2

Consider a squared surface S consisting of 25 locations (k = 5) depicted in the Figure 2.9. Further suppose that all locations have the same probability of being affected by the corrosion initiation process equal to one. Hence, all elements of the matrix SpT are equal to 1 and all surface locations belong to the initial location set [2]. Moreover, it is assumed that at the considered time the corrosion is initiated only at the location (i,j) indicated by "5". In other words, only one 'arrival' of the Poisson process $N_1(t)$ is observed. This results in $level(i,j)$ = 1 and $level(k,l)$ = 0 for the remaining surface points. This surface (with mentioned corrosion levels) will be regarded as the current state of the surface S. On the other hand, the surface with all potential locations being visited by the extension process will be referred as the updated state of the surface.

In this example we also assume that the intensity function of the extension process is the same for all locations and equals $\nu(i,j)=1$, for all $(i,j)\in S$.

[2] This is because all elements of matrix SpT are greater than or equal to the corresponding elements of the matrix RnU, which are drawn independently from the uniform distribution on the interval [0, 1]

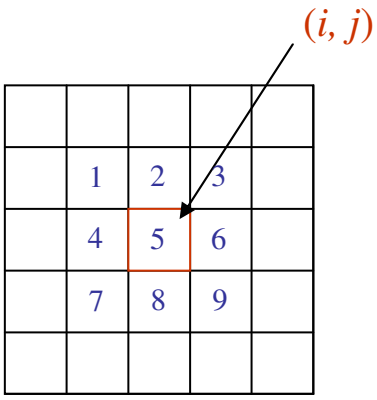

Figure 2.9 *Example of a discrete surface.*

A spatial dependency between corrosion spots on particular locations is introduced by the maximum allowable depth level between surface neighbors (the parameter *steps*), which is chosen to be equal 1 (unit).

For the surface point 5 affected already by the corrosion, the set of potential extension locations consist of eight elements, i.e. $\{1,2,3,4,6,7,8,9\}$.

When considering extension at location 6 (equivalently denoted by the location $(i,j+1)$), the number of its neighbors with corrosion level at least equal to

$$level(i,j+1) - steps + 1,$$

has to be checked. More precisely, we check the cardinality of the set $D_{i,j+1}$, which in this case is defined as:

$$D_{i,j+1} := \{(k,l): (k,l) \text{ is neighbor of } (i,j+1) \text{ and } level(k,l) \geq level(i,j+1) - steps + 1\} =$$
$$= \{(k,l): (k,l) \text{ is neighbors of } (i,j+1) \text{ and } level(k,l) \geq 0 - 1 + 1\}.$$

Since all neighboring locations of the point 6 have the corrosion level greater than or equal to 0 (all belong to the set $D_{i,j+1}$), the first extension condition is satisfied. Thus, it remains to determine how much the corrosion level at the location 6 will increase. To do this, the following intensity set $I_{i,j+1}$ have to be determined:

$$I_{i,j+1} := \{(k,l): (k,l) \text{ is neighbor of } (i,j+1) \text{ and } level(k,l) > level(i,j+1)\} \cup \{(i,j+1)\}$$

In our example, location 5 is the only one with corrosion depth bigger than the one at location 6. As a result, the set $I_{i,j+1}$ consists of two elements; that is $I_{i,j+1} = \{(i,j), (i,j+1)\}$.

Therefore, the extension process at location 6 will be governed by the Poisson process with the intensity

$$\lambda_{i,j+1} = \nu(i,j) + \nu(i,j+1) = 1+1 = 2\,.$$

However, in order to be consistent with the maximum allowable difference level (*steps*), which in our example equals 1, before the extension is made the following upper bound is calculated:

$$b := steps + \min\{level(k,l) : (k,l)\, all\ neighbors\ of\ (i,j+1)\} - level(i,j+1) = \\ = 1+0-0 = 1$$

Finally, the new depth level of location 6 can be calculated and is equal to:

$$level(i,j+1)' = \min\{N_2(i,j+1), b\}\ ,$$

where Poisson number $N_2(i,j+1)$ has intensity $\lambda_{i,j+1} = 2$.

The consideration of possible corrosion extension can be carried out in a similar manner for the remaining locations. After that, all corrosion levels on surface S are updated and stand for the current state of the surface at the next time point.

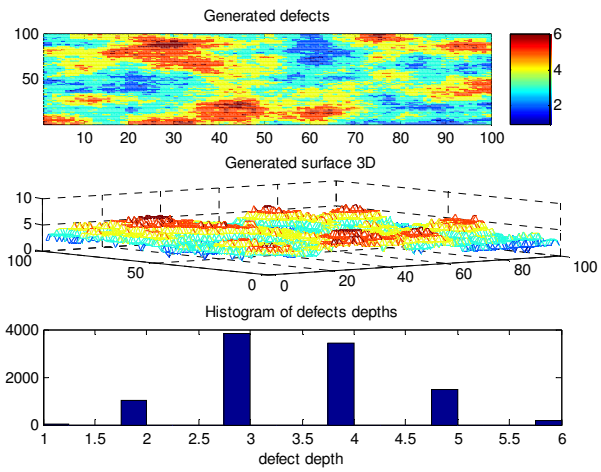

steps = 1

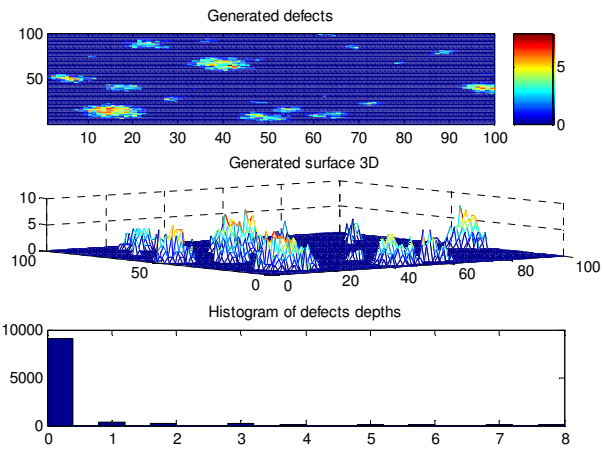

steps = 6

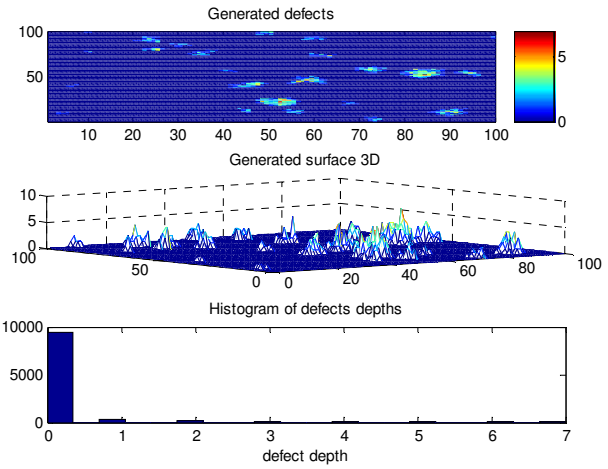

steps = 4

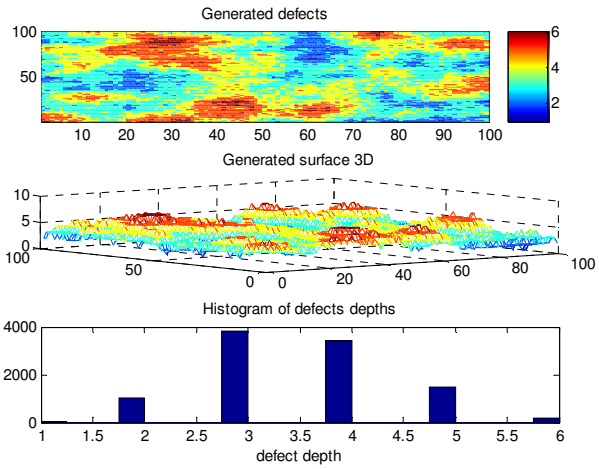

steps =1

Figure 2.10 *Examples of corroded surfaces generated by the Poisson model.*

3. Inspection schemes

The main subject of this chapter is to introduce and to check the performance (in simulation experiments) of the designed sampling inspection schemes. These are: the regular inspection scheme, the adaptive inspection scheme and the sequential random scheme. All of mentioned sampling methods are further used for the inspection purpose of corroded surfaces generated by the gamma and Poisson models (the detailed descriptions of these techniques are presented in previous chapter).

The inspection schemes proposed below are defined by some parameters that need to be specified before the inspection procedure is performed. Therefore, depending on the available knowledge about the considered surface, different inspection schemes will be more appropriate. This issue will be also covered in subsequent lines.

3.1. Regular inspection scheme

In the next paragraphs a description of one of the designed sampling inspection schemes is presented. Concretely, in section 3.1.1 one can find the outline of the mechanism and the properties of the regular inspection scheme (RIS). On the other hand, section 3.1.2 shows the application of the mentioned inspection method. It presents the simulated inspection results for the corrosion surfaces generated with the Poisson as well as the gamma model. These results give an indication of the performance of the considered scheme for different types of corroded surfaces. It is worth to mention that for the simulation purposes two *Matlab* routines [3] (one for the Poisson model and one for the gamma model) were created and implemented.

3.1.1. Framework of the regular inspection scheme

A regular inspection scheme is a very trivial and simple inspection scheme that is defined by one parameter i.e. *the inspection coverage*. This parameter defines the proportion of the considered surface that will be examined during the inspection process. In the inspection scheme proposed here (called also the inspection scheme 1) when choosing particular value of the inspection scheme coverage, say c, ($c \cdot 10$) points on every 10 points will be examined. Mentioned points are not selected randomly but they follow some pattern that assures their even spread. For instance, when c = 0.5 on every 10 discrete surface points five of them will be inspected, in this case every 2^{nd} point will be examined. Of course,

[3] In the Appendix C the description of the software developed for the simulation purposes is presented.

due to the discreteness of the surfaces the pre-specified inspection coverage is not always satisfied precisely, however in all cases it is very close to the desired value. An essential feature of the inspection scheme 1 is that the inspected coverage is established in advance before the inspection process is initialized. As a result, the total inspection costs can be assessed beforehand. However, since this inspection scheme is not dynamic (i.e. it is completely defined before its application), it requires some kind of confidence about the considered surface structure. An appropriate prior knowledge about the defects distribution allows avoiding situations when *the inspection coverage* parameter is over or under estimated.

Examples of surfaces to be inspected in other words, the applied patterns for different values of the scheme parameter - *inspection coverage* - are presented below (Figure 3.1). In these figures the yellow area denotes the inspected surface while the green area the not inspected one. Additionally presented, the true percentage of the inspected area shows that the used inspection pattern has the desired inspection coverage. The chosen surface size is k = 25.

<table>
<tr>
<td> 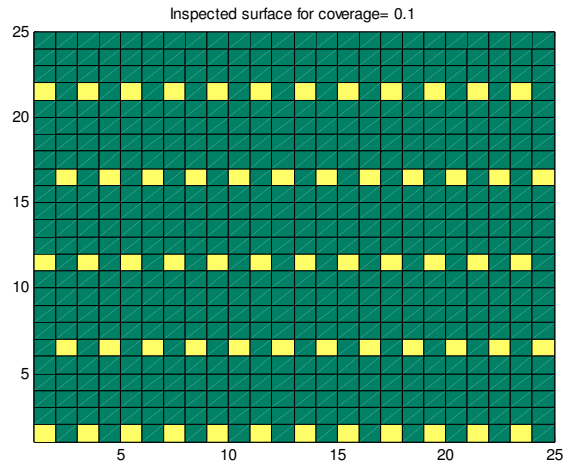
</td>
<td> 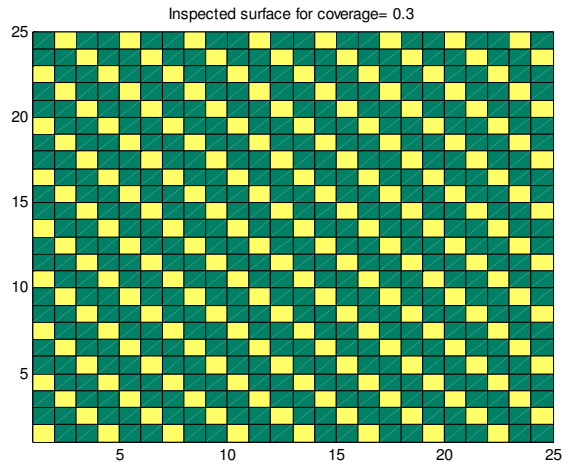
</td>
</tr>
<tr>
<td>the inspection coverage = 0.1
(true inspected coverage = 0.1008)</td>
<td>the inspection coverage = 0.3
(true inspected coverage = 0.3344)</td>
</tr>
</table>

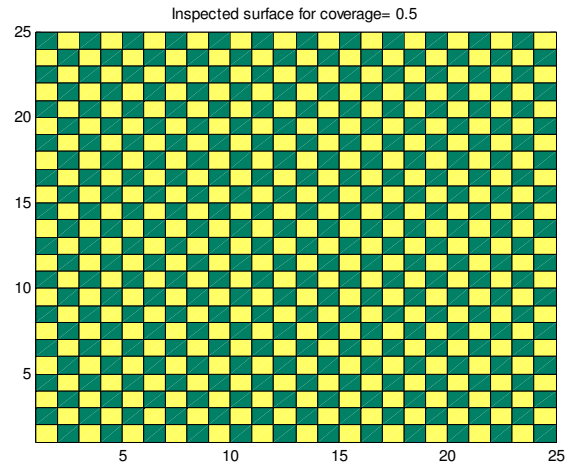

the inspection coverage = 0.5
(true inspected coverage = 0.5008)

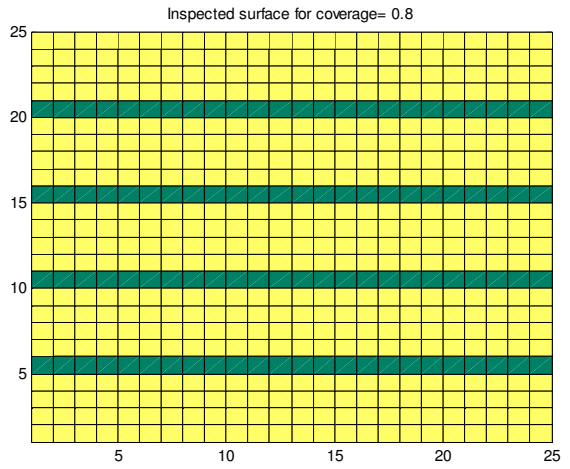

the inspection coverage = 0.8
(true inspected coverage = 0.7936)

Figure 3.1 *Examples of the inspection patterns within RIS for different values of the inspected coverage parameter.*

3.1.2. Simulation

Let us now present some results obtained when applying the regular inspection scheme in simulation experiments. These experiments were performed for two proposed techniques of generating corrosion surfaces, namely the gamma and the Poisson method. The analysis was carried out with respect to the parameters characteristic for those methods as well as with respect to the parameter of the inspection scheme 1.

Simulation settings of the regular inspection scheme for corrosion surfaces generated by the gamma model.

In order to analyze the performance of the inspection scheme 1 the following parameters of the gamma corrosion generation technique were used. It is worth to point out that they were kept unchanged during entire analysis.

- the shape parameter a = 1.5;
- the scale parameter b = 0.5;

(It is worth to note that the expected value of the gamma distributed variable with these parameters (i.e. a = 1.5 b = 0.5) is equal to $E(X) = ab$ = 0.75. Moreover, simulated expected maximum value from the 625 i.i.d. gamma variables appeared to be equal 5.5. We have simulated 625 gamma variables since in the simulation experiments the surfaces consisting of 25x25 = 625 locations were considered.);

- the L_p norm parameters p = 2 and q = 0.5;

(Note that with this setting the applied L_p norm reduces to the simple Euclidean norm that represents the real distance measured with in discrete units).

On the other hand, different values of parameter d reflecting the correlation factor between corroded points were examined under the regular inspection scheme considered here. It appeared that the latter value has strong influence on the appropriateness of the applied inspection coverage. In different words, for some class of values of parameter d, the inspection of a small percentage of surface brought equally reliable results as when applying more extended inspection.

During performed simulation experiment the square of gamma corroded surface of size $n = k \times k$ = 25x25 grid points was generated 300 times. (A sensitivity analysis with respect to number of simulations parameter can be found in the Appendix B-1.) For each surface the same pattern of inspected points (the same inspection coverage) was applied. The number of wrong decisions (for definition see below) and differences between the maximum of all real defects and the maximum of defects recorded during inspection (in each simulated surface) were used as driving criterions when performing the study. The latter quantity is represented by histogram plots. Plots of the cumulative distribution functions of the actual maximum defects and the maximum of those recorded during inspections are presented as well.

- *the number of wrong decisions* – counts the number of situations when among the inspected points *the critical defect* (defined below) was not recorded (found) while it was present on the simulated surface. In other words, it counts the number of bad acceptance decisions when after the inspection procedure the considered surface is judged as a good one (without evidence of the critical defect) while it does not reflect the reality. This quantity shows when the applied inspection scheme performs well, whether it results in a small number of wrong decisions or possibly leads to severe consequences;

- *the critical defect size* is a defect size defined in advance by the inspector and depends on the considered surface. Existence of a pit depth of this size is equivalent with component failure and the surface is judged as a defective one.

Obviously, the proper choice of *the critical defect size* is important and strongly affects the simulation results. Therefore, attention should be paid when setting the value of this parameter simultaneously taking into account important characteristics of the considered surface.

In the performed simulation experiments the critical defect size was chosen regarding the previously chosen gamma surface parameters and was equal to 3 (units). The accompanied figures with some characteristic plots of the considered corroded areas confirm the rightness of the applied value of the critical defect. From these plots one can see that for the gamma distribution with parameters a = 1.5 and b = 0.5, the value 3 is located in its tail and has a small probability of being exceeded.

Simulation results of the regular inspection scheme for corrosion surfaces generated by the gamma model.

The simulation experiments brought the following results of the performance of RIS applied for the surfaces generated by the multivariate gamma model.

- *the correlation parameter* d = 1

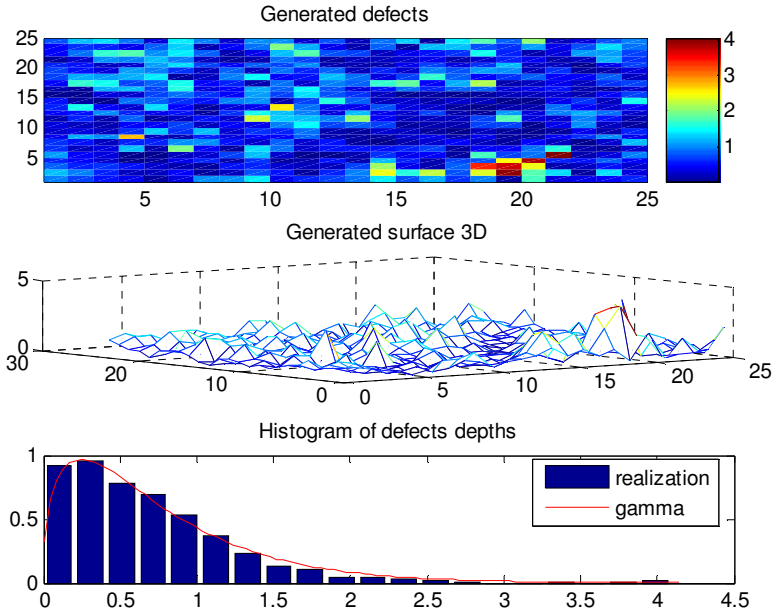

Figure 3.2 a) *The characteristic plots of the corroded surface with the correlation parameter d = 1.*

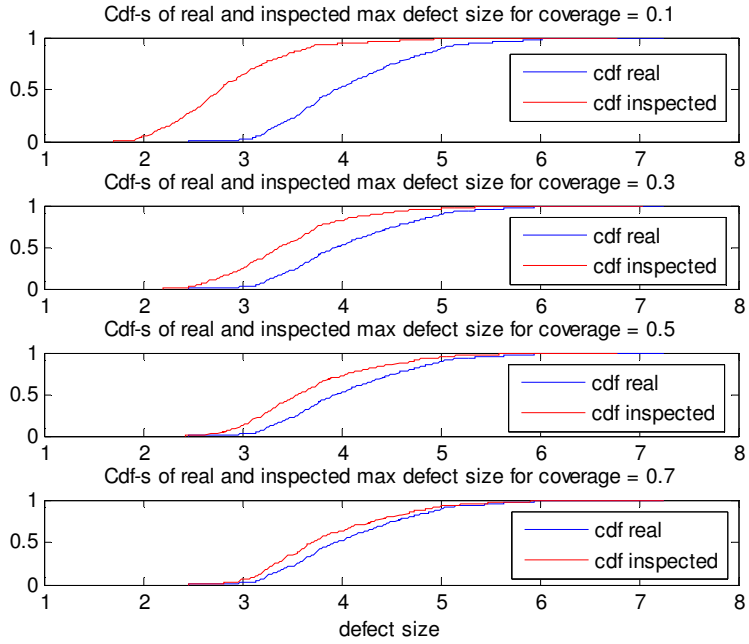

Figure 3.2 b) *The cumulative distribution functions of the real maximum defects and the maximum defects recorded during RIS for different inspection coverage and d = 1.*

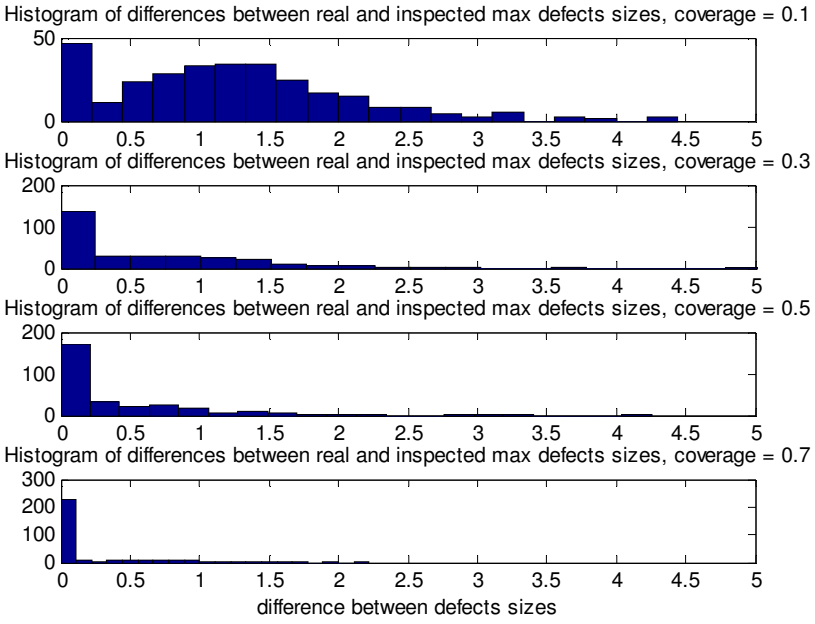

Figure 3.2 c) *The histograms of differences between the real maximum defects and the maximum defects recorded during RIS for different inspection coverage and d = 1.*

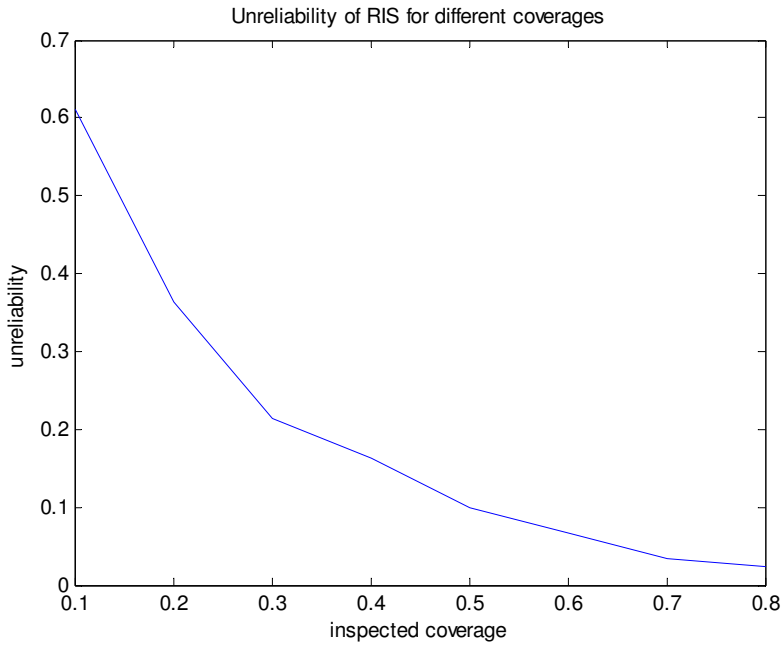

Figure 3.2 d) *The unreliability function of the regular inspection scheme for d = 1.*

correlation parameter d = **1**, number of simulations = 300								
Inspected coverage	0.1	0.2	0.3	0.4	0.5	0.6	0.7	0.8
Number of wrong decisions	183	109	64	49	30	20	10	7

Table 3. 1 *The number of the wrong acceptance decisions against the inspection coverage within the regular scheme for d = 1.*

The results obtained when the correlation parameter was equal to d = 1 show that with an increasing inspection coverage the difference between the cumulative distribution functions of the real and found maximum defects become smaller (see Figure 3.2 b). The red curve representing the distribution of maximum sizes of inspected points indeed approaches the blue one illustrating the real maximum defects distribution. Similar inferences can be gathered when looking at the histogram graph – Figure 3.2 c, illustrating the differences between the real maximum defects and the maximum of those inspected. One can observe that with the 0.7 inspection coverage the histogram is concentrated around zero, what means that in most cases the maximum defect was recorded (found) during inspection process.

The so-called unreliability function of the regular inspection scheme is presented in the Figure 3.2 d. This function is a function of the inspected coverage and is defined as a proportion of the number of wrong decisions (defined at the beginning of this section) among performed simulations. It can be seen that in the considered case, i.e. with d = 1, the

unreliability function is decreasing and reaches a value close to zero for a large inspection coverage (0.8). This can be interpreted as that in the majority of simulations if the critical defect was present on the generated surface, it was also recorded among the inspected points and it further leads to the correct surface classification. The accompanied Table 3.1 shows how the unreliability function was obtained, i.e. shows the number of wrong decisions that was made with a given inspection coverage.

Looking now at the results presented below for the correlation parameter d = 0.5, one can gather similar inferences about the significant influence of the used inspection coverage on the unreliability of the regular inspection scheme. However, here this inspection scheme seems to work (perform) better in terms of a smaller number of wrong acceptance decisions for small inspection coverage. It is because a smaller value of the parameter d introduces more dependency between generated defects' depths what further causes that the corroded surface has more smooth structure.

- *the correlation parameter* d = 0.5

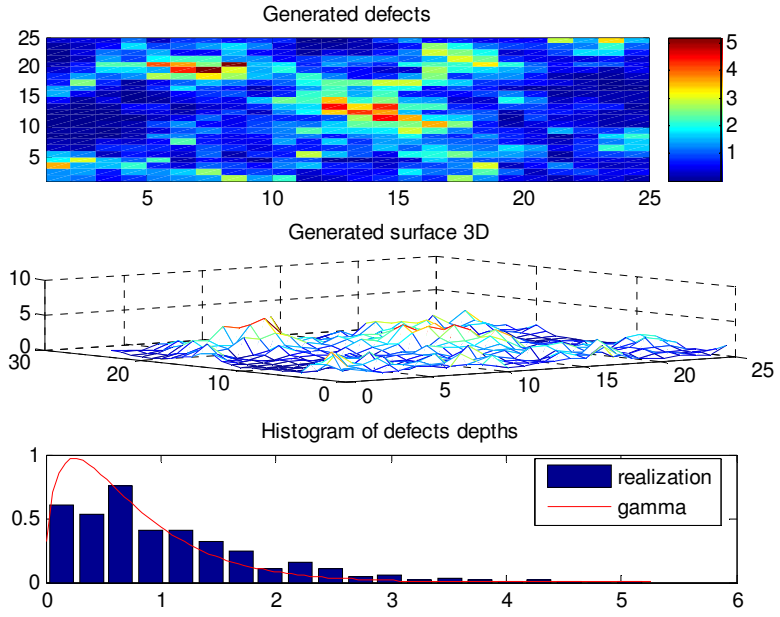

Figure 3.3 a) *The characteristic plots of the corroded surface with the correlation parameter d = 0.5.*

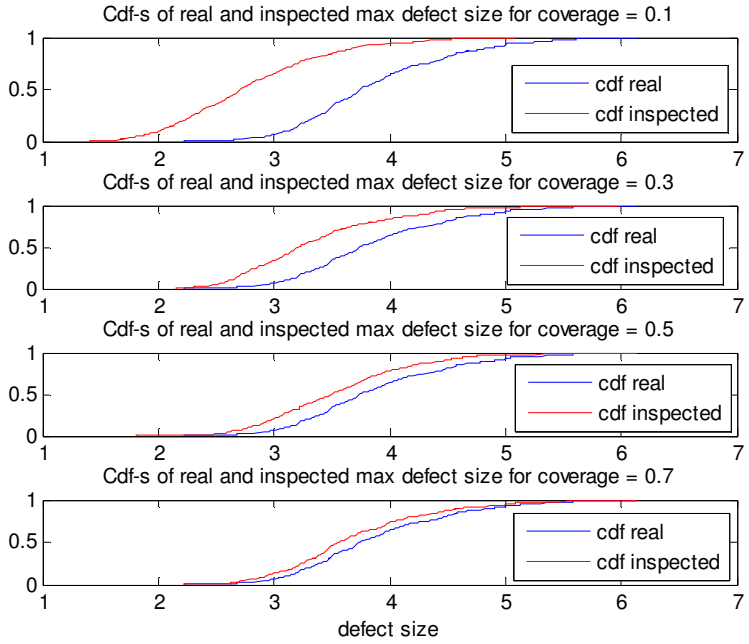

Figure 3.3 b) *The cumulative distribution functions of the real maximum defects and the maximum defects recorded within RIS for different inspection coverage and d = 0.5.*

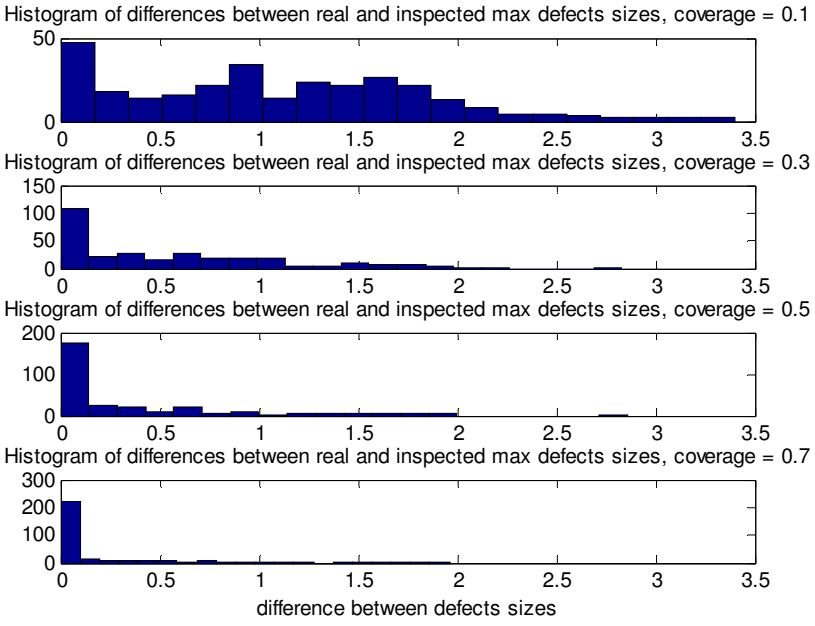

Figure 3.3 c) *The histograms of differences between the real maximum defects and the maximum defects recorded within RIS for different inspection coverage and d = 0.5.*

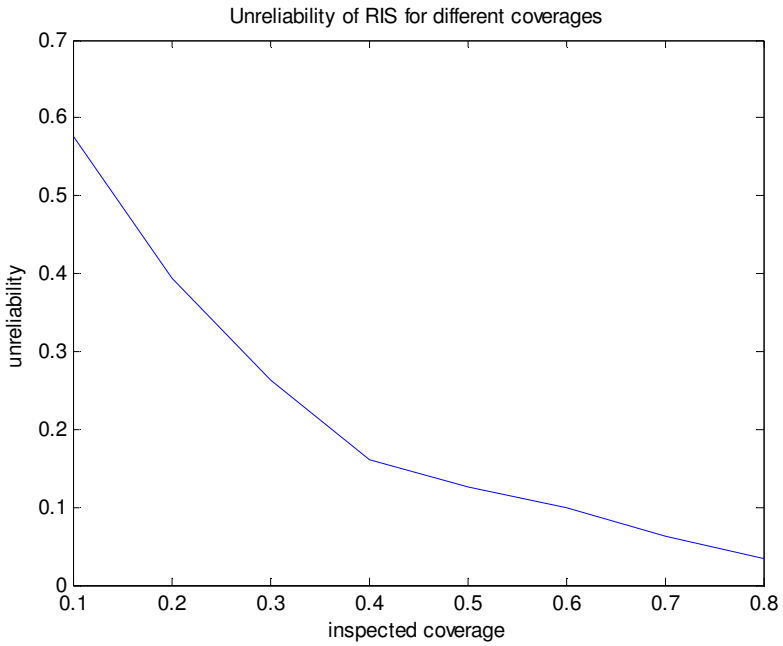

Figure 3.3 d) *The unreliability function of the regular inspection scheme for d = 0.5.*

Correlation parameter d = **0.5**, number of simulations = 300								
Inspected coverage	0.1	0.2	0.3	0.4	0.5	0.6	0.7	0.8
Number of wrong decisions	173	118	79	48	38	30	19	10

Table 3. 2 *The number of the wrong acceptance decisions against the inspection coverage within the regular scheme for d = 0.5.*

Let's now check how the inspection scheme 1 performs when the correlation parameter is equal to d = 0.05. From the subsequent figures (Figures 3.4 b-d) one can conclude that an enlargement of the inspection coverage does not bring so significant improvement in the performance of the considered scheme as it was in the previous cases (for d = 1 and d = 0.5). Moreover, one can see that the inspection of only 30 % of the total surface leads to reasonable inspection results. Concretely, in the majority of cases the maximum defect was recorded among inspected points. As a result, more extended inspection seems to be redundant and will be only connected with higher expenses.

Looking now at the values of the unreliability function (Figure 3.4 d) and the values gathered in the accompanied Table 3.3, one can see that for all inspection coverages used, RIS performs well resulting in at most 10 % (see the number of wrong decisions for the smallest inspection coverage, i.e. equal to 0.1) of wrong surface classifications. Reminding

that to obtain such unreliability with d = 0.5 or d = 1 we had to inspect about 60 % of the considered surface, the latter inference is confirmed. As a consequence, for the inspection of the surfaces characterized by the clustered defects' distribution, the application of the regular scheme with small inspection coverage seems to be reasonable. This will result in inspection plan of good reliable obtained with small inspection effort (measured in terms of inspected coverage).

- *the correlation parameter* d = 0.05

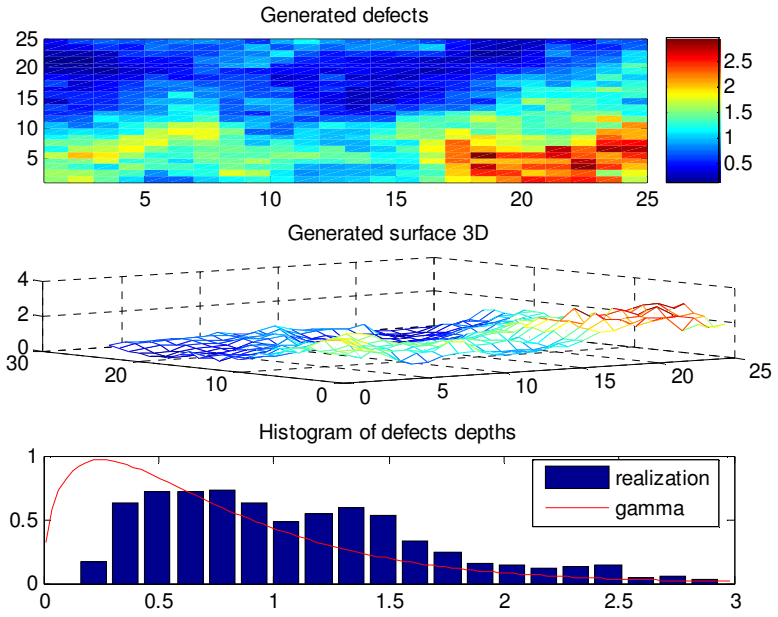

Figure 3.4 a) *The characteristic plots of the corroded surface with the correlation parameter d = 0.05.*

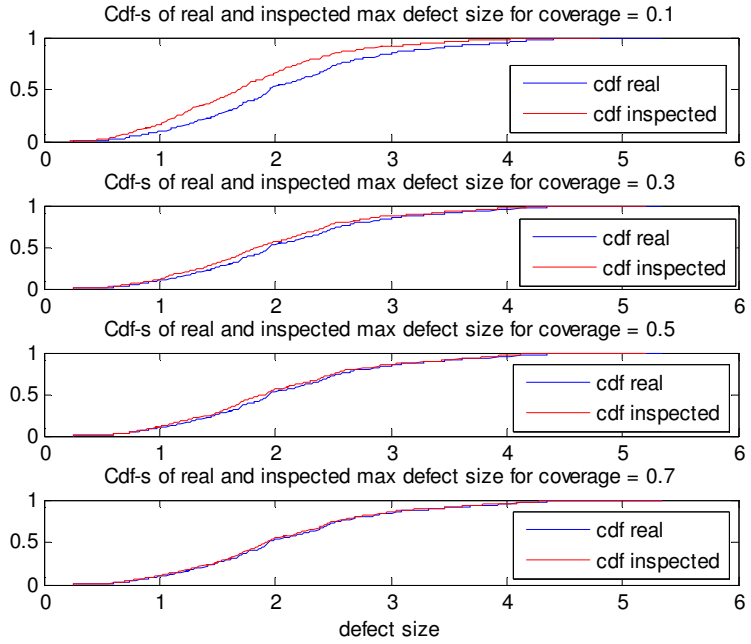

Figure 3.4 b) *The cumulative distribution functions of the real maximum defects and the maximum defects recorded during RIS for different inspection coverage and d = 0.05.*

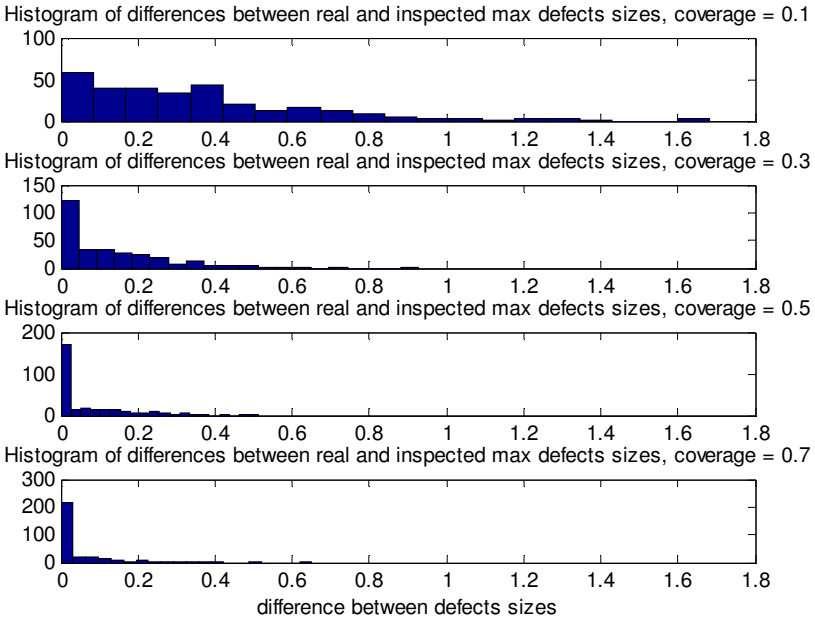

Figure 3.4 c) *The histograms of differences between the real maximum defects and the maximum defects recorded during RIS for different inspection coverage and d = 0.05.*

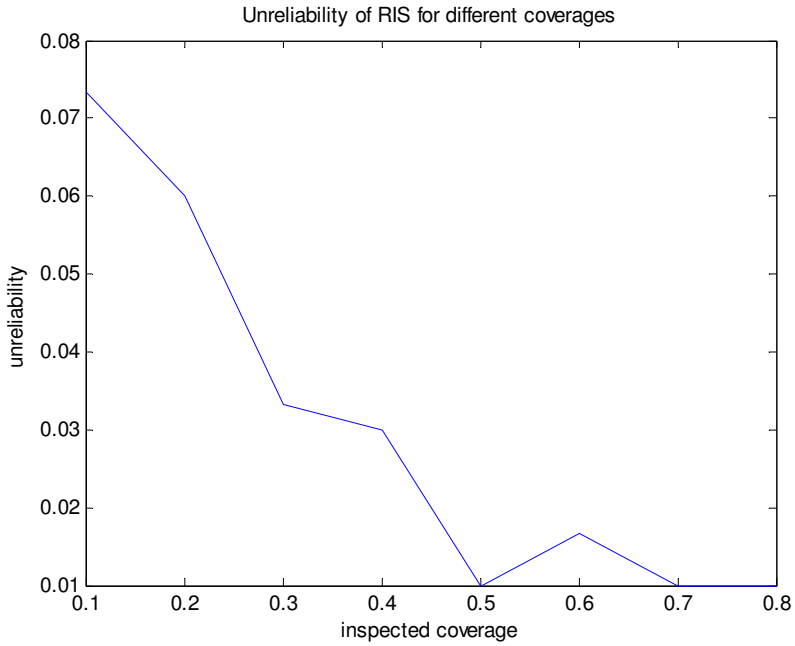

Figure 3.4 d) *The unreliability function of the regular inspection scheme for d = 0.05.*

Correlation parameter d = **0.05**, number of simulations = 300								
Inspected coverage	0.1	0.2	0.3	0.4	0.5	0.6	0.7	0.8
Number of wrong decisions	22	18	10	9	3	5	3	3

Table 3. 3 *The number of the wrong acceptance decisions against the inspection coverage within the regular scheme for d = 0.05.*

Simulation settings of the regular inspection scheme for corrosion surfaces generated by the Poisson model.

When performing the simulation experiments with the regular inspection scheme and the corrosion surface generated by the Poisson method, the following parameters of this method were fixed:

- the parameters of the Poisson process corresponding to the corrosion initiation process (number of arrivals) : $\lambda = 0.2$ and $q = 2.11$;

- the intensity of the corrosion extension process of the affected points was given by the function ν given in the matrix form $\nu = \frac{1}{5.2} \cdot \text{ones}(k,\ k)$, where $\frac{1}{5.2}$ is the so-called extension factor;
- the probability of the corrosion initiation is assumed to be high, i.e. equal to 1, and the same on the entire surface (equivalent with the homogeneity assumption of the corrosion initiation process). This assumption is expressed in the corrosion initiation matrix SpT = ones(k, k).

Such a setup was made based on [18] were similar model using the Poisson process to simulate the corrosion, is introduced. However, it would be desirable to perform separate parameters estimation for model considered in this report. This would improve its effectiveness and give more realistic model. As it was in [18], it can be suggested to ask the experts' opinion about possible values of these parameters.

It is worth to point out that with $\lambda = 0.2$ and q = 2.11, the Poisson process modeling the arrivals of spots has not stationary increments. In different words, the number of corrosion initiations depends on time. This is a realistic assumption since taking into account the aging process and exposure to weathering conditions of steel structures; it is likely that the number of arrivals grows in time. One more remark concerning chosen parameters should be made. With assumed constant expansion rate of the corrosion process (see function ν) we assume constant purity of the surface which as it often appears is in accordance with reality.

Of course the values listed above were not changed during the carried out simulation analysis. The observations were made at time $Tmax$ = 10 units (measured since the considered surface is made and used). In different words, the maximum time at which the corrosion processes were active was bounded by 10.

The variable parameter was the maximum allowable depth level between neighboring locations, simply denoted by $steps$. Together with this parameter an appropriate value of the critical defect size was fixed for the purpose of analysis. The latter can be explained by the fact that with bigger value of the variable $steps$ bigger (deeper) defects may be generated resulting in different criticality levels. Such dependence is confirmed in the figures with graphical illustrations of generated surfaces.

It is worth to point out that the parameter *steps* has a similar impact on generated surfaces like the correlation parameter d within the gamma model for generating corrosion.

Simulation results of the regular inspection scheme for corrosion surfaces generated by the Poisson model.

Let us start our study from the situation when the parameter $steps$ equals 1 unit. With this setup the corroded surfaces generated by the Poisson technique are rather smooth and the deepest defects reach value of 5 units (see Figure 3.5 b). The latter fact caused that the criticality level (*the critical defect size*) was fixed at 3 units' level.

Analyzing the graphics presented in figures 3.5 b and 3.5 c one can observe the visible, significant improvement of the performance of the regular inspection scheme when enlarging inspection coverage from 0.1 to 0.3. In this case the cumulative distribution function of the inspected maximum defects (red line) is much closer to the cumulative distribution function corresponding to the actual maximum defects (blue line). Similarly, the differences between the real maximum defects and maximum of those recorded during inspections become smaller.

On the other hand, the further coverage enlargement seems to be not necessary since the results gathered during simulation experiments with the coverages bigger than 0.3 look very similar (see appropriate subplots in Figure 3.5 b-c). Therefore when dealing with such surfaces the regular inspection scheme with small inspection areas is worth to apply since it brings reliable and satisfactory results. The latter conclusion can be confirmed by the unreliability plot (Figure 3.5 d) and the accompanied Table 3.4. From there one can draw the inferences that even with only 0.3 inspection coverage it is rather unlikely (number of wrong decisions equals to 0) to wrongly judge considered corroded surface.

- $steps$ = 1, *the critical defect size* = 3

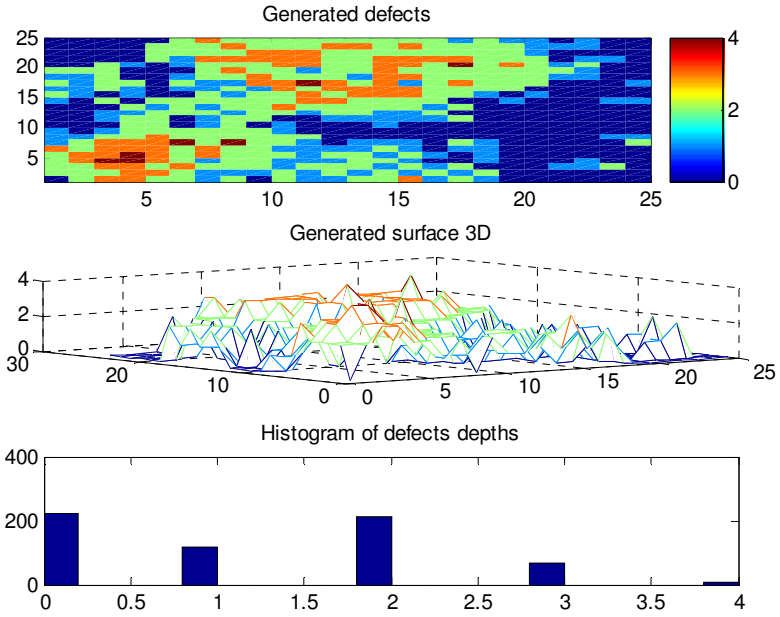

Figure 3.5 a) *The characteristic plots of the corroded surface with steps = 1.*

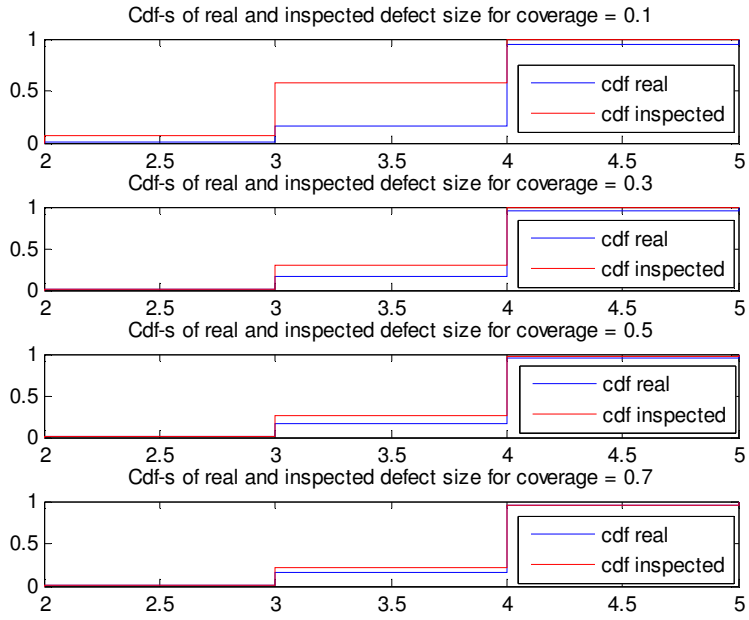

Figure 3.5 b) *The cumulative distribution functions of the real maximum defects and the maximum defects recorded during RIS for different inspection coverage and steps =1.*

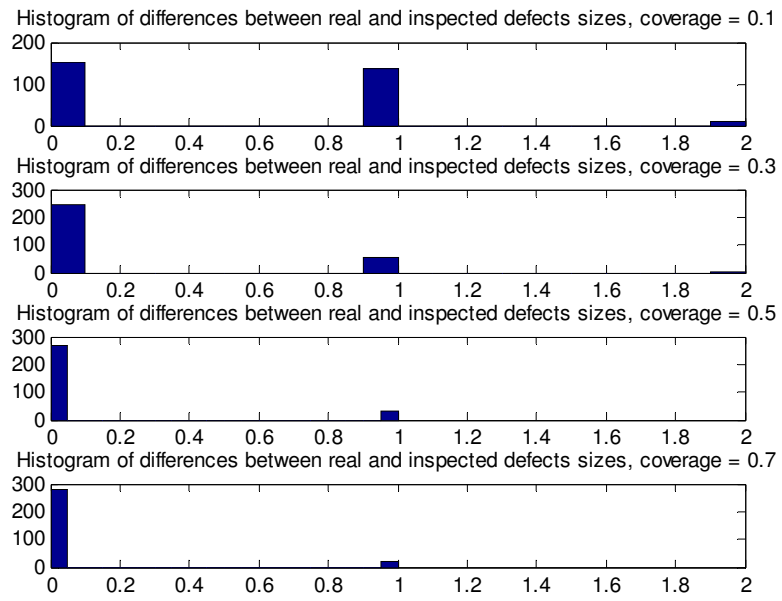

Figure 3.5 c) *The histograms of differences between the real maximum defects and the maximum defects recorded during RIS for different inspection coverage and steps =1.*

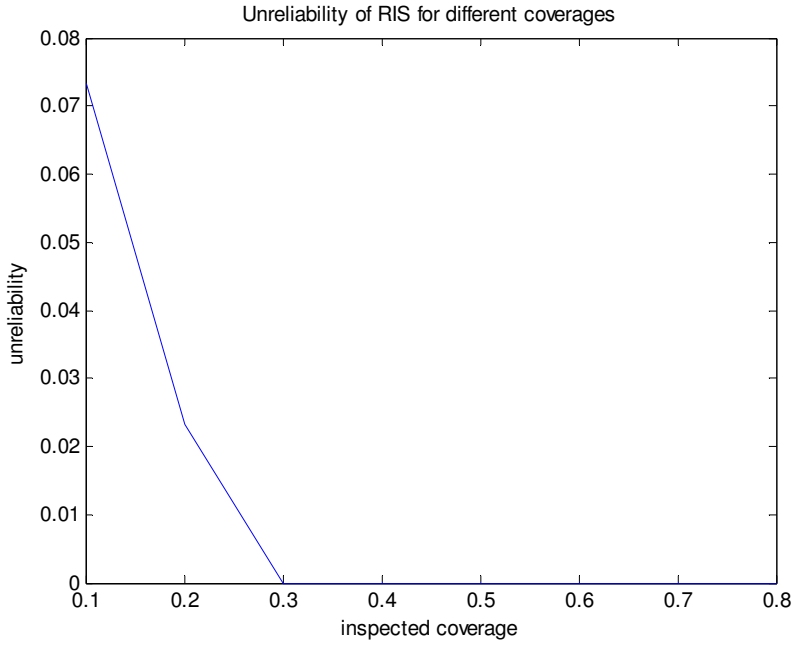

Figure 3.5 d) *The unreliability function of the regular inspection scheme for steps = 1.*

steps = **1**, number of simulations = 300								
Inspected coverage	0.1	0.2	0.3	0.4	0.5	0.6	0.7	0.8
Number of wrong decisions	22	7	0	0	0	0	0	0

Table 3. 4 *The number of the wrong acceptance decisions against the inspection coverage within the regular scheme for steps = 1.*

Increasing the value of the parameter *steps* deeper corrosion spots can be generated by the Poisson technique. Simultaneously, the corroded surfaces have more variable structures and the surface locations seem to be less correlated. Therefore, let's check now the performance of the inspection scheme 1 when the variable *steps* has a value of 2 units and the critical defect size equals 4 units.

- *steps* = 2, *the critical defect size* = 4

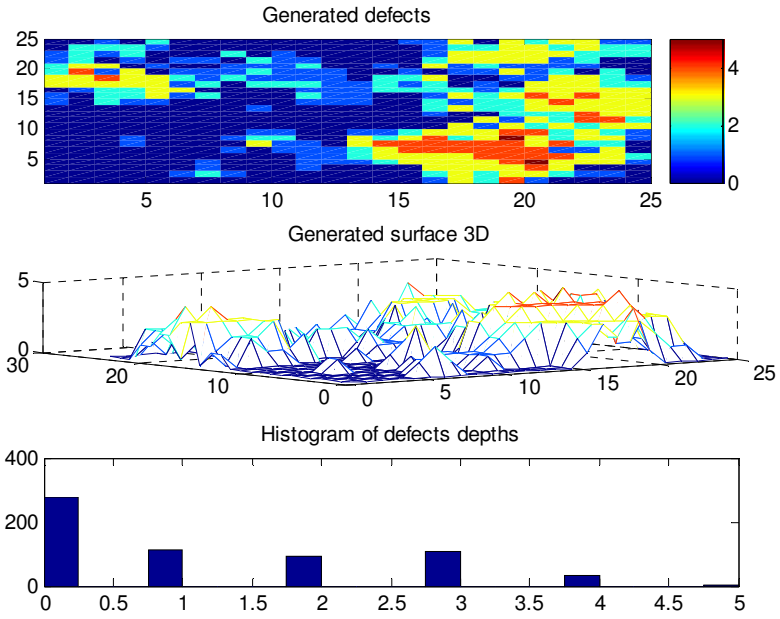

Figure 3.6 a) *The characteristic plots of the corroded surface with steps = 2.*

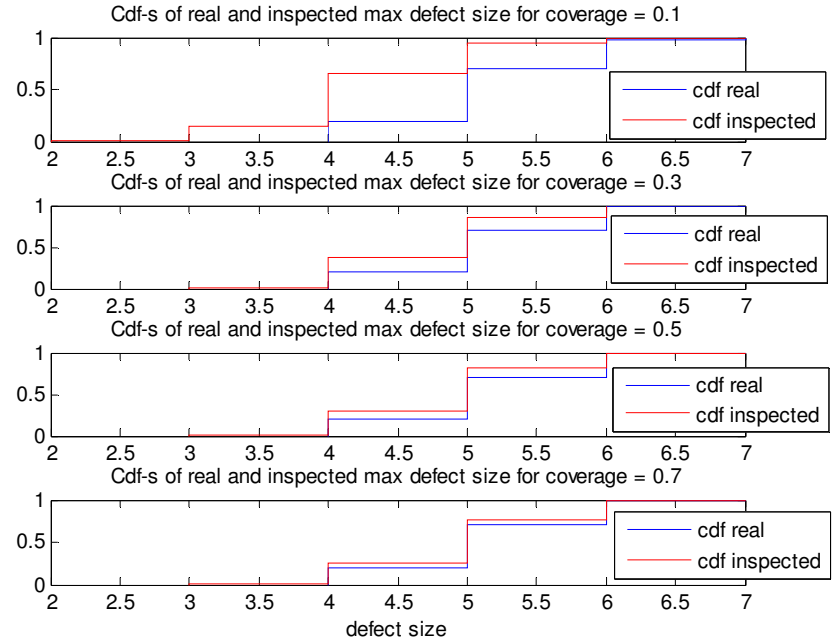

Figure 3.6 b) *The cumulative distribution functions of the real maximum defects and the maximum defects recorded during RIS for different inspection coverage and steps = 2.*

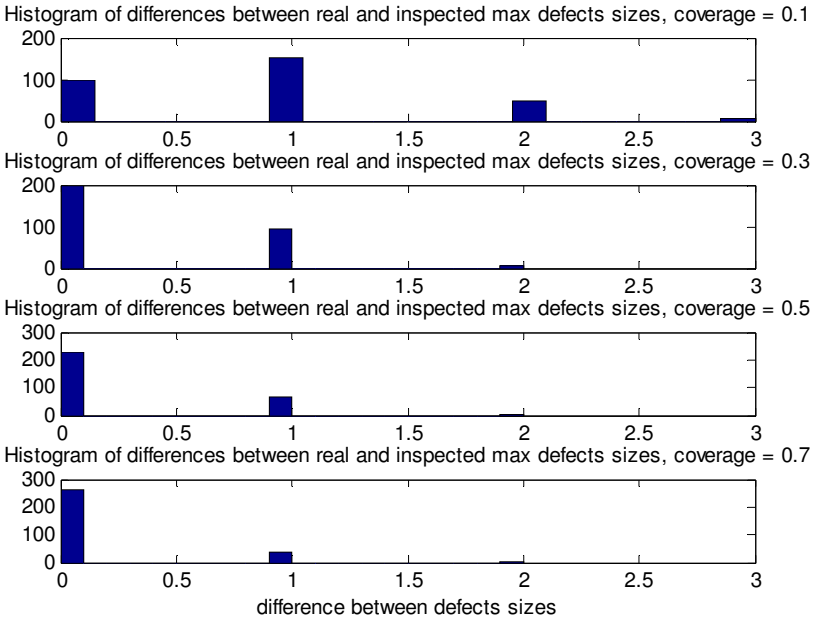

Figure 3.6 c) *The histograms of differences between the real maximum defects and the maximum defects recorded during RIS for different inspection coverage and steps= 2.*

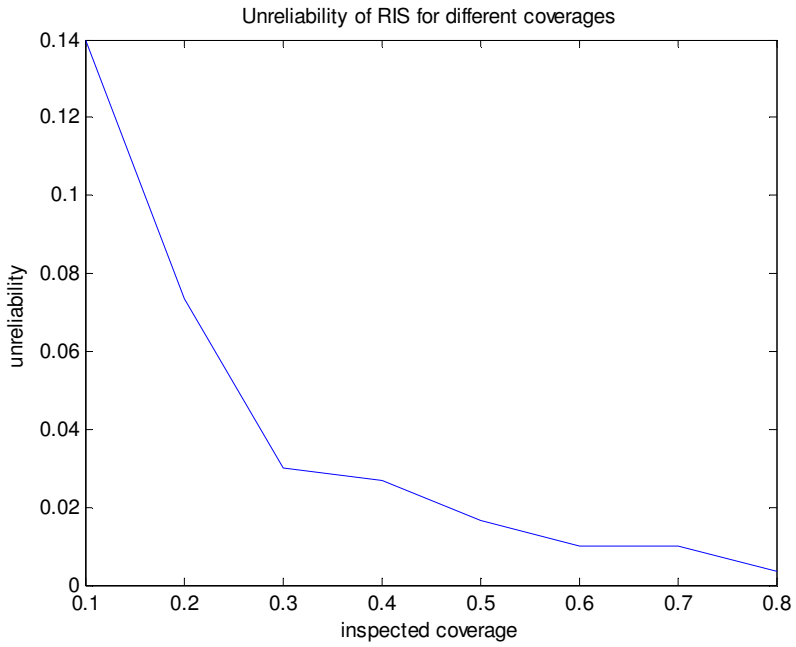

Figure 3.6 d) *The unreliability function of the regular inspection scheme for steps = 2.*

steps = **2**, number of simulations = 300								
Inspected coverage	0.1	0.2	0.3	0.4	0.5	0.6	0.7	0.8
Number of wrong decisions	42	22	9	8	5	3	3	1

Table 3. 5 *The number of the wrong acceptance decisions against the inspection coverage within the regular scheme for steps = 2.*

As one could expect the corroded surface are coarser than in previous case (i.e. when *steps* = 1) and the domain of the defects' depths is wider; that is, it takes values from the interval [0, 6] (see the cumulative distribution plots in the Figure 3.6 b). The results show the improvement of the performance of the regular inspection scheme with bigger inspection coverage. This trend is especially seen for the values of coverage smaller than 0.4 where for each additional 10% of inspection area the number of wrong acceptance decisions becomes two times smaller (see Table 3.5). On the other hand, the inspections of coverages larger than 0.5 reveal almost the same performance of the inspection scheme. Therefore, in this case, the inspection coverage equals 0.5 seems to be the reasonable choice.

It is worth to note that the overall unreliability of the regular inspection scheme is worse than the unreliability obtained when the parameter *steps* was equal to 1 unit. For the smallest inspection coverage, 0.1, the unreliability function takes a value 0.14 while in the previous case oscillated around 0.07. Moreover, in order to obtain faultless surfaces'

classifications the inspection with the 0.3 coverage was sufficient for $steps$ = 1 and to obtain a similar efficiency for $steps$ = 2, the examination of 0.8 surface's area is required (compare Table 3.4 and Table 3.5).

Finally let's look at the results obtained during the simulation experiments when the maximum allowable depth level between neighboring locations ($steps$) had the biggest (analyzed here) value and was equal 3 units. As a consequence, the criticality level was attenuated and fixed at 5 units' level. Of course similar trends regarding larger defects' depths and bigger structure's variability can be observed.

Analyzing the cumulative distribution functions of the real maximum defects and the maximum defects recorded during the inspection procedure, the improvement of the performance of scheme 1 when increasing inspection coverage is clearly visible. In opposite to the previous cases (i.e. when $steps$ = 1 and 2) this trend is also observed for bigger coverages (larger than 0.5). For example, with the inspection coverage equals 0.5 the maximum defect was recorded among inspected points in 220 out of 300 cases while for 0.7 inspection coverage the maximum defect was found in almost all, 280, cases (see the Figure 3.7c with the histograms of the differences between the maximums of real and inspected defects' sizes).

In Figure 3.7 d, the unreliability function shows that in this case the performance of the regular inspection scheme strongly depends on the applied inspection coverage. Moreover, this function has a rather wide set of values with an upper bound equal to 0.27. Therefore, in order to make correct surface classification bigger inspection effort should be involved.

Concluding, when dealing with corroded surfaces having a structure similar to the one presented in Figure 3.7 a) and the criticality at 5 units' level, it is advised to apply bigger inspection coverages (larger than 0.6) when using the inspection scheme 1.

- $steps$ = 3, *the critical defect size* = 5

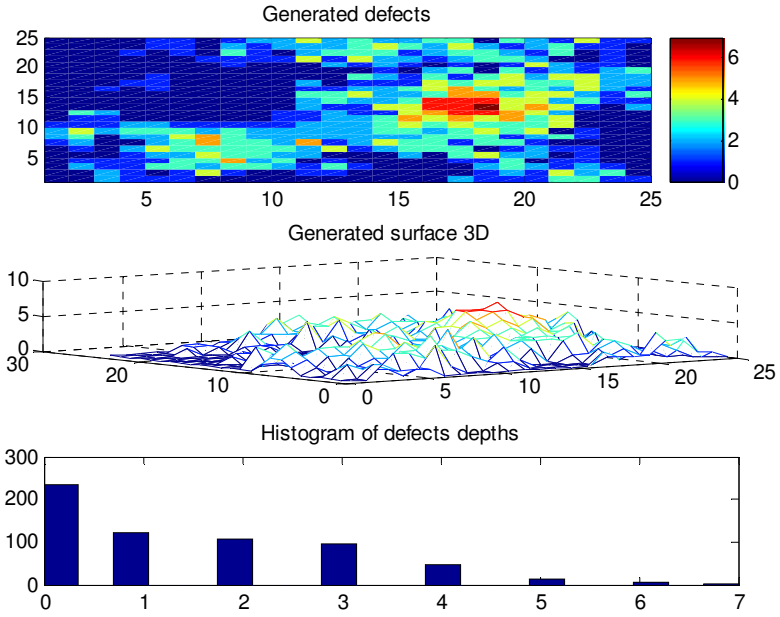

Figure 3.7 a) *The characteristic plots of the corroded surface with steps = 3.*

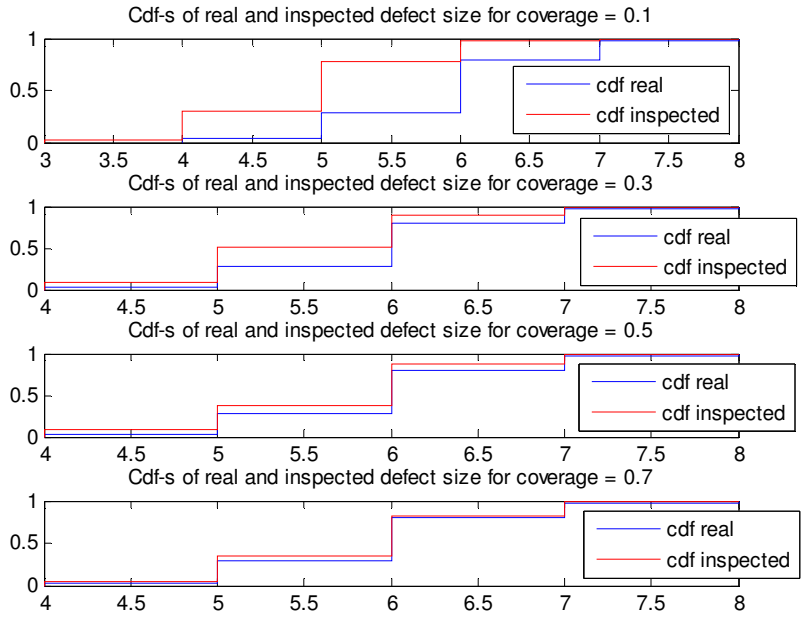

Figure 3.7 b) *The cumulative distribution functions of the real maximum defects and the maximum defects recorded during RIS for different inspection coverage and steps=3.*

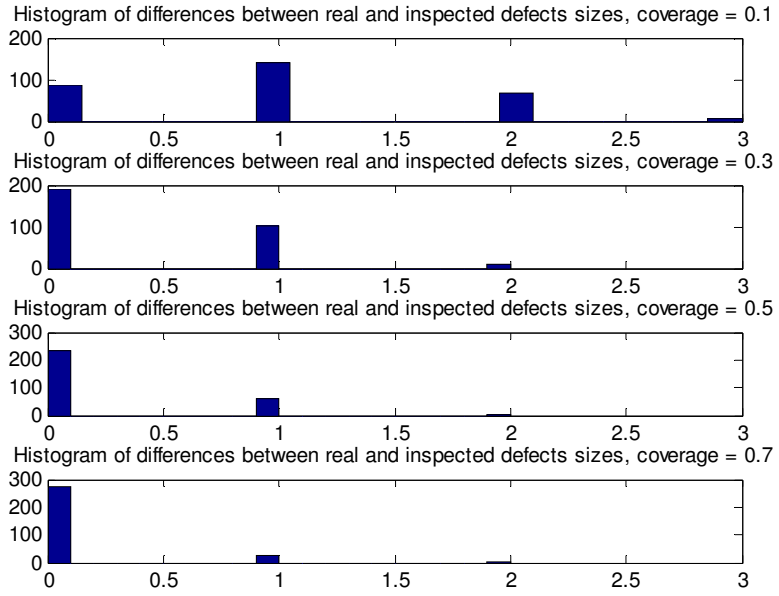

Figure 3.7 c) *The histograms of differences between the real maximum defects and the maximum defects recorded during RIS for different inspection coverage and steps=3.*

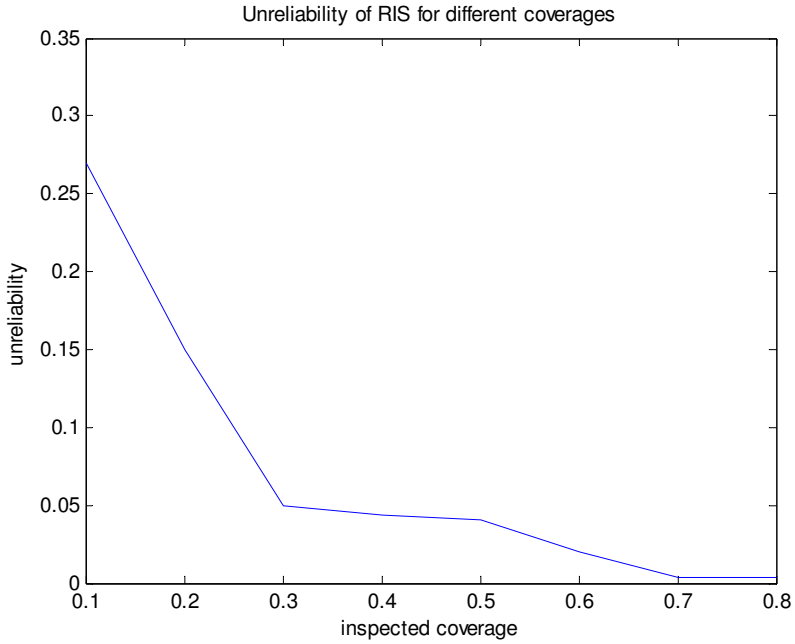

Figure 3.7 d) *The unreliability function of the regular inspection scheme for steps = 3.*

steps = **3**, number of simulations = 300								
Inspected coverage	0.1	0.2	0.3	0.4	0.5	0.6	0.7	0.8
Number of wrong decisions	81	45	15	13	12	6	1	1

Table 3. 6 *The number of the wrong acceptance decisions against the inspection coverage within the regular scheme for steps = 3.*

Conclusions

When the regular inspection scheme was applied for corroded surfaces generated by both the gamma and the Poisson model, the simulations give some kind of overview of its performance under different conditions. Throughout the analysis one could seen that its effectiveness and reliability was dependent on the surface's structure. In some cases the application of small inspection coverage is reliable while in other cases the inspection of a large area was necessary to obtain a correct surface classification. Based on those results, or performing similar simulation experiments using created *Matlab* routines, it is possible to design an optimal regular sampling plan (with the optimal inspection coverage) that will balance the accuracy of the forecasts against the inspection's costs. The costs' analysis was outside the scope of this project; however, it would be desirable to include them in future work.

3.2 Adaptive inspection scheme

The main goal of this paragraph is to introduce and to check the performance of an adaptive inspection scheme (AIS). This scheme (further also called the inspection scheme 2) can be classified as the semi-dynamic sampling scheme and consists of two stages: the first-initial inspection step (the first stage) and the adaptive inspection step (the second stage). It has to be pointed out that the initial inspection makes up a non-dynamic part of this scheme. It is because the initial inspected coverage is fixed (cannot be changed) and the points inspected at this stage are selected according to established pattern. On the other hand, the second part of scheme 2 is dynamic one and its structure depends on (is adapted to) the particular situation (hence the name of this scheme). The detailed description of designed adaptive inspection scheme is given in section 3.2.1.

The inspection scheme 2 is designed for simulation of a sampling inspection of corroded surfaces that are generated using the gamma or Poisson model (described in Chapter 2). However, when analyzing the performance of the adaptive scheme we restrict ourselves to the squared surface S with limited dimension sizes depending on the chosen

corrosion simulation technique. Concretely, for the gamma corrosion surfaces the possible dimensions are k = 25, 30, …, 45, 50 while in the Poisson case they can be equal k = 25, 30, …, 95, 100. Recall that the difference between the possible dimension sizes is due to the fact that the gamma technique with bigger dimensions requires more computational effort (connected with calculation of the correlation matrix). These simulation results are presented in section 3.2.2.

3.2.1 Framework of the adaptive inspection procedure

The adaptive inspection scheme has the following structure:

Step 1 – Initial inspection

An initial inspection examines a number (depending on and proportional to the considered surface dimension) of evenly spread squares of size 2x2, and covers about 10 % of a total surface area. For example, when the chosen surface size equals k = 25, the initial inspection examines 16 squares each of them consisting of 4 grid points. As a result the initial sample size (coverage) equals 64 grid points which is equivalent to about 10% of total surface ($\frac{64}{25 \cdot 25} = \frac{64}{625} = 0.1024$).

A decision about the application of a further (additional) inspection depends on the following two conditions:

Conditions for terminating an inspection at initial stage:

- presence of at least one inspected point with depth deeper than *the critical defect size*. In such situation the examined surface is classified as defective and is no longer inspected.
- no defects of size bigger than *the extension condition* recorded among initially inspected points.

Where:

- *the critical defect size* is a defect size defined in advance by the inspector and depends on the considered surface. Existence of a pit depth of this size is equivalent with component failure (surface is judged as defective) and therefore an additional inspection effort is not required.

- *the extension condition* is the parameter that forces the inspection extension. The pit depth smaller than this value is considered as not dangerous for the considered component, for example, it can be regarded as inherited unevenness of surface. On the other hand, finding the defect bigger than the extension parameter results in additional inspection. Also this parameter is specified by the inspector before the inspection process is carried out. It is worth to point out that the extension condition could be defined based on different kinds of criteria: 1) insignificant defects, which could be based on a mechanical assessment; 2) natural variations not related to the corrosion damage (e.g. related to the fabrication process, producing uneven thickness); 3) the detection limit of the inspection technique used.

Step 2 – Adaptive inspection

When the results of the initial inspection (recorded defect sizes) do not give the basis for its termination at this stage (in other words: the condition for termination inspection at the initial level are not satisfied), an adaptive inspection procedure is applied. The latter process is multiple and complex in the sense that it can be repeated several times depending on the previously obtained results. One level of considered adaptive inspection presents as follows.

Remind that from the model assumption, a first level of the adaptive inspection takes place if among the initially inspected points no pits deeper than the critical defect size were recorded and at least one of these points has a depth greater than the extension condition. Then, all 'neighbors' of points with depth greater than the extension condition are inspected and their depth is recorded. After this procedure a decision about further action, that is whether to stop inspecting or to perform the next adaptive inspection, is made regarding the following three conditions.

Conditions for terminating inspection after the additional inspection stage are:

- presence of at least one additionally inspected point with the depth deeper than *the critical defect size*. In such situation the examined surface is classified as defective and no longer inspected and maintenance is planned.
- no defects of size (depth) bigger than *the extension condition* were recorded among additionally inspected points.
- the totally inspected coverage, i.e. the sum of initially and additionally inspected area, is bigger than the pre-specified *maximal inspected coverage*.

Where:

- *the maximal inspected coverage* determines the percentage of the entire surface that can be examined during the inspection process. This parameter is defined in advance by the inspector and its value may depend upon inspection costs or other influential criterions.

For the definitions of *the critical defect size* and *the extension condition* reader is referred to the paragraph describing the initial inspection step.

If at least one of these conditions is satisfied the overall inspection process is terminated, otherwise another additional inspection is performed. Of course the following inspection stages are carried out in a similar way: that is, the same termination or extension conditions are used. As a result the number of stages of the whole inspection procedure is not specified in advance and strongly depends on the considered surface and the chosen termination criterions.

3.2.2 Simulation

In this section the performance of the introduced adaptive sampling scheme will be verified based on the simulation experiments. During these studies, the different values of *the extension condition* parameter will be examined. It will be shown that its choice strongly affects the dynamic characteristics of the inspection method considered here and as a consequence brings different results. With 'characteristics' we mean the number of additional inspections as well as the overall inspected coverage.
As for the regular sampling scheme, a separate performance analysis of inspection scheme 2 is made for the corroded surfaces generated by the gamma and the Poisson model. Moreover, in order to compare both inspection plans, the same values of the parameters of the corrosion processes are applied.

Simulation settings

The simulation procedure was performed implementing two *Matlab* programs: one working with the gamma and one with the Poisson method. (For details concerning the software description reader is referred to the Appendix C).

The value of *the maximal inspected coverage* parameter was fixed to be equal 1. This setting implies that the adaptive inspection will terminate when a defect of the critical size is recorded or all measured defects have smaller sizes than *the extension condition* level. As a further consequence, the required inspection coverage can be determined.

In this case the simulations were performed 300 times. This number was fixed based on a sensitivity analysis which results are presented in the Appendix 2.

Like it was in the case of the regular inspection scheme, the performance of inspection scheme 2 is mainly judged based on the unreliability function. However, because of the dynamic character of this scheme, in the sense of a not constant inspection size, the average of the inspected coverage is used when determining the mentioned unreliability. The cumulative distribution plots of the real maximum defects and the inspected maximum defects as well as the histograms of the differences between them, allow better performance's analysis.

Simulation results of the adaptive inspection scheme for corrosion surfaces generated by the gamma model.

Let us start the analysis of the performance of AIS applied to surfaces generated by the gamma model. Taking into account, the chosen values of the parameters within the considered method, during the simulation experiments three different values of the extension condition (denoted also as th1) were examined; that is equal to 1, 1.5 and 2 units. Remind also that *the critical defect size* was chosen at 3 units' level.

- *the correlation parameter* d = 1

When considering the corroded surfaces where defects are independently[4] distributed (note that independence is assumed by choosing a high value of the correlation parameter d, here equal to 1), the following simulation results were obtained.

[4] Note that with correlation parameter d equal to 1 there is still some correlation between defects depths at locations close to each other, say within the distance of 4 units. On the other hand, those which share greater distance are uncorrelated (see Figure 2.4).Therefore, when using this value of d we will contend the independence between defects.

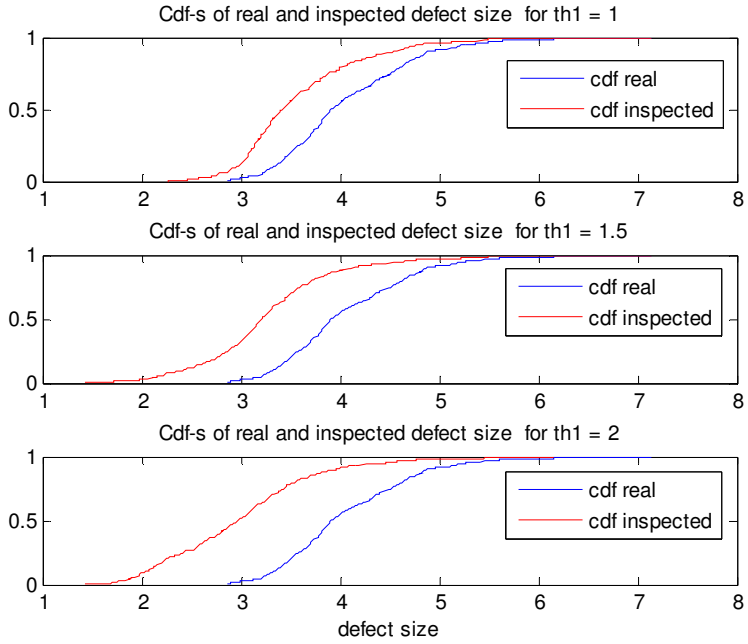

Figure 3.8 a) *The cumulative distribution functions of the real maximum defects and the maximum defects recorded during AIS for different values of the extension condition and d=1.*

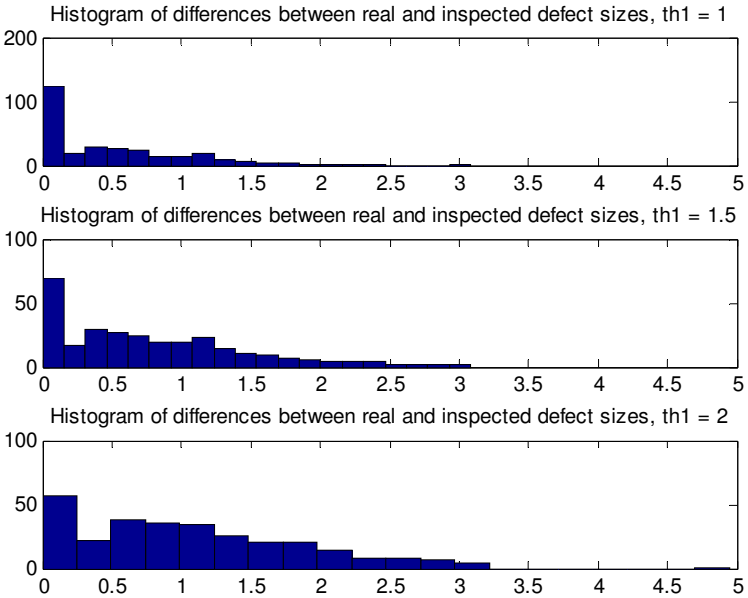

Figure 3.8 b) *The histograms of differences between the real maximum defects and the maximum defects recorded during AIS for different values of the extension condition and d=1.*

Correlation parameter $\hat{d}$ = **1**, *the critical defect size* = 3			
the extension condition	th1 = 1	th1 = 1.5	th1 = 2
Mean inspected coverage	0.225	0.149	0.116
Mean number of additional inspections	1.7433	1.6433	0.87667
Mean inspected coverage when wrong acceptance	0.4012	0.1752	0.1209
Unreliability	0.09	0.287	0.487
Number of wrong acceptances	27	86	146

Table 3. 7 *The simulation results of the adaptive inspection scheme for d =1.*

Looking at Figure 3.8a) and 3.8b), one can observe that when the extension condition equals 1 unit, the adaptive inspection gives more reliable information about the defect distribution, than when choosing this value to be equal to 1.5. The cumulative distribution functions of the real maximum defect (blue lines) and the inspected maximum defect (red lines) are more close to each other in the first case. However, it has to be pointed out, that the mean inspected coverage is about 8% higher for the smaller value of the extension condition (see Table 3.7 above). Therefore, one can intuitively expect better performance of AIS when its driving parameter equals 1 than when it equals 1.5. Indeed, the values of the unreliability function presented in Table 3.7 confirm this. More precisely, the un-detection probability obtained in the first case, 0.09, is about three times smaller than in the second case, i.e. 0.287.

On the other hand, the same table shows that with the further increase of the value of the extension condition, i.e. when it is equal to 2 units, the average inspected coverage does not change a lot. The difference between the latter value within the adaptive inspection with th1 = 1.5 and th1 = 2, is equal to 3%. Thus, even that the increment in this parameter value is the same as it was in previously compared cases (th1 = 1 and th1 = 1.5), the change in the average inspected coverage does not revel the same behavior. However, one can see that the change in the value of the extension condition from 2 to 1.5 causes (on the average) about 3% bigger the total inspection coverage but simultaneously leads to a quite big improvement in the inspection reliability, equivalent with about 20% decrease in the number of wrong surfaces' classifications.

During the simulation experiment the information about the value of the mean inspected coverage when surfaces were wrongly classified, was also recorded. This quantity (see fourth row in Table 3.7) shows that even when inspecting about 40% of the considered surface, an improper acceptance can be done. This is caused mainly by the variable structure of the surface (the assumed independence of the defect distribution). As a result, the information gathered from the inspection does not give us a reliable estimate of the possible defect distribution in the non-inspected part.

For the purpose of the analysis of the inspection cost the number of additional inspections seems to be also an interesting quantity [5]. It is because when the expenses, connected with a setup of the inspection process, are high it is better to find and apply the optimal extension condition parameter that requires less inspection steps and simultaneously brings sufficiently reliable inspection results. In the situation with correlation parameter d = 1, one can see that there is almost no difference in the average number of additional inspections for an extension condition equal to 1 or 1.5; that is, it is 1.7433 and 1.6433, respectively. On the other hand, when th1 equals 2, significantly less inspection steps are performed. The latter can be explained by the distribution of the defect depths on the generated surfaces. Looking at Figure 3.2 a) one can see that in this case the defects of smaller sizes, say not bigger than 1.5, are more likely to being observed than those greater than 1.5. As a result, when choosing the extension condition parameter equal to 2, more rarely the defect of this size will be recorded among initially inspected points causing earlier termination of the inspection process.

Figure 3.8c) presenting the unreliability plots of inspection schemes 1 and 2 allows the comparison of their performance. It can be clearly seen that for the same inspection coverage, the adaptive sampling scheme gives more reliable results than the regular inspection scheme. The red plot, corresponding to the unreliability of AIS, lies below the blue curve that illustrates the unreliability of RIS. For example, one can see, that in order to get a (good) reliability equal to 0.1, it is necessary to inspect in average about 22% of the surface area when applying the adaptive scheme. On the other hand, the same reliability is obtained for the regular inspection scheme after inspecting about 50% of the surface. It has to be pointed out that the actual coverage resulting from AIS may reach even 60% when the wrong decision is made (see Figure 3.8d) but this is approximately an upper bound of the coverage.

[5] Note that the costs analysis is not a goal of this study; however, its performance could be desirable extension of this work.

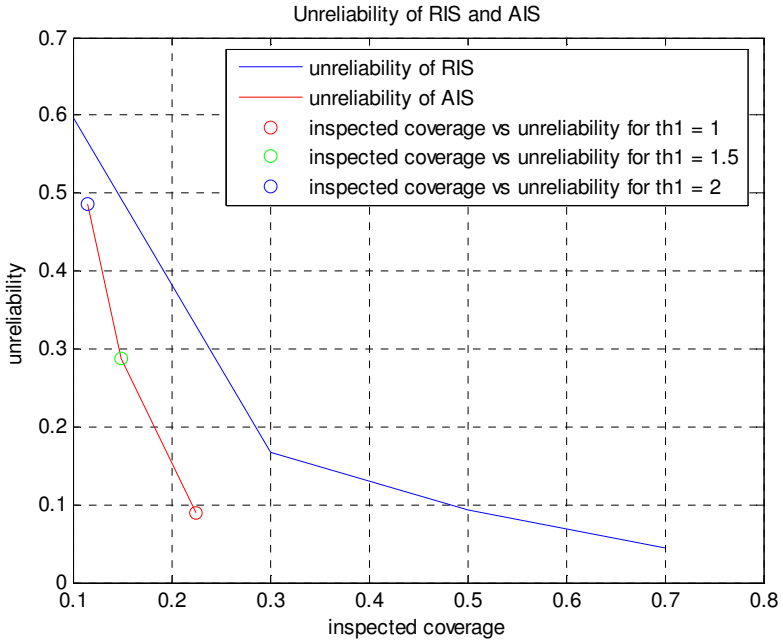

Figure 3.8 c) *The unreliability plots of the inspection schemes 1 and 2 for d = 1.*

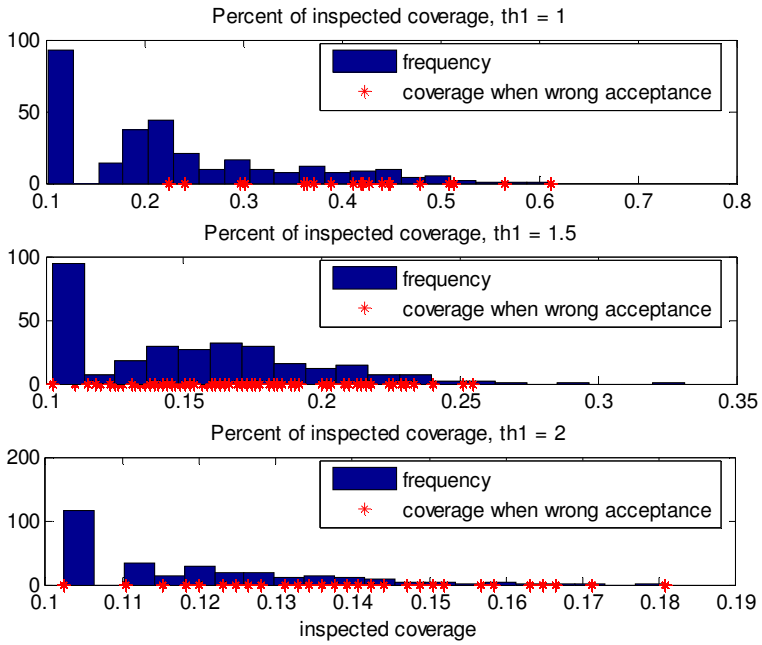

Figure 3.8 d) *The histograms of the inspected coverage within AIS for different values of the extension condition and d = 1.*

One can conclude that when dealing with corroded surfaces that possess similar structure's characteristics to those presented in Figure 3.2a, the adaptive inspection scheme with the extension condition equal to 1 unit is worth to apply. When implementing this inspection plan, reliable inspection results can be obtained with not big inspection effort.

When performing simulation experiments for the adaptive inspection scheme applied for the surfaces generated by the gamma model with the correlation parameter equals to 0.5, we obtain the following results.

- *the correlation parameter* d = 0.5

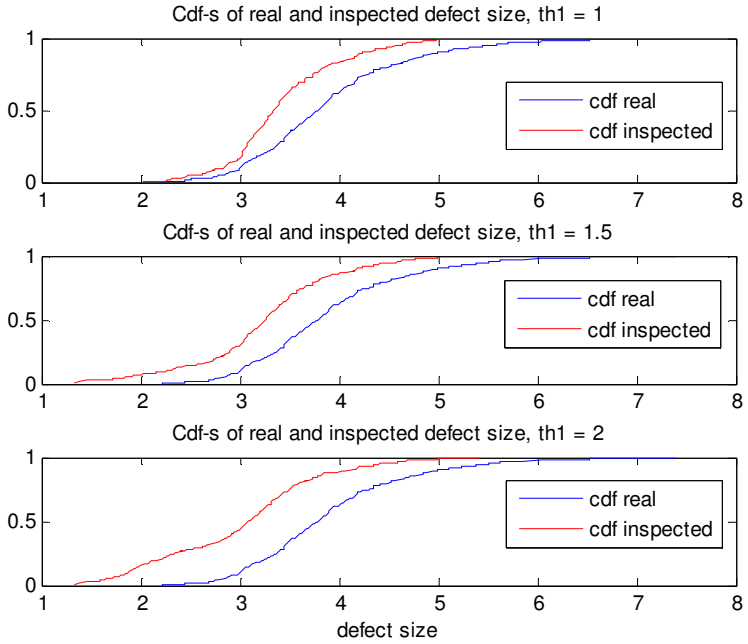

Figure 3.9 a) *The cumulative distribution functions of the real maximum defects and the maximum defects recorded during AIS for different values of the extension condition and d = 0.5.*

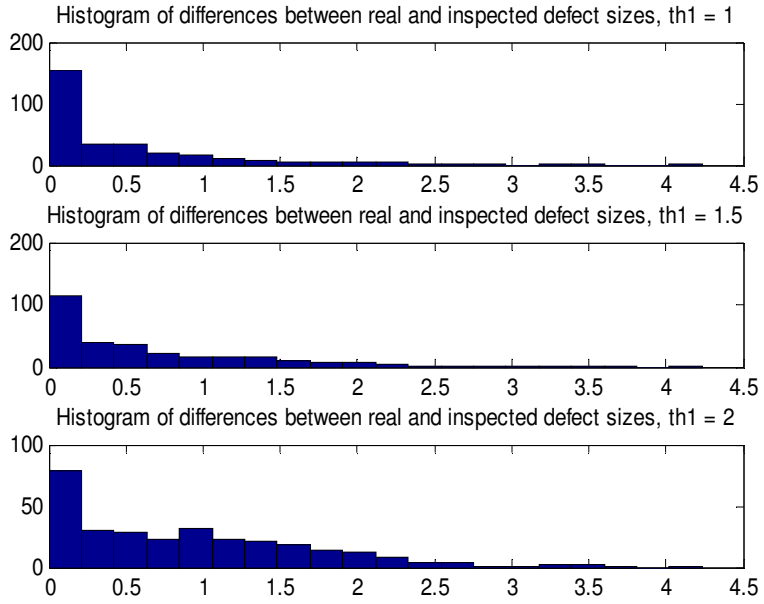

Figure 3.9 b) *The histograms of differences between the real maximum defects and the maximum defects recorded during AIS for different values of the extension condition and d = 0.5.*

Correlation parameter d = **0.5**, *the critical defect size* = 3			
the extension condition	th1 = 1	th1 = 1.5	th1 = 2
Mean inspected coverage	0.223	0.1469	0.1156
Mean number of additional inspections	1.9567	1.5367	1.9567
Mean inspected coverage when wrong acceptance	0.3883	0.1720	0.1210
Unreliability	0.07	0.207	0.343
Number of wrong acceptances	21	62	103

Table 3. 8 *The simulation results of the adaptive inspection scheme for d = 0.5.*

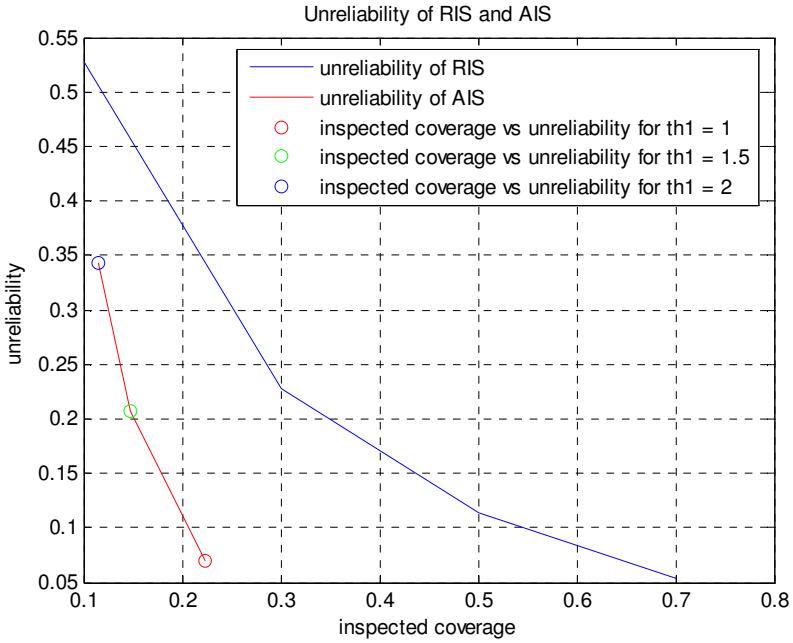

Figure 3.9 c) *The unreliability plots of the inspection schemes 1 and 2 for d = 0.5.*

Analyzing the results presented in Table 3.8 one can observe that the average inspected coverage for the applied extension condition values are similar to those obtained in the previous case, i.e. when d = 1. Here, however, the reliability of the considered adaptive inspection scheme is better, that is, it shows smaller number of wrong acceptance decisions for a given inspection coverage. Again, we can explain this by the surface's structure, which in this case is smoother as the defects are more correlated.

Looking at the Figures 3.9a) and 3.9b), it can be seen that choosing a smaller value of the extension condition parameter it is more probable to record the real maximum defect during the inspection procedure.

When comparing the performance of the inspection scheme 1 and 2, measured in terms of the values of the unreliability function, we can conclude that also in this case the adaptive scheme works better (see corresponding curves in Figure 3.9c above). Therefore, one can expect the general superiority of AIS with respect to RIS. However, in order to fully confirm this statement one more situation has to be analyzed. More precisely, let's check the performance of the adaptive inspection scheme applied to surfaces where corroded spots are highly correlated, i.e. where the correlation parameter is very small, say d = 0.05.

- *the correlation coefficient* d = 0.05

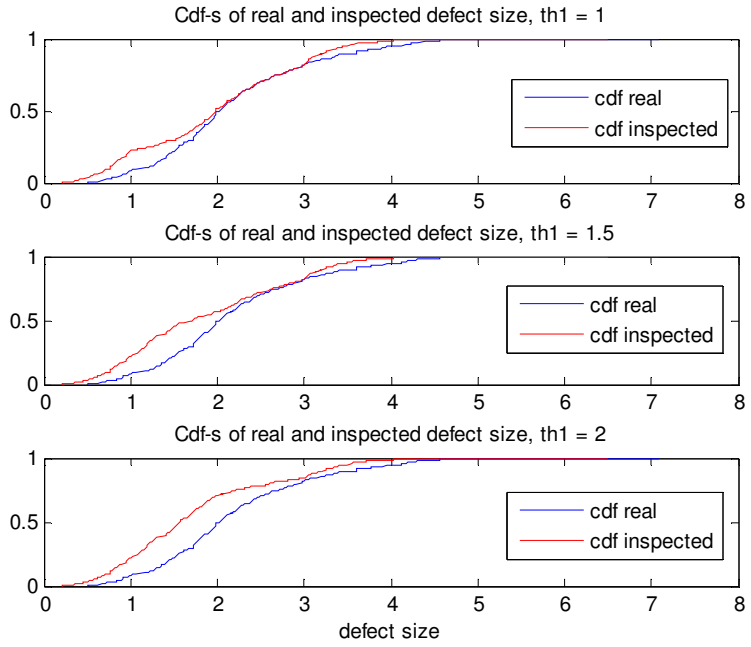

Figure 3.10 a) *The cumulative distribution functions of the real maximum defects and the maximum defects recorded during AIS for different values of the extension condition and d = 0.05.*

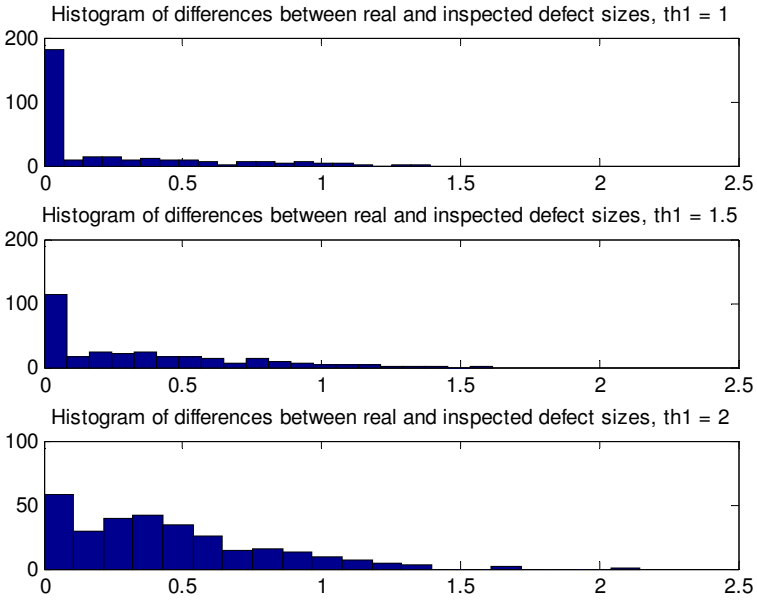

Figure 3.10 b) *The histograms of differences between the real maximum defects and the maximum defects recorded during AIS for different values of the extension condition and d = 0.05.*

Correlation parameter d = **0.05**, *the critical defect size* = 3			
the extension condition	th1 = 1	th1 = 1.5	th1 = 2
Mean inspected coverage	0.3192	0.1688	0.1168
Mean number of additional inspections	4.5067	2.2733	0.6367
Mean inspected coverage when wrong acceptance	0	0.1872	0.1464
Unreliability	0	0.003	0.027
Number of wrong acceptances	0	1	8

Table 3. 9 *The simulation results of the adaptive inspection scheme for d = 0.05.*

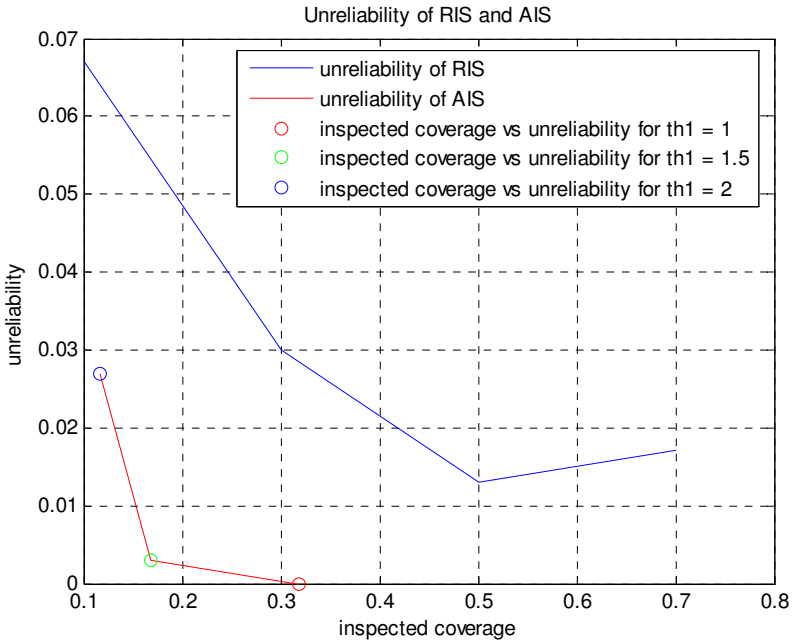

Figure 3.10 c) *The unreliability plots of the inspection schemes 1 and 2 for d = 0.05.*

Figure 3.10c shows that the adaptive inspection scheme gives in general more reliable inspection results. Even that the reliability of the regular inspection scheme has improved significantly (what is strongly connected with the assumed dependency of the defects' distribution), its values are still worst when comparing to the values of the reliability within inspection scheme 2 (see blue and red curves in the figure above, respectively).

Looking at Figure 3.10 b it can be observed that the histogram for th1 = 1 has a thin but long tail, almost as large as for th1 = 1.5 and slightly less than for th1 = 2. This indicates that the adaptive inspection with the smallest value of the extension condition (th1 = 1) brings accurate results: in majority of situations the maximum defect was found (zero difference) and only in small number of situations the difference between the real maximum defect and the maximum defect among inspected points was significant (up to 1.3). Therefore, the magnitude of the difference between maximal defects could be used as another measure of the reliability of inspection scheme.

It is worth to note that for such highly correlated surface structures, the average number of additional inspections is usually higher than when assuming independency between surface's locations (compare appropriate rows of Table 3.7 and 3.9). This fact can be explained in the following way. When the correlation between defect sizes is high, in the case when a defect of size bigger than the extension condition value is found, one can expect that its neighbors will have similar large depths. With a high probability they will justify the necessity of the next inspection step. Therefore, when the setup costs of the inspection procedure are big and one suspects a high dependency between the defects within the considered surface, it is better to enlarge the initial inspection coverage. However, within the adaptive inspection scheme designed here the initial inspection coverage is constant. Therefore, in order to improve its effectiveness and to extend applications' area, an option that allows changing the initial inspection size should be added. Such fully dynamic adaptive sampling scheme that would incorporate the possibility of flexible initial inspection coverage seems to be desirable.

Simulation settings of the adaptive inspection scheme for corrosion surfaces generated by the Poisson model.

It has to be pointed out that due to the discrete nature of the Poisson distribution generated defects have integer sizes. Therefore, only the integer values are reasonable choices for the values of the extension parameter. Because, for example, defects greater than 1 are simultaneously greater than 1.5, hence applying the extension condition equal to 1 or 1.5 will result with the same additional inspection coverage. As a result, when applying the adaptive inspection scheme for the surfaces generated by the Poisson model with parameter $steps$ equal to 1 unit and the critical defect size equal to 3 units, only the values of the extension condition parameter equal to 1 and 2 were reasonable to use.

Simulation results of the adaptive inspection scheme for corrosion surfaces generated by the Poisson model.

When applying the adaptive scheme to inspect the corroded surfaces generated by the Poisson model, the following results were obtained.

- *steps* = 1, *the critical defect size* = 3

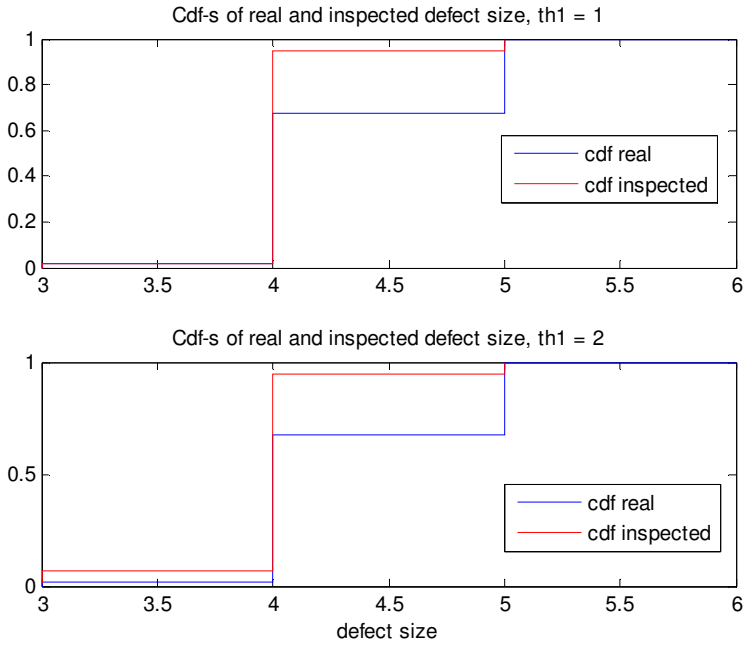

Figure 3.11 a) *The cumulative distribution functions of the real maximum defects and the maximum defects recorded during AIS for different extension conditions and steps=1.*

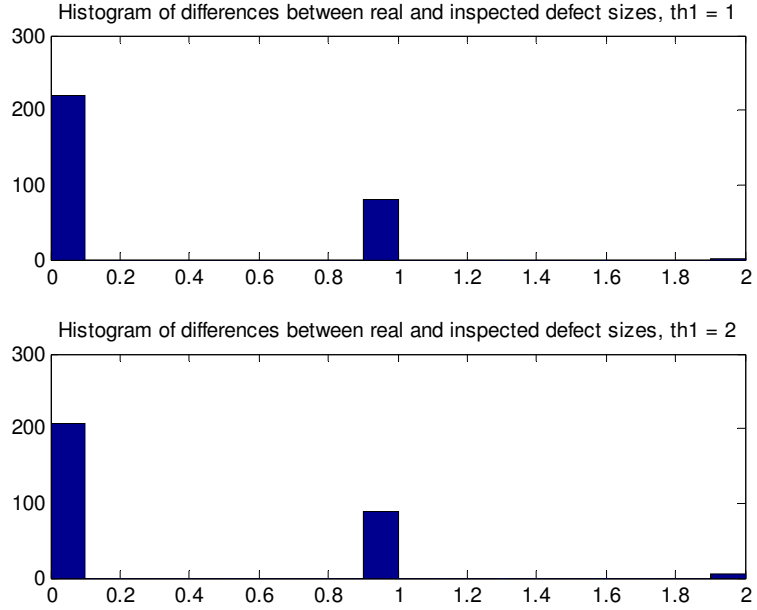

Figure 3.11 b) *The histograms of differences between the real maximum defects and the maximum defects recorded during AIS for different extension conditions and steps=1.*

steps = **1**, *the critical defect size* = 3		
the extension condition	th1 = 1	th1 = 2
Mean inspected coverage	0.1607	0.1127
Mean number of additional inspections	0.4533	0.4100
Mean inspected coverage when wrong acceptance	0	0.1354
Unreliability	0	0.0467
Number of wrong acceptances	0	14

Table 3. 10 *The simulation results of the adaptive inspection scheme for steps = 1.*

Looking at Figure 3.11a) one can conclude that there is almost no difference between the cumulative distribution functions when choosing the value of the extension condition equal to 1 or 2. In both cases, for a small defects' sizes (not greater than 4) the cumulative distribution functions of the inspected maximum defects (red curves) are very close to the cumulative distribution functions of the real maximum defects (blue lines). On the other hand, the same curves differ from each other for bigger values of defects when th1 = 1 as well as when th1 = 2. However, we do not have to worry about these differences since they can be explained in the following way: in performed AIS the critical defect size was chosen to be equal 3 units and a detection of defect of this size caused the termination of the inspection procedure, as a result due to these terminations the bigger defects were not recorded.

The histograms of differences between the real maximum defects and the defects inspected during AIS with the values of th1 equal to 1 and 2 (Figure 3.11b), show similar results. Taking into account the mean inspected coverage and the unreliability of the adaptive scheme for different values of the extension parameter (see third and sixth row in Table 3.10, respectively), using bigger value of this parameter seems to be more reasonable. It is because for th1 = 2 in the majority of situations (about 95 %) the surfaces were classified correctly with inspecting on the average about 11% of surface area. On the other hand, when applying the value of th1 equal to 1 one can obtain 'perfect' scheme reliability (100% of correct surfaces' classifications); however it requires about 5% bigger inspection coverage. Therefore, when assessing the value of the extension parameter of AIS that will be applied for inspecting surfaces similar to the one presented in Figure 3.5a, one advices to include the costs criterion. With severe consequences of failure (high costs of the failure repair) one will prefer to avoid dangerous situations performing more extended inspection. On the other hand, when the inspection procedure is connected with high expenses one could accept a bit bigger risk of failure (due to wrong surface classification) but invests less in the inspection process.

Figure 3.11c) presents the probability that the critical defect size will be not detected during both AIS and RIS procedure for different values of the mean inspection coverage. It is clearly seen that for given inspection coverage the adaptive inspection scheme performs better than the regular scheme, bringing more reliable surfaces' classifications. For example, one can see that with the inspection coverage equal to 0.1 AIS shows the unreliability equal

to about 0.05 while in case of RIS it is equal to about 0.19. (Again, it has to be pointed out that due to the non constant inspection coverages within AIS its reliability is defined as the function of the average inspected coverage. Thus, it may happen that the wrong acceptance decision will be made when the upper bound of resulted coverages was realized. On the other hand, the mean value of inspected coverage for RIS is constant; therefore its reliability can be interpreted in direct way.)

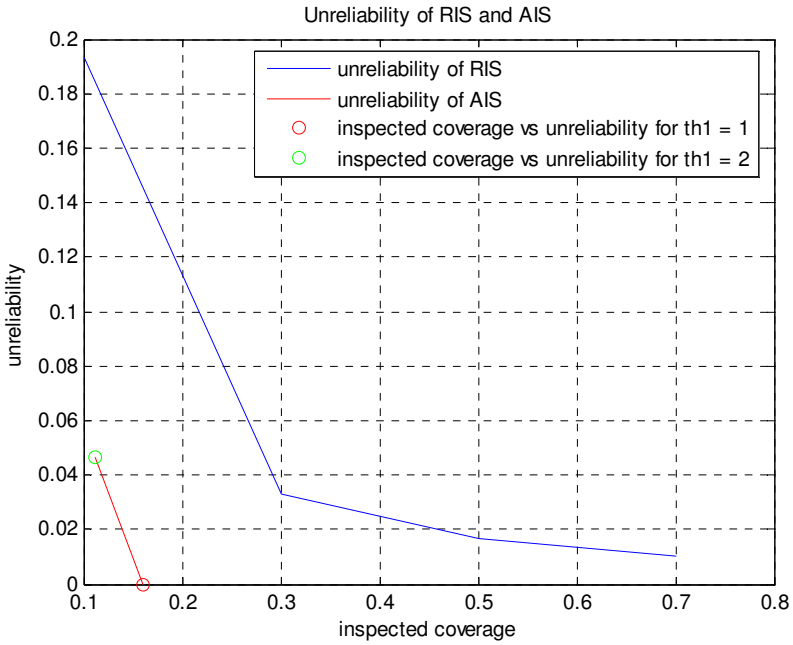

Figure 3.11 c) *The unreliability plots of the inspection schemes 1 and 2 for steps = 1.*

When applying the adaptive inspection scheme with the extension parameter equal to 1, 2 and 3 to the surfaces generated by the Poisson model with parameter *steps* equal to 2, the following results were obtained. (Note that the values of the extension condition were chosen based on the expected defects sizes (see Figure 3.6 a) and they are consistent with the assessed value of the critical defect size that equals 4 units.)

- *steps* = 2, *the critical defect size* = 4

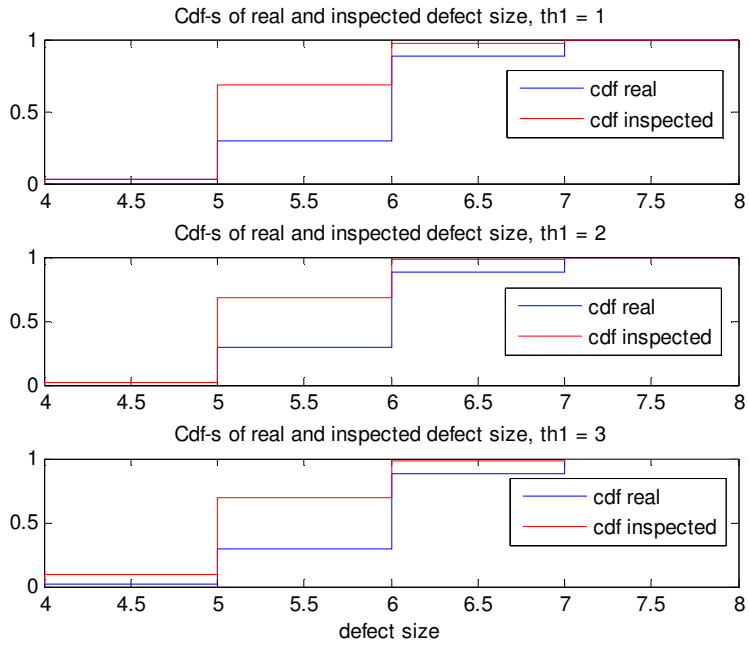

Figure 3.12 a) *The cumulative distribution functions of the real maximum defects and the maximum defects recorded during AIS for different extension conditions and steps = 2.*

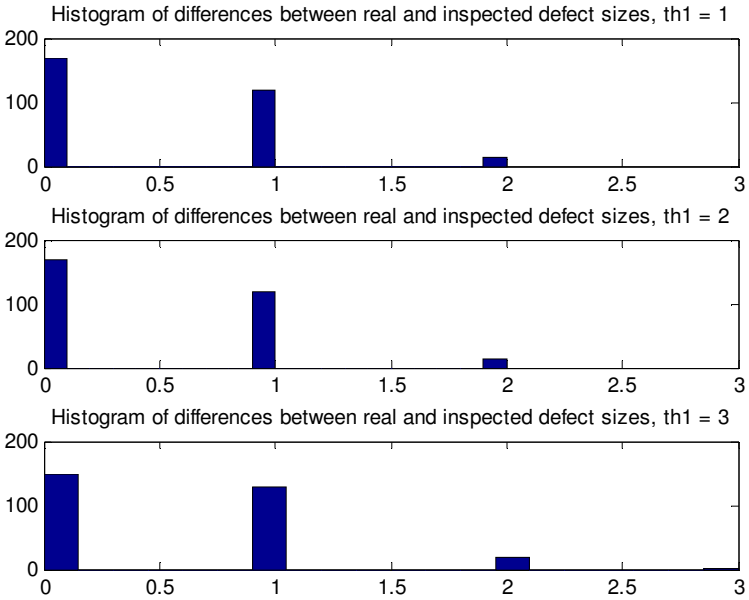

Figure 3.12 b) *The histograms of differences between the real maximum defects and the maximum defects recorded during AIS for different extension conditions and steps = 2.*

steps = **2**, *the critical defect size* = 4			
the extension condition	th1 = 1	th1 = 2	th1 = 3
Mean inspected coverage	0.1871	0.1575	0.1152
Mean number of additional inspections	0.5600	0.6033	0.4567
Mean inspected coverage when wrong acceptance	0	0	0.1342
Unreliability	0	0	0.067
Number of wrong acceptances	0	0	20

Table 3. 11 *The simulation results of the adaptive inspection scheme for steps = 2.*

Table 3.11 shows that for all chosen values of the extension parameter the adaptive inspection scheme brings reliable and satisfactory results. One can observe that with the mean inspection coverage oscillating around 15 % in the majority of situations correct surfaces' classifications were made. Obviously, depending on the applied value of th1 a bit different outcomes of the simulation experiments were recorded. However, when analyzing plots and histograms presented in Figure 3.12a) and 3.12b) these differences appear to be insignificant. It is also worth to note that the mean number of additional inspections that were carried out is equal to 0.5. This means that usually the whole inspection procedure was terminated at its initial stage or only one additional inspection step was required. This fact would stand for the advantage of AIS especially when the costs of setup of the inspection procedure are high.

As one could expect, when comparing the reliability of the adaptive inspection scheme and the regular scheme, the first one presents much better results (see Figure 3.12c).

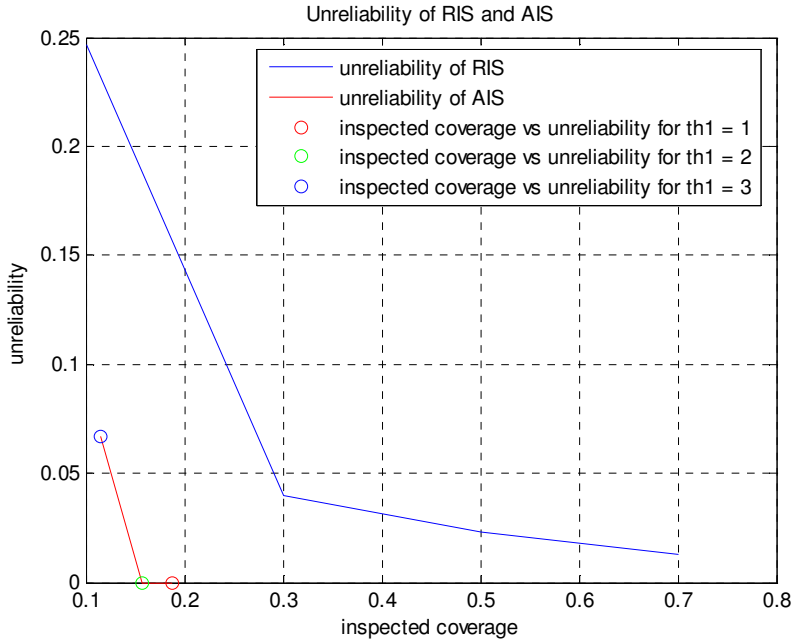

Figure 3.12 c) *The unreliability plots of the inspection schemes 1 and 2 for steps = 2.*

So far we present the simulation results of the adaptive inspection scheme when surfaces generated by the Poisson model had rather smooth structures (i.e. the maximum allowable difference between neighboring locations ($steps$) was equal to 1 and 2). Therefore, let us now check the performance of this scheme applied to the surfaces that have more variable structures that can represent the pitting corrosion process. This process can be modeled by the Poisson technique with a big value of the parameter $steps$. Below, we present the outcomes of the simulation experiment where this value was equal to 3. It has to be pointed out that this setup was made in order to be consistent with the parameters applied when the performance of RIS was analyzed. However, to generate surfaces possessing locations both highly corroded and unaffected by the corrosion, it is advised to choose bigger values of the parameter $steps$ [6]. As it was in previous cases, the analysis was carried out with respect to the extension condition parameter which in this situation was equal to 2, 3 and 4. On the other hand, the value of the critical defect size was chosen to be equal 5 units.

[6] An example of such surface is presented in the Appendix A-5 where the performance analysis of AIS for surfaces representing uniform and pitting type of corrosion is conducted.

- *steps* = 3, *the critical defect size* = 5

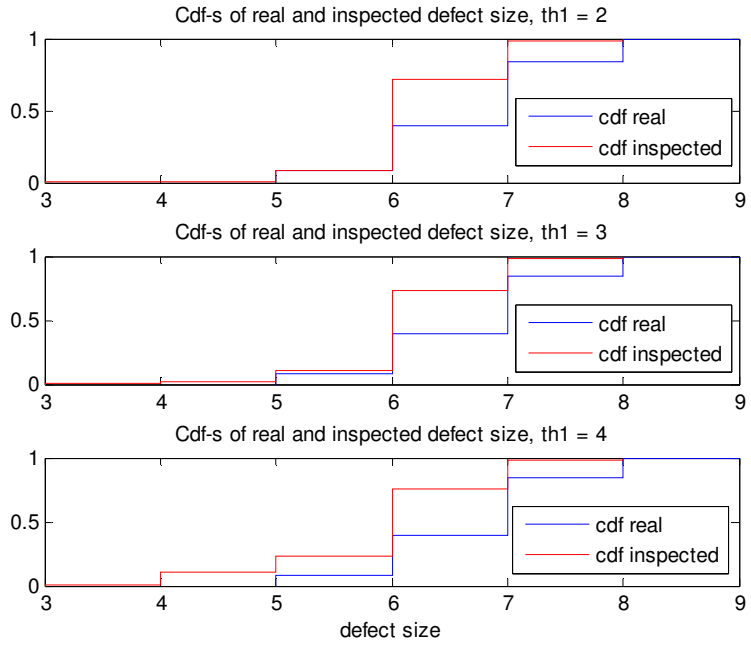

Figure 3.13 a) *The cumulative distribution functions of the real maximum defects and the maximum defects recorded during AIS for different extension conditions and steps = 3.*

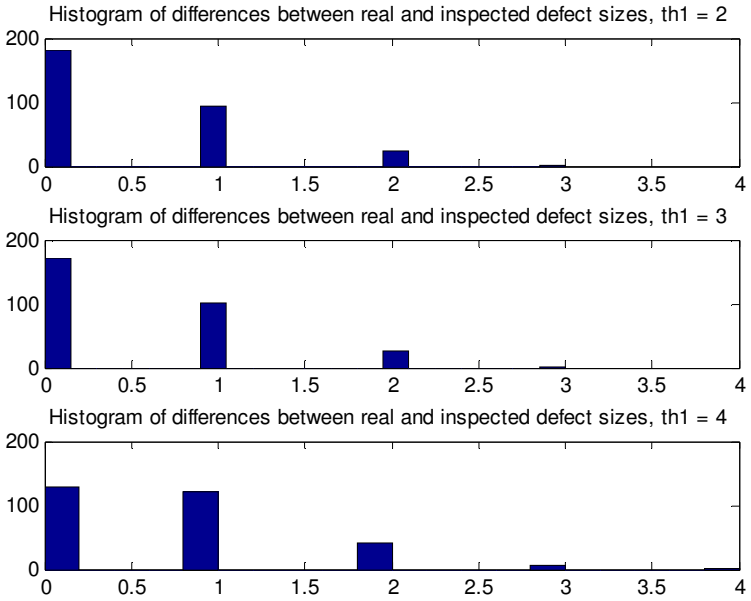

Figure 3.13 b) *The histograms of differences between the real maximum defects and the maximum defects recorded during AIS for different extension conditions and steps = 3.*

steps = **3**, *the critical defect size* = 5			
the extension condition	th1 = 2	th1 = 3	th1 = 4
Mean inspected coverage	0.1968	0.1515	0.1129
Mean number of additional inspections	1.1333	1.0167	0.5533
Mean inspected coverage when wrong acceptance	0.4448	0.2203	0.1211
Unreliability	0.003	0.023	0.15
Number of wrong acceptances	1	7	45

Table 3. 12 *The simulation results of the adaptive inspection scheme for steps = 3.*

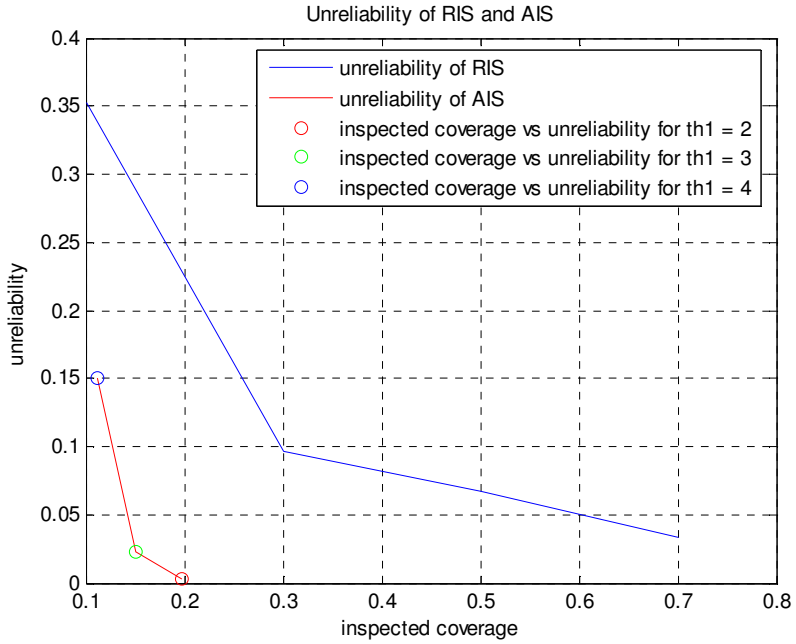

Figure 3.13 c) *The unreliability plots of the inspection schemes 1 and 2 for steps = 3.*

From the plots presented in Figure 3.13a) one can see that the change of the extension parameter mainly causes the differences between the cumulative distribution functions of the real maximum defects (blue curves) and the cumulative distribution functions of inspected maximum defects (red curves) for the small values of defect size. This is especially seen when comparing the first and the third subplot in the mentioned figure, where for th1 = 2, $F_{inspected}(5) = F_{real}(5)$ while for th1 = 4 $F_{inspected}(5) \approx \frac{1}{2} F_{real}(5)$. This means that when applying the adaptive inspection scheme with the extension parameter equal to 4, it is possible to underestimate (based on inspection results) the risk of having the critical defect on the surface. However, when looking at the results gathered in Table 3.12 one can observe that even with this value of th1, the AIS shows good performance bringing

about 15% of wrong surfaces' classifications. The same table shows that increasing the value of extension condition of 1 unit causes the reduction in the mean inspected coverage of about 5%. This obviously will influence the inspection costs that have to balance against the possible risk of un-detecting the critical defect (unreliability).

Figure 3.13c) showing the unreliability plots of both adaptive and regular inspection scheme allows drawing the general conclusion about superiority of AIS.

Conclusions

Within AIS, the extension condition parameter is a driving one and strongly influences the size of the inspected part of the surface. Logically, choosing a small value of this parameter a big inspected coverage will be obtained, and the other way around. On the other hand, surfaces having different dependency structures require different inspection coverages for their appropriate classifications. These two facts imply the dependence between the performance of the adaptive inspection scheme and the applied value of its extension condition.

The analysis has shown that no matter whether one has to inspect the surfaces that are subject to uniform or pitting corrosion process, it is advised to use the adaptive inspection scheme instead of the regular scheme. Of course, this statement could change when including the costs' criterion. However, under assumption about equal unit costs of both schemes, the superiority of AIS seems to be justified.

3.3 Sequential random scheme

A sequential random scheme (SRS) can be classified as a dynamic scheme. The reason for this is that the inspection coverage is not established in advance and strongly depends on considered surface. What is more, within this sampling scheme the initial inspection size (coverage) can be freely chosen by the inspector. This feature stands for the advantage of the sequential random scheme. Remind that in the adaptive inspection scheme even that the total inspection coverage could vary from case to case; the initial inspection size was always equal to about 10%.

In the sequential random scheme points subject to inspection do not follow a regular (fixed) pattern. They are simply drawn randomly from the surface of interest. The number of steps (additional inspections) when this sampling scheme is applied also depends on the particular situation. However, as it will be shown during the simulation experiments, the number of steps in the majority of cases is smaller than in the adaptive scheme. More extended analysis of the properties and performance of SRS is presented in section 3.3.2.

For the inspection sampling scheme described here, we consider two termination criterions. Firstly, the critical defect size with an assumption that a detection of defect bigger than the pre-specified critical defect size will terminate inspection procedure. Secondly, the probability of exceeding the critical defect size for the non-inspected part of the surface. In different words, this criterion (parameter) expresses the maximum risk that one is able to accept that the critical defect is present among non-examined surface locations. The latter implies that the sequential sampling scheme is a risk-based inspection strategy in which the risk is used as a driving criterion when determining optimal inspection coverage. In [12], [13] or [14] one can find more examples of the risk-based inspection models.

It is clearly seen that the value of this exceeding probability is strictly connected with the critical defect size and both parameters have to be assessed by the inspector before initialization of the inspection process.

Before the detailed description of the sequential random sampling plan will be given (see section 3.3.1), the following fact has to be pointed out. The additional sample size of its each inspection step will be calculated (determined) using one of two methods that are based on the extreme value theory. The first one uses the gamma distribution while the second one the generalized extreme value distribution (GEV). The choice of these distributions is motivated as follows.

The generalized extreme value distribution usually reflects the distribution of the minimum or the maximum value among a large set of independent, identically distributed random quantities representing measurements or observations. Therefore has a variety of applications including natural phenomena such as floods, rainfalls, air pollution and (what is the most important for us) corrosion. Other features of this distribution will be pointed out in the subsequent paragraph while for more details regarding theory and applications of GEV reader is referred to [9], [10], [11] or [22].

On the other hand, the reason of applying the gamma distribution is that this distribution was used in the multivariate-gamma model to represent the corrosion depth on each surface location. Therefore, we will assume that the maximum defect among non-inspected parts (locations) of the surface follows also this distribution.

In our corrosion generating models, the random variables representing the defect spots are not independent. However, the lack of independence will be ignored when the size of additional inspection coverage will be calculated using both GEV and the gamma distribution. Therefore, it can be recommended to develop the mathematical model that would incorporate the possibility of including dependence. For example, as it is suggested in [29] or [30], one can use the so-called *extremal index* as a measure of dependence.

It has to be mentioned that this sampling scheme is designed to work only with the surfaces on which corrosion is generated by the gamma model. This can be motivated as follows. The distribution of defects generated by the Poisson model represents the discreet distribution. On the other hand, the gamma and GEV distribution used in sequential scheme

in fitting procedure when determining the additional sample size belong to the family of continuous distributions. Therefore, one could expect more reliable simulation results when investigating the performance of SRS applied for the gamma corroded surfaces.

2.3.1 Framework of the sequential random sampling scheme

The sequential random sampling scheme can be summarized as the following two-steps procedure.

Step 1 – Initial inspection

During the initial inspection some number of surface locations is examined. This number strictly corresponds to and agrees with the initial coverage pre-specified by the inspector. The latter is given as a proportion between inspected points and the total number of surface points. The locations that have to be inspected initially are then selected randomly from the entire surface and form the so-called initial inspection data. Given this initial inspection data, an estimate is made of the distribution of the initially inspected points.

At the next level of the initial inspection within the sequential random sampling procedure, the fitted distribution is created for recorded data points. As it was mentioned before, one can apply the gamma fit or the generalized extreme value fit. The parameter estimation for the gamma fit is done using the maximum-likelihood method. On the other hand, the fitting methods for the parameters of the generalized extreme value distribution are taken from [23], where the method of moments was applied for the parameter estimation. It has to be mentioned that in order to verify whether the recorded observations follow the assumed distribution the Kolmogorov-Smirnov test [7] was performed. However, the statistical uncertainty due to the error inherent in parameters estimated from small samples was not taken into account.

To familiarize ourselves with both distributions the formulas for the cumulative distribution functions of the gamma and GEV distribution are presented below.

Introduced in Definition 2.4 (see Chapter 2) the gamma random variable $X \sim Gamma(x \mid a,b)$, has the following form of the cumulative distribution function:

$$F(x) = \int_0^x \frac{1}{b^a \cdot \Gamma(a)} \cdot y^{a-1} \cdot \exp(-\frac{y}{b}) dy \,, \qquad (3.1)$$

[7] For the description of the Kolmogorov-Smirnov test reader is referred, for example, to [15] or [17].

where $\Gamma(a) = \int_0^\infty t^{a-1} \cdot \exp(-t)dt$. The variable $a > 0$ stands for the shape parameter, while $b > 0$ represents the scale parameter.

On the other hand, the cumulative distribution function of the generalized extreme value distribution with parameters $\xi \in (-\infty, \infty)$, $\mu \in (-\infty, \infty)$ and $\psi \in (0, \infty)$, (corresponding to the shape, location and scale parameter, respectively), is given by:

$$F(x) = \exp\{-[1 + \xi(x-\mu)/\psi]_+^{-1/\xi}\} \tag{3.2}$$

where, $x_+ = \max\{x, 0\}$.

Note that the Gumbel distribution (defined below) arises as a limiting case [8] of equation (3.2) as $\xi \to 0$. It is also worth noticing that the GEV distribution has a bound at $x_0 = \mu - \frac{\psi}{\xi}$, which for $\xi < 0$ stands for an upper bound and for $\xi > 0$ is a lower bound.

Definition 3.1

A random variable X is said to have a **Gumbel distribution** with location parameter $\mu \in (-\infty, \infty)$ and scale parameter $\psi \in (0, \infty)$, if its probability density function is given by:

$$f(x) = \frac{1}{\psi} \cdot \exp\left(-\frac{x-\mu}{\psi}\right) \cdot \exp\left\{-\exp\left(-\frac{x-\mu}{\psi}\right)\right\}.$$

In order to fit these distributions for further inspection planning, the following assumptions are made. Firstly, we assume that the data gathered from a part of the surface that has been covered by the inspection represents the distribution of corrosion within the entire surface. Secondly, we assume that the amounts of corrosion at different surface points are independent [9]. It has to be pointed out that the latter assumption is the most conservative one and gives a fit that is an upper-bound approximation. This is because assuming independence is equivalent to assuming the smallest information about the non-inspected locations, and as a result one can expect all realizations of defects sizes to occur there.

[8] For a simple proof of the statement, the reader is referred to the Appendix B.

[9] When performing simulation some kind of the validation of these two assumptions can be made based on the plots created during the extrapolation procedure (see Appendix C-3 and help files attached to the *Matlab* applications).

These two assumptions imply that the cumulative distribution function of the maximum defect depth for the non-inspected part of the surface is simply the M-element product of the already-found fitted distribution. Such an approach is called an extrapolation procedure. The parameter M counts the number of non-inspected surface locations.

Thus, the following probability can be derived:

$$P\left(\max\{X_1, X_2,..., X_M\} \le x\right) = P\left(X_1 \le x, X_2 \le x,..., X_M \le x\right) = \\ = \prod_{i=1}^{M} P\left(X_i \le x\right) = P\left(X \le x\right)^M \tag{3.3}$$

As a result we obtain the following formula for the distribution of the maximum of M independent gamma variables:

$$F_M(x) = \left(\int_0^x \frac{1}{b^a \cdot \Gamma(a)} \cdot y^{a-1} \cdot \exp(-\frac{1}{b} y) dy \right)^M \tag{3.4}$$

Note that, the maximum of independent, gamma random quantities is no longer a gamma variable. However, it is worth to mention that the maximum of M independent gamma distributed random quantities $X_i \sim Gamma(x|\ a,b),\ i = 1,\ldots,\ M$, belongs to the domain of attraction of the Gumbel distribution.

On the other hand, when assuming the GEV distribution in the extrapolation procedure, the cumulative distribution function of the maximum of M independent variables presents as follows:

$$F_M(x) = F(x)^M = (\exp\{-[1+\xi(x-\mu)/\psi]_+^{-1/\xi}\})^M = \\ = \exp(-\{1+\xi[x-\mu+\psi(1-M^{\xi})/\xi]/\psi M^{\xi}\}_+^{-1/\xi}) \tag{3.5}$$

Hence, the maximum of M independent GEV distributed random variables follows also a GEV distribution with parameters

$$\mu_M = \mu - \frac{\psi(1-M^{\xi})}{\xi}\ ,\ \ \psi_M = \psi \cdot M^{\psi}\ ,\ \xi_M = \xi\ .$$

It is worth to note that GEV distribution of equation (3.4) has the same bound as GEV distribution of equation (3.5), that is $x_M = x_0 = \mu - \frac{\psi}{\xi}$. As a result, for $\xi < 0$ and $M \to \infty$, we have that

$$E(\max\{X_1, X_2, \ldots, X_M\}) \xrightarrow[M \to \infty]{} x_0 .$$

The latter fact means that no matter how large the value of M is, the extrapolation procedure gives us a sensible predictor that does not exceed the upper bound x_0 of the GEV distribution fitted to the data. This fact is of big importance for a reliable defect prediction applied to the corrosion surfaces consisting of a large number of locations. Moreover, Cottis et al. (see [24] and [25]) have found experimental evidence for the use of $\xi < 0$ for the fitted GEV distribution in corrosion applications.

As it was mentioned before, in order to incorporate the dependence between amounts of corrosion at different locations, the extremal index, denoted by θ, can be used. Then, the counterpart of the formula (3.3) presents as follows; [29, 30]:

$$\begin{aligned} &P\left(\max\{X_1, X_2, \ldots, X_M\} \le x\right) = P\left(X_1 \le x, X_2 \le x, \ldots, X_M \le x\right) = \\ &= P\left(X_i \le x\right)^{\theta \cdot M} \end{aligned} \tag{3.6}$$

Note that, when $\theta = 1$, we have independent case and the latter formula is the same as formula (3.3). On the other hand, choosing value of θ in the interval (0, 1) the dependence between defects depths is modeled.

Using one of the cumulative distribution functions (i.e. formulas (3.4) or (3.5)), the probability of exceeding the critical defect size for the non-inspected surface part is calculated.

Similarly to the previous inspection schemes, the definition of the critical defect size reads:

- *the critical defect size* is a defect size defined in advance by the inspector and depends on the considered surface. Existence of a pit depth of this size is equivalent with component failure (surface is judged as defective).

Hence, the exceedance probability is determined as follows:

$$P_{Ex}(\textit{the critical defect size}) = 1 - F_M(\textit{the critical defect size}) \tag{3.7}$$

Conditions for terminating this inspection procedure are:

- when the latter probability (given by formula 3.7) is smaller than the maximum allowable exceedance probability pre-specified by the inspector, the inspection procedure is terminated at the initial stage. This is because extrapolation suggests that the risk of having a critical defect among the non-inspected surface locations is small and acceptable for us. In the opposite case, additional samples (points) are taken resulting in an additional inspection step;
- obviously, when a defect greater than the critical defect size is recorded among the inspected points, further inspection is unnecessary, as the surface is classified as a defective one.

Step 2 – Sequential adaptive inspection

The number of samples (additional locations) that will be examined during the additional inspection procedure is determined in the following way. Based on the extrapolation, one can assess how many additional measurements will cause that the maximum allowable exceedance probability condition will be satisfied. In other words, the following probabilities are calculated:

$$P_{Ex}(\textit{the critical defect size}) = 1 - F_{M-n}(\textit{the critical defect size}) \qquad (3.8)$$

where $n = 1,2,\ldots,M$ denotes number of additional samples.

Then, the sample size is defined as the smallest n for which

$$1 - F_{M-n}(\textit{the critical defect size})$$

is acceptable for us (smaller than the maximum allowable exceeding probability).

Having determined the sample size, n not yet inspected locations are selected randomly. New measurements obtained in this way and those previously recorded are a base for the derivation of a new distribution fit. The latter is determined according to the initially chosen distribution (gamma or GEV) and the current exceedance probability is calculated as in (3.7), but now using the updated cumulative distribution function, say, $F'(x)$. If the exceedance probability is sufficiently small (satisfies the maximum allowable probability condition) or if a defect larger than the critical defect size was found among new inspected points, then the inspection procedure is terminated. In the opposite case, another sample is drawn and a new probability distribution is fitted. The additional inspection procedure can be

repeated several times as long as one of the termination criterions is not satisfied or, alternatively, when the whole surface is inspected.

3.3.2 Simulation

In this section we will present the simulation results when the sequential random scheme was applied for the corroded surfaces generated by the gamma model. Because this scheme allows using one of two distributions when calculating the size of additional sample, two separate performance analysis were made. However, one can also find some remarks comparing both approximation options.

Simulation settings

As it was mentioned before SRS gives a possibility of choosing different initial inspection coverages. This value, together with the critical defect size and the maximum allowable exceeding probability, are three parameters that fully describe applied inspection plan. When the critical defect size and the exceeding probability can be quite easily assessed by the inspector based on available knowledge about the considered surface, the appropriate estimation of the initial coverage is more difficult task. Therefore, the simulation experiments were performed with respect to this parameter. In each experiment the corroded surfaces of size 25x25 were simulated 300 times. As it was in the previous cases, the number of simulation was fixed based on the sensitivity analysis which results are presented in the Appendix A, section 3.

In order to make a reliable comparison between the performance of the sequential random scheme and previously described inspection plans (i.e. RIS and AIS), the same values of the parameters of the gamma corrosion generating model were applied. To remind them, they are listed below.

The parameters of the gamma model within the simulations of the sequential random scheme:

- the shape parameter a = 1.5;
- the scale parameter b = 0.5;
- the $\mathrm{L_p}$ norm parameters p = 2 and q = 0.5;
- the correlation parameter d = 1, 0.5 and 0.05;

Due to the specific character of the sequential random scheme three values of the critical defect size were examined. They were equal to 3, 6 and 9 units. By the specific character we mean its almost perfect reliability (see the simulation results presented in

sections below), which is a result of the assumed rules for terminating the sequential random inspection scheme. Therefore, the influence of the critical defect parameter on the total inspected coverage within SRS was analyzed during the study.

On the other hand, the value of the parameter reflecting the maximum allowable probability of exceeding the critical defect size was chosen based on the assumed gamma distribution function and was equal to 0.01.mNote that with the chosen parameters of gamma distribution, the probabilities of observing a defect deeper than the critical defect size present as follows:

- $P(X_i > \textit{the critical defect size}) = 1 - Gamma(\textit{the critical defect size} \mid a,b) = \\ = 1 - Gamma(3 \mid 1.5,0.5) = 0.0074$
- $P(X_i > \textit{the critical defect size}) = 1 - Gamma(\textit{the critical defect size} \mid a,b) = \\ = 1 - Gamma(6 \mid 1.5,0.5) = 2.5 \cdot 10^{-5}$
- $P(X_i > \textit{the critical defect size}) = 1 - Gamma(\textit{the critical defect size} \mid a,b) = \\ = 1 - Gamma(9 \mid 1.5,0.5) = 7.5 \cdot 10^{-8}$

Simulation results of the sequential random scheme with GEV distribution fit

When applying the sequential random scheme for the corroded surfaces on which the defects are assumed to be independently distributed (the correlation parameter d equal to 1), the following results were obtained.

- the correlation parameter d = 1

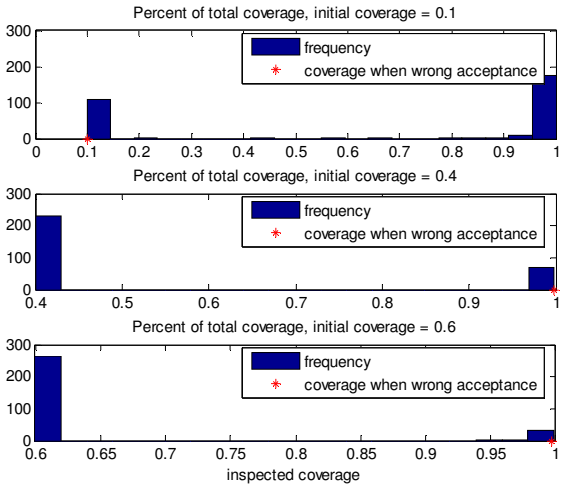

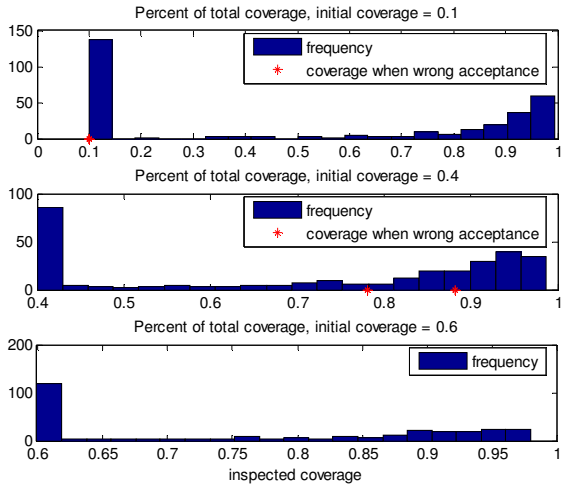

a) the critical defect = 3 b) the critical defect = 6

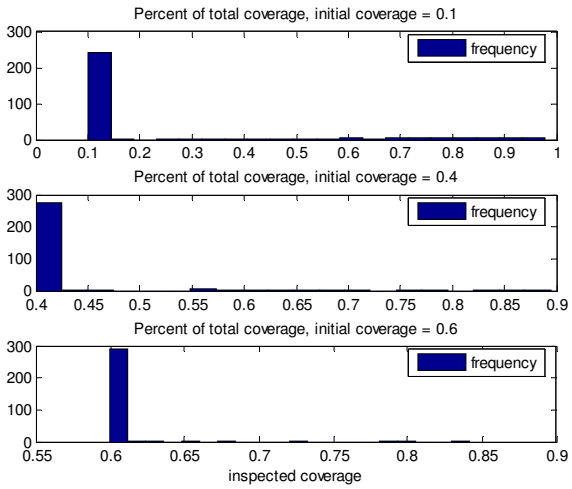

c) the critical defect = 9

Figure 3.14 *The histograms of the inspected coverage within SRS (with GEV fit) for d = 1.*

As it was mentioned before, the characteristic feature of the sequential random scheme is its perfect reliability. However, in order to reach such a good efficiency the inspection of 100 % coverage is required in many cases when the critical defect is equal to 3 and 6. This conclusion can be drawn when looking at Figure 3.14 where the histograms of total inspection coverage are presented. From this figure one can observe that when the criticality level (the critical defect size) is equal to 3 units (see subplot a) after initial inspection of 10% of surface, the examination of its all not-inspected locations is necessary to reduce the uncertainty of having the critical defect. Such histogram of the bathtub shape can be explained in the following way. With assumed defects distribution the probability of observing the defect of size bigger than the critical defect size was close to the fixed exceedance probability. Therefore, either the critical defect was recorded during initial inspection, or if not, the risk (assessed on those initial measurements) of having a large defect in the non-inspected part of the surface was so significant that leads to 100% inspection. On the other hand, it can be seen than when enlarging the initial inspection coverage to 40% or 60%, the overall inspection procedure was in the majority of situations terminated at this stage (see Figure 3.14a and the mean number of inspection steps in Table 3.13a). This fact can be explained that when inspecting more it is more likely to detect the critical defect during the initial inspection process. Therefore, one should expect that this condition was the reason causing the termination.

Figure 3.14c shows that when increasing the value of the critical defect size the inference about termination of the inspection after its initial stage can be drawn. However, in this case, this fact has an opposite explanation. Remind that with assumed parameters of the

gamma distribution, the probability of drawing the gamma number bigger than 9 is very small and equal about $7.5 \cdot 10^{-8}$. Therefore, it is rather unlikely to observe many of defects of this size among initially inspected points. As a consequence, the fitted GEV distribution will also assign a small cumulative probability for observing defects bigger than this value. Finally, taking into account relatively big maximum allowable probability of exceeding the critical defect, 0.01; the extrapolation shows no evidence for further inspection and suggests its termination.

In tables below (Table 3.13 a – c) the detailed simulation results are gathered. It is worth to note that independently of the applied value of the critical defect parameter, the unreliability of the sequential random scheme shows very small value and is near to 0.

Correlation parameter d = **1**, *the critical defect size* = 3			
the initial coverage	Init cover = 0.1	Init cover = 0.4	Init cover = 0.6
Mean inspected coverage	0.6622	0.5388	0.6445
Mean number of inspection steps	1.6533	1.2367	1.1167
Unreliability	0.0033	0.0033	0.0033
Number of wrong acceptances	1	1	1

Table 3.13 a) *The simulation results of SRS (with GEV fit) for d= 1 and the critical defect size= 3.*

Correlation parameter d = **1**, *the critical defect size* = 6			
the initial coverage	Init cover = 0.1	Init cover = 0.4	Init cover = 0.6
Mean inspected coverage	0.51339	0.71502	0.7646
Mean number of inspection steps	1.8133	2.0867	1.8767
Unreliability	0.0133	0.0067	0
Number of wrong acceptances	4	2	0

Table 3.13 b) *The simulation results of SRS (with GEV fit) for d= 1 and the critical defect size= 6.*

Correlation parameter d = **1**, *the critical defect size* = 9			
the initial coverage	Init cover = 0.1	Init cover = 0.4	Init cover = 0.6
Mean inspected coverage	0.20791	0.42026	0.60536
Mean number of inspection steps	1.22	1.09	1.0533
Unreliability	0	0	0
Number of wrong acceptances	0	0	0

Table 3.13 c) *The simulation results of SRS (with GEV fit) for d= 1 and the critical defect size= 9.*

Let us now check the performance of SRS with the generalized extreme value fit distribution applied to the surfaces generated by the gamma model with the correlation parameter equal to 0.5. Also in this case, the analysis focuses on the study of the total inspection coverage value obtained under different criticality assumptions (different values of the critical defect size).

The simulation experiment brought the results presented in Figure 3.15 and Tables 3.14 a-c. Looking at them, one can draw the inferences similar to those obtained in the previous case (i.e. when the correlation parameter d was equal to 1). That is, it can be seen that with weak criticality level condition (the critical defect size = 9), the trend of terminating the inspection procedure at the initial stage is observed (compare subplots c in Figure 3.14 and 3.15). However, when choosing the critical defect equal to 6 and assuming that the surface locations are more correlated (d = 0.5), the size of the coverage that was necessary to inspect during additional inspection steps was usually smaller than in the independent case (compare the mean inspected coverages in Table 3.13 b and 3.13 c). For example, one can see that when applying the initial coverage equal to 0.1, with d = 1 in about 70 situations total surface was finally inspected while with d = 0.5 this situation had place only about 30 times. This is of course connected with bigger surface variability, which causes that the prediction of the defects distribution in non-inspected part is less accurate.

As one could expect, the reliability of the sequential random scheme shows very satisfactory results. In the performed simulation experiment wrong acceptance decisions were recorded only in one case, that is, when the critical defect was equal to 3 (see Table 3.14 a).

- the correlation parameter d = 0.5

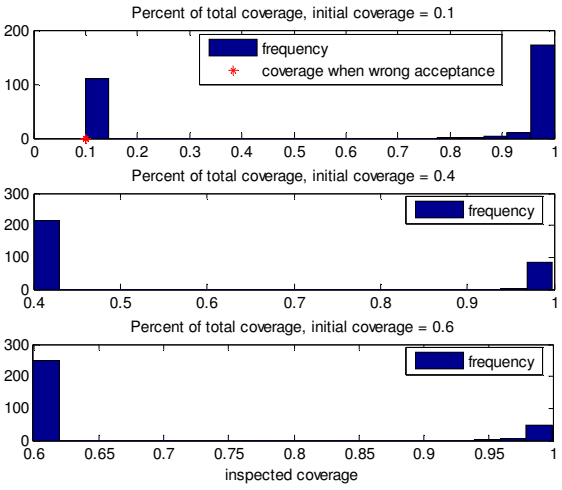

a) the critical defect = 3

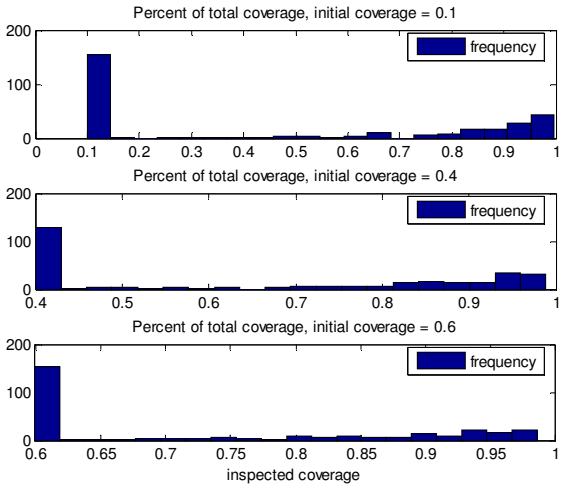

b) the critical defect = 6

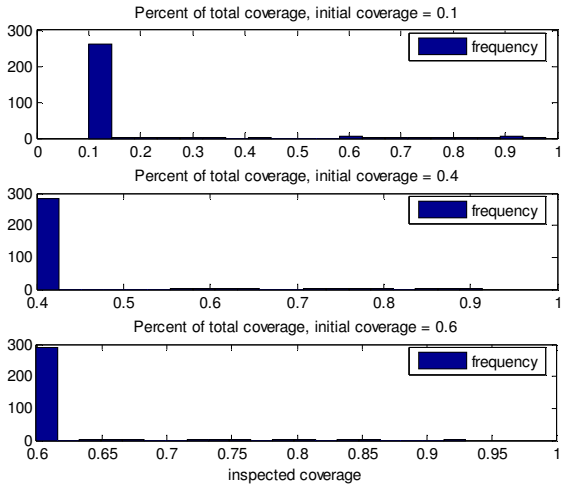

c) the critical defect = 9

Figure 3.15 *The histograms of the inspected coverage within SRS (with GEV fit) for d= 0.5.*

Correlation parameter d = **0.5**, *the critical defect size* = **3**			
the initial coverage	Init cover = 0.1	Init cover = 0.4	Init cover = 0.6
Mean inspected coverage	0.65764	0.56931	0.66771
Mean number of inspection steps	1.6767	1.3267	1.2167
Unreliability	0.02	0	0
Number of wrong acceptances	6	0	0

Table 3.14 a) *The simulation results of SRS (with GEV fit) for d= 0.5 and the critical defect size = 3.*

Correlation parameter d = **0.5**, *the critical defect size* = **6**			
the initial coverage	Init cover = 0.1	Init cover = 0.4	Init cover = 0.6
Mean inspected coverage	0.45436	0.6587	0.73362
Mean number of inspection steps	1.6667	1.8567	1.64
Unreliability	0	0	0
Number of wrong acceptances	0	0	0

Table 3.14 b) *The simulation results of SRS (with GEV fit) for d= 0.5 and the critical defect size = 6.*

Correlation parameter d = **0.5**, *the critical defect size* = **9**			
the initial coverage	Init cover = 0.1	Init cover = 0.4	Init cover = 0.6
Mean inspected coverage	0.16514	0.41737	0.60605
Mean number of inspection steps	1.13	1.0633	1.0467
Unreliability	0	0	0
Number of wrong acceptances	0	0	0

Table 3.14 c) *The simulation results of SRS (with GEV fit) for d= 0.5 and the critical defect size = 9.*

The last step of the performance analysis of SRS (with GEV distribution) is devoted to study the properties of this scheme when is applied to corroded surfaces with highly correlated locations. Recall that within the gamma corrosion generating model, a strong dependence between simulated defects' depths is expressed by the small values of the correlation parameter d. Fixing this value to be equal to 0.05 we obtain the following results.

- the correlation parameter d = 0.05

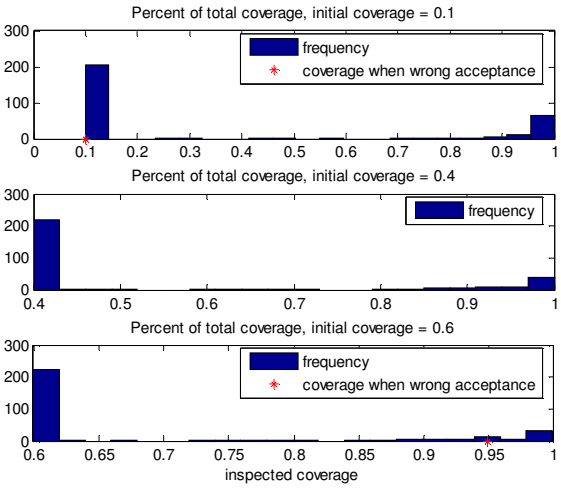

a) the critical defect = 3

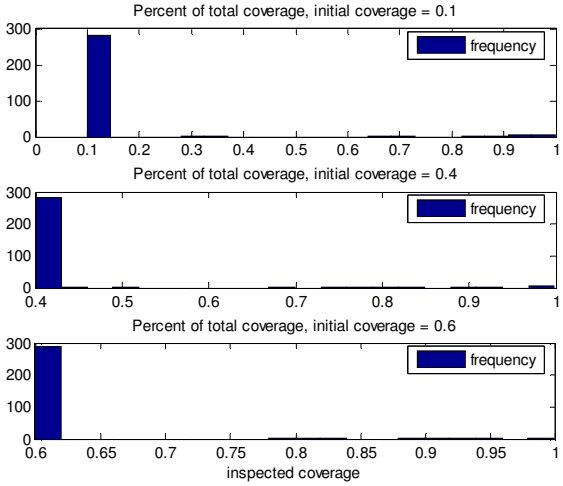

b) the critical defect = 6

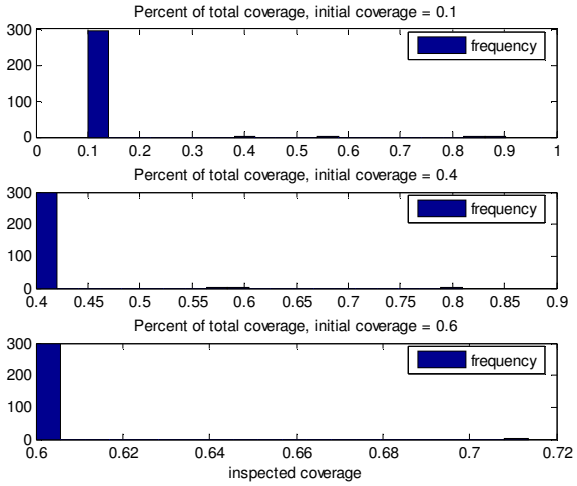

c) the critical defect = 9

Figure 3.16 *The histograms of the inspected coverage within SRS (with GEV fit) for d= 0.05.*

Analyzing the histograms presented in Figure 3.16, it is clearly seen that independently of the value of the critical defect size the majority of the simulated inspection procedures was terminated after the initial inspection. However, for smaller values of the defect size (see, for example, subplot 3.16a) some additional inspections were required, but then the additionally inspected coverage was not as large as in previously examined cases, i.e. with d = 1 and d = 0.5. These results suggest that the course of the sequential random scheme, in the sense of the number of inspection steps and the size of inspected coverage, strongly depends on the properties of the surface. However, the reliability and quality of its results are always maintained on the perfect level (see Tables 3.15 a-c).

Correlation parameter d = **0.05**, *the critical defect size* = **3**			
the initial coverage	Init cover = 0.1	Init cover = 0.4	Init cover = 0.6
Mean inspected coverage	0.35985	0.53862	0.68524
Mean number of inspection steps	1.4267	1.3933	1.3833
Unreliability	0.0067	0	0.0033
Number of wrong acceptances	2	0	1

Table 3.15 a) *The simulation results of SRS (with GEV fit) for d= 0.05 and the critical defect size = 3.*

Correlation parameter d = **0.05**, *the critical defect size* = **6**			
the initial coverage	Init cover = 0.1	Init cover = 0.4	Init cover = 0.6
Mean inspected coverage	0.14616	0.42138	0.61148
Mean number of inspection steps	1.07	1.0633	1.06
Unreliability	0	0	0
Number of wrong acceptances	0	0	0

Table 3.15 b) *The simulation results of SRS (with GEV fit) for d= 0.05 and the critical defect size = 6.*

Correlation parameter d = **0.05**, *the critical defect size* = **9**			
the initial coverage	Init cover = 0.1	Init cover = 0.4	Init cover = 0.6
Mean inspected coverage	0.10699	0.40263	0.60038
Mean number of inspection steps	1.02	1.0133	1.0033
Unreliability	0	0	0
Number of wrong acceptances	0	0	0

Table 3.15 c) *The simulation results of SRS (with GEV fit) for d= 0.05 and the critical defect size = 9.*

Simulation results of the sequential random scheme with gamma distribution fit

Due to the fact that in the gamma model for generating corroded surfaces, the gamma distribution is used to represent the defects' sizes, we decide to check the performance of the sequential random scheme when this distribution is used in the extrapolation procedure.

For the value of the correlation parameter d equal to 1, the simulation experiments brought the following results.

- the correlation parameter d = 1

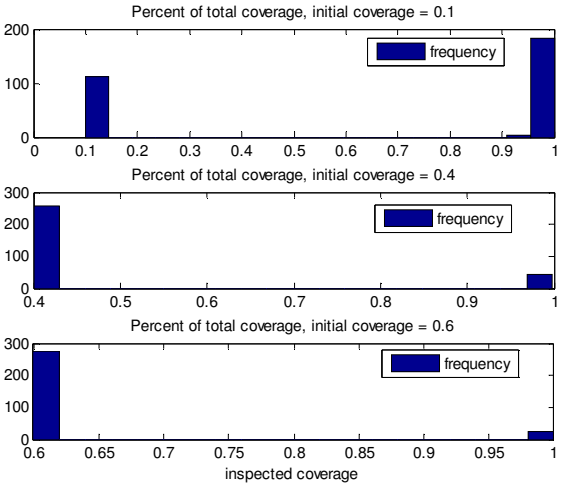

a) the critical defect = 3

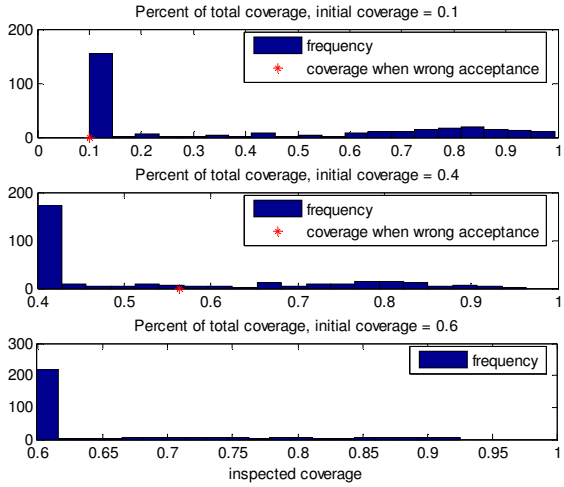

b) the critical defect = 6

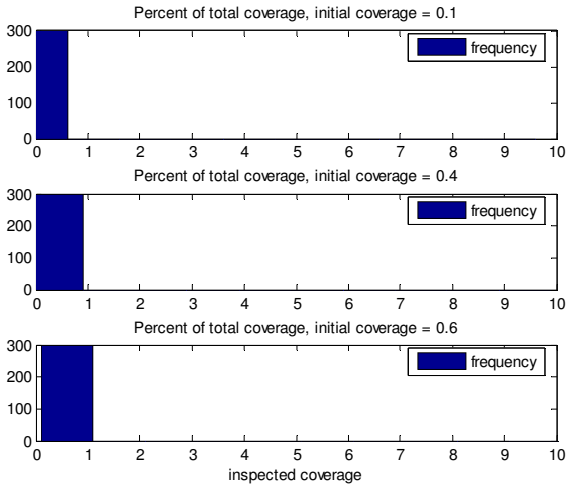

c) the critical defect = 9

Figure 3.17 *The histograms of the inspected coverage within SRS (with gamma fit) for d= 1.*

The histograms in Figure 3.17 show a visible influence of the applied value of the critical defect size on the total inspected coverage. It can be especially seen when comparing the subplots illustrating results of SRS with the initial coverage equal to 0.1. One can observe that when increasing value of the critical defect size the number of situations at which the inspection was terminated at the initial stage increases as well. With the critical defect size equal to 3, 6 and 9 units, in 110, 170 and 300 out of 300, simulated inspection situations, respectively, the additional inspection was not performed. This trend could be expected, when recalling the results obtained when the sequential scheme with GEV fit was applied to inspect similar surfaces (see Figure 3.16). However, when using the gamma fit for the extrapolation within SRS, one can see that with the critical defect size value equal to 6 units if the adaptive inspection was required to carry out, rather rarely the total surface was inspected. On the other hand, when the sequential random scheme (with the same parameters) but with GEV fit distribution was applied to inspect surfaces with independent defect distribution (d = 1), larger inspection coverage had to be examined and more often 100% inspection was involved (compare Figures 3.14b and 3.17b, and the mean inspected coverage in Tables 3.13b and 3.16b). Although the extrapolation with the gamma distribution is mathematically incorrect, it may still lead to reliable predictions of the non-inspected defect distribution, and as a consequence good performance of the inspection scheme.

Correlation parameter d = **1**, *the critical defect size* = **3**			
the initial coverage	Init cover = 0.1	Init cover = 0.4	Init cover = 0.6
Mean inspected coverage	0.65795	0.4856	0.63445
Mean number of inspection steps	1.6333	1.1567	1.0933
Unreliability	0	0	0
Number of wrong acceptances	0	0	0

Table 3.16 a) *The simulation results of SRS (with gamma fit) for d=1 and the critical defect size = 3.*

Correlation parameter d = **1**, *the critical defect size* = **6**			
the initial coverage	Init cover = 0.1	Init cover = 0.4	Init cover = 0.6
Mean inspected coverage	0.40253	0.53184	0.648
Mean number of inspection steps	1.6567	1.5767	1.4067
Unreliability	0.0033	0.0033	0
Number of wrong acceptances	1	1	0

Table 3.16 b) *The simulation results of SRS (with gamma fit) for d=1 and the critical defect size = 6.*

*Correlation parameter d = **1**, the critical defect size = **9***			
the initial coverage	Init cover = 0.1	Init cover = 0.4	Init cover = 0.6
Mean inspected coverage	0.1	0.4	0.6
Mean number of inspection steps	1	1	1
Unreliability	0	0	0
Number of wrong acceptances	0	0	0

Table 3.16 c) *The simulation results of SRS (with gamma fit) for d=1 and the critical defect size = 9.*

Let us now check whether the assumption about gamma distributed maximum defect size affects the reliability of SRS when inspecting surfaces with some dependence between defects' distribution. In order to allow such study 300 surfaces were generated by the gamma model with correlation parameter d equal to 0.5. On these surfaces the sequential inspection procedure was simulated and the following results were obtained.

- the correlation parameter d = 0.5

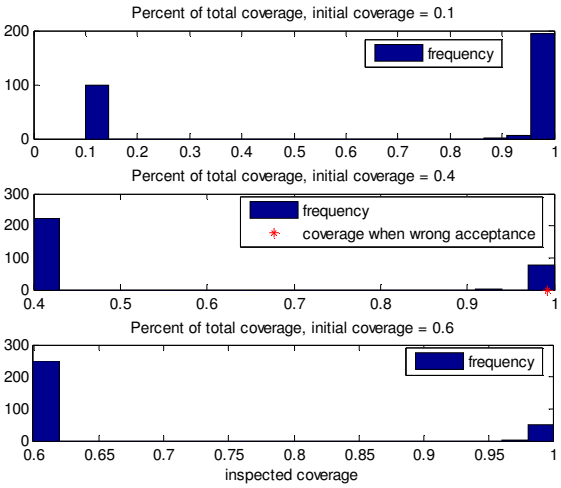

a) the critical defect = 3

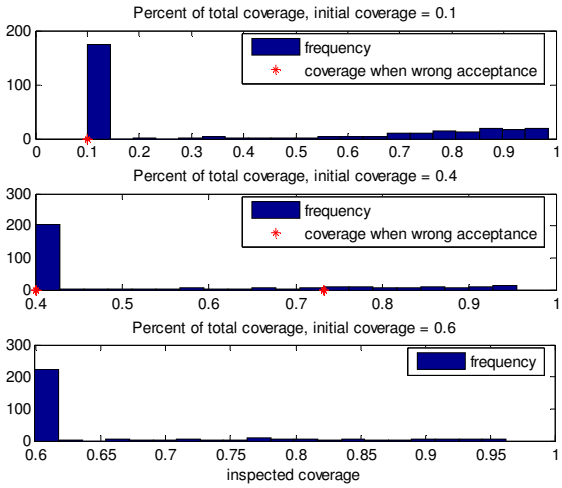

b) the critical defect = 6

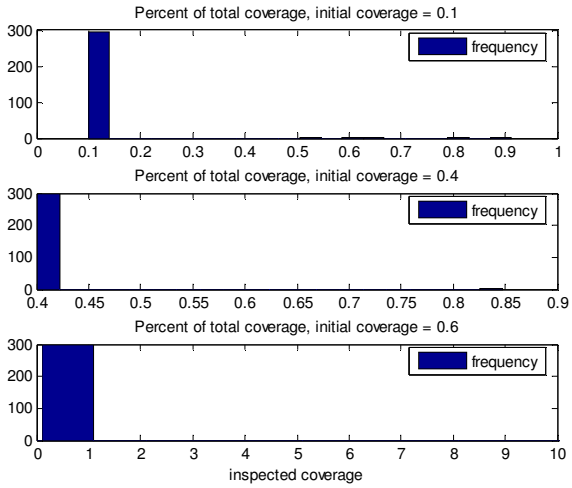

c) the critical defect = 9

Figure 3.18 *The histograms of the inspected coverage within SRS (with gamma fit) for d= 0.5.*

Correlation parameter d = **0.5**, *the critical defect size* = **3**			
the initial coverage	Init cover = 0.1	Init cover = 0.4	Init cover = 0.6
Mean inspected coverage	0.69502	0.55233	0.6683
Mean number of inspection steps	1.7033	1.2833	1.2
Unreliability	0	0.0033	0
Number of wrong acceptances	0	1	0

Table 3.17 a) *The simulation results of SRS (with gamma fit) for d= 0.5 and the critical defect size = 3.*

Correlation parameter d = **0.5**, *the critical defect size* = **6**			
the initial coverage	Init cover = 0.1	Init cover = 0.4	Init cover = 0.6
Mean inspected coverage	0.38823	0.52072	0.65593
Mean number of inspection steps	1.5933	1.5167	1.3933
Unreliability	0.01	0.0167	0
Number of wrong acceptances	3	5	0

Table 3.17 b) *The simulation results of SRS (with gamma fit) for d= 0.5 and the critical defect size = 6.*

Correlation parameter d = **0.5**, *the critical defect size* = **9**			
the initial coverage	Init cover = 0.1	Init cover = 0.4	Init cover = 0.6
Mean inspected coverage	0.10932	0.40149	0.6
Mean number of inspection steps	1.0167	1.0033	1
Unreliability	0	0	0
Number of wrong acceptances	0	0	0

Table 3.17 c) *The simulation results of SRS (with gamma fit) for d = 0.5 and the critical defect size = 9.*

Analyzing the values gathered in Tables 3.17a-c, one can see that a slippery use of the gamma distribution when assessing risk of having the critical defect among non-inspected surface locations does not influence the reliability of inspection results. In the worst case 5 out of 300 simulated surfaces were wrongly classified, what still gives almost perfect, equal to 98% reliability (see Table 3.17b). Similarly to the previous situation (i.e. when d = 1), the histograms of inspected coverages (Figure 3.18) show decreasing trend in required inspection effort when applying bigger values of the critical defect parameter. Moreover, the same plots indicate that with bigger initial inspection more often the inspection was terminated at first stage (the total inspected coverage was equal to the initial). It can be explained in the following way: with smaller value of the critical defect parameter, performing more measurements it was more likely to detect defect of this size; while choosing bigger value of the critical defect parameter the information gathered from those measurements was sufficient to reject a hypothesis that the critical defect may be present among non-inspected surface locations. This inference can be confirmed when looking at the increasing, with bigger value of the initial coverage parameter, the mean number of inspection steps (see Tables 3.17a-c).

Generating the corroded surfaces using the gamma model with the correlation parameter d = 0.05, we are able to examine the performance of the sequential random scheme (with gamma fit) for the inspection of surfaces with clustered defects' distribution.

During the simulation experiments, choosing different criticality levels, we have simulated the sequential inspection on 300 of such surfaces. The total inspection size and the number of inspection steps were recorded in each case. As before, the number of wrong surface classifications was counted and used as measure of the scheme reliability. Obtained results are presented in Tables 3.18a-c and Figure 3.19. They confirm the perfect reliability of SRS as wrong acceptance was observed only in one case (see Table 3.18a). It can be also seen that the characteristic defects' distribution caused that in the majority of situations the inspection procedure was terminated after the initial step. Due to the same reason when the critical defect was chosen to be equal 9, in some situations, when inspecting initially 10%, the additional inspection of all remaining locations was required (see Figure 3.19c).

- the correlation parameter d = 0.05

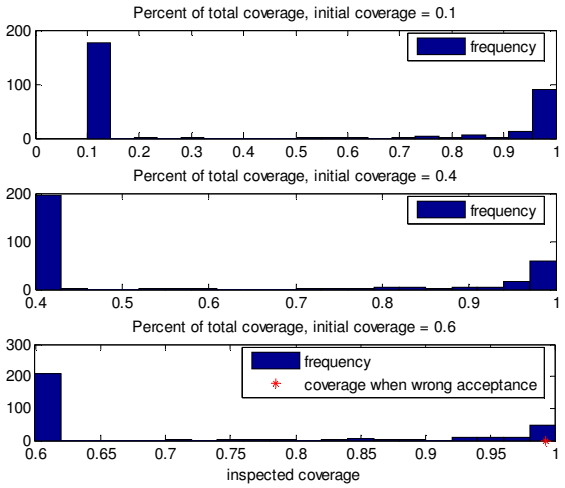

a) the critical defect = 3

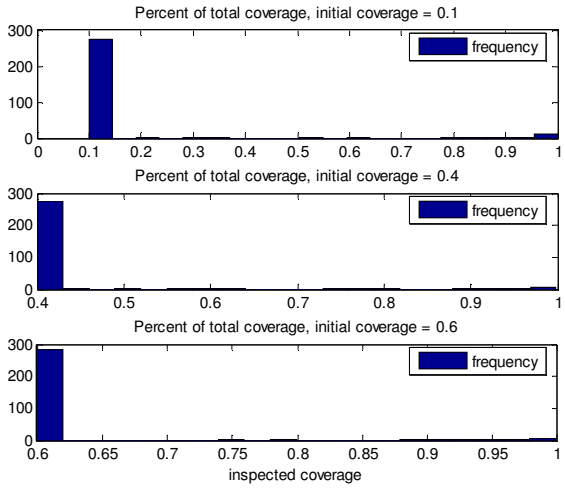

b) the critical defect = 6

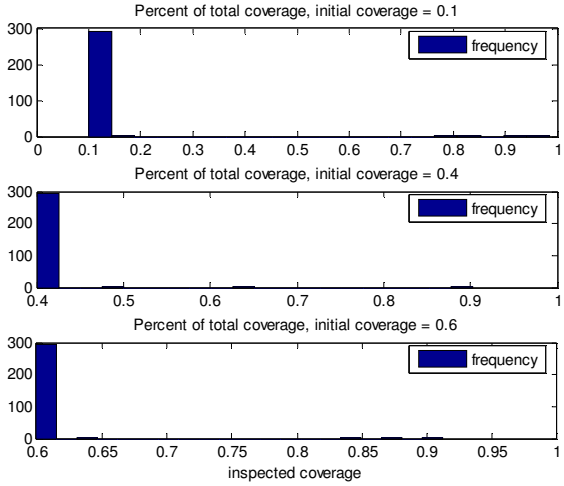

c) the critical defect = 9

Figure 3.19 *The histograms of the inspected coverage within SRS (with gamma fit) for d = 0.05.*

Correlation parameter d = **0.05**, *the critical defect size* = **3**			
the initial coverage	Init cover = 0.1	Init cover = 0.4	Init cover = 0.6
Mean inspected coverage	0.44113	0.58322	0.70756
Mean number of inspection steps	1.6167	1.5067	1.4533
Unreliability	0	0	0.0033
Number of wrong acceptances	0	0	1

Table 3.18 a) *The simulation results of SRS (with gamma fit) for d= 0.05 and the critical defect size = 3.*

Correlation parameter d = **0.05**, *the critical defect size* = **6**			
the initial coverage	Init cover = 0.1	Init cover = 0.4	Init cover = 0.6
Mean inspected coverage	0.15949	0.4339	0.61691
Mean number of inspection steps	1.1133	1.11	1.08
Unreliability	0	0	0
Number of wrong acceptances	0	0	0

Table 3.18 b) *The simulation results of SRS (with gamma fit) for d= 0.05 and the critical defect size = 6.*

Correlation parameter d = **0.05**, *the critical defect size* = **9**			
the initial coverage	Init cover = 0.1	Init cover = 0.4	Init cover = 0.6
Mean inspected coverage	0.11558	0.40686	0.60292
Mean number of inspection steps	1.03	1.0333	1.02
Unreliability	0	0	0
Number of wrong acceptances	0	0	0

Table 3.18 c) *The simulation results of SRS (with gamma fit) for d= 0.05 and the critical defect size = 9.*

Conclusions

Throughout the analysis of the performance of the sequential random scheme it could be seen that its reliability is independent of the distribution of defects on corroded surface as well as of the assumed distribution applied in the extrapolation procedure. On the other hand, the initial inspection coverage and the critical defect size have appeared to be influential parameters affecting the size of additionally inspected surface. In some cases, the information gathered from a small number of initially taken measurements was sufficient to decide about the termination of inspection while in other cases led to 100% inspection. Therefore, the optimization of the initial coverage parameter seems to be prioritized task improving the overall performance of the sequential scheme. This would result in the costly-optimal and almost perfectly reliable inspection plan.

Comparison of the sequential random scheme with the adaptive inspection schemes

Simulation experiments have shown that independently of the corrosion structure, the sequential sampling scheme always performs well bringing very reliable inspection results. However, it could be also seen that in some situations this perfect effectiveness was connected with big inspection effort. On the other hand, the reliability of the adaptive inspection schemes was rather variable and has depended on the distribution of defects on considered surface. However, in many cases, this inspection plan also led to very satisfactory reliability. Therefore, let us now compare both schemes. Note that both the sequential and the adaptive sampling plan share the feature that the total inspected coverage is not

established in advance. Therefore, their reliability is defined as a function of the mean inspected coverage. It is also worth to mention that since the regular inspection scheme appeared to be rather less effective than the adaptive scheme, it is not considered here.

Since the performance of the sequential sampling scheme was examined only on the corroded surfaces generated by the gamma model, the comparing analysis is restricted to these cases. Moreover, to be consistent with the chosen value of the critical defect size applied when simulating the adaptive inspection scheme, the criticality level equal to 3 units is fixed for the SRS.

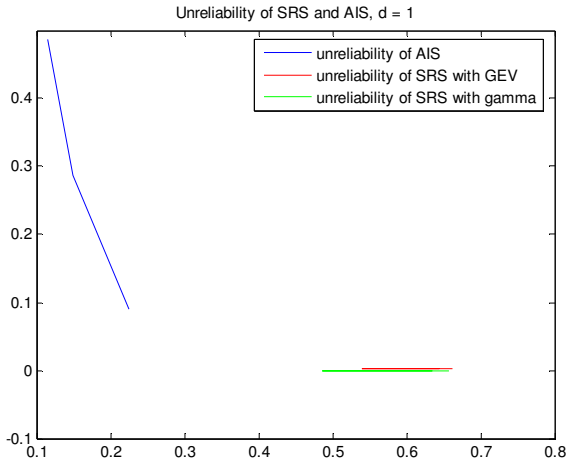

a) the correlation parameter d = 1

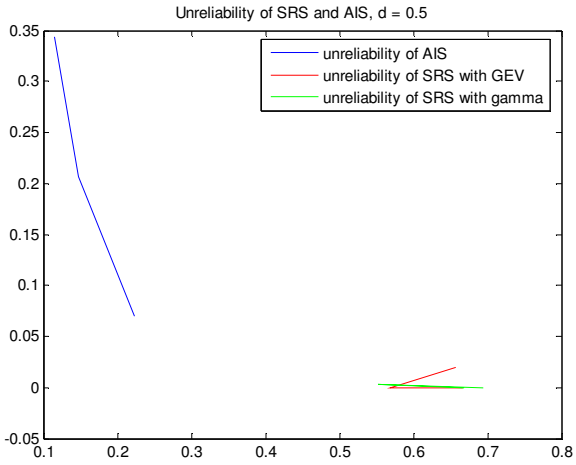

b) the correlation parameter d = 0.05

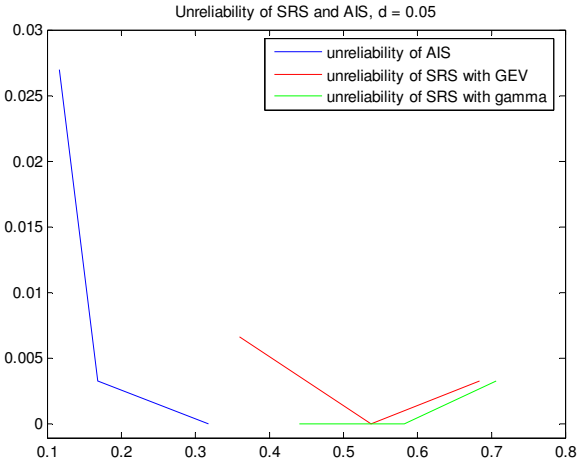

c) the correlation parameter d = 0.05

Figure 3.20 *1The unreliability plots of AIS and SRS*

The unreliability plots presented in Figure 3.20 show that independently of the structure of the corroded surface, the mean total inspected coverage for the adaptive inspection scheme is much smaller than in case of the sequential random scheme. On the other hand, as one could expect, the sequential scheme shows better reliability. However, when looking at the plot 3.20c) corresponding to the results obtained when the correlation parameter d was equal to 0.05, one can observe that the adaptive inspection bring results of the reliability very similar to the sequential scheme and simultaneously requires significantly less coverage to be examined. Similar inference can be drawn when comparing the performance of both schemes applied to surfaces generated by the gamma model with parameter d = 0.5. The adaptive inspection scheme with the extension parameter th1 = 1, inspecting on the average 22% of the surface, shows the unreliability equal to 0.07 (see also Table 3.8). On the other hand, the minimal average inspection coverage for SRS is equal to 44%. Therefore, it is rather difficult to state in general which of these two dynamic schemes is better. When one is able to accept some risk of wrong surface classification, it can be advised to apply the adaptive inspection that involves less inspection effort. In situations, when the consequences of wrong acceptance of corroded surfaces are severe, the sequential plan with perfectly reliable results should be chosen. Thus, the cost-criterion analysis seems to be necessary in order to design an optimal sampling scheme.

4. Conclusions and recommendations

A properly planned inspection procedure is of big importance for any industrial process. In the oil industry special attention is given to inspect steel components that are subject to corrosion. Their reliability is necessary to avoid failure that may lead to oil release and pollution of the natural environment. Obviously, the more one inspects the better information one can gain. On the other hand, the inspection procedure can - and quite often is - connected with high expenses. Therefore, finding the optimal inspection plan balancing costs and risk of failure is desirable. In this thesis, the so-called sampling inspection approach is considered as a possible solution.

In this study, the following three sampling inspection schemes were introduced: the regular inspection scheme, the adaptive inspection scheme, and the sequential random scheme.

The regular inspection scheme represented the non-dynamic, one-step inspection model. According to this scheme the inspected points were selected according to some pattern that assured their even spread. An essential feature of the regular scheme was that the total inspection coverage was completely defined before its application.

On the other hand, the other two inspection plans, namely the adaptive and sequential schemes were designed as the multi-step procedures, in which the total inspection coverage was variable.

In case of the adaptive inspection scheme, after the initial inspection, which examined about 10% of the surface area its further adaptive stage was dependent on some conditions. The so-called extension criterion was used as a condition that forced additional inspection effort. According to this condition, all neighboring locations of inspected points with corrosion depths bigger than the chosen value of the extension condition, were examined in the adaptive step.

Within the sequential random scheme, after the initial inspection of unrestricted size, the additional inspected coverage was determined based on the estimated risk of having the critical defect among non-inspected surface locations. In this scheme all inspected points were selected randomly. All plans were defined by some parameters that appeared to have influence on the performance of the inspection procedure.

The performance analysis was based on simulation experiments in which the corrosion surfaces were generated by two proposed models. The Poisson and gamma model allowed simulating surfaces with different probability distributions for the defects. As a result, the reliability of the designed sampling schemes was verified when they were applied to surfaces of different structure. Moreover, it could be seen that the Poisson model was more general and universal, in the sense, that it allows generating more types of corroded surfaces. In opposite to the gamma corrosion generating technique, using the Poisson model one is

able to simulate surfaces where not all locations are affected by the corrosion mechanism. This would be very useful for modeling the pitting type of corrosion.

When judging the effectiveness of the inspection plans, the so-called unreliability function was used. This function was defined as a function of the mean inspected coverage and expresses the non-detection probability of the critical defect.

Throughout the study one could see that the sequential random scheme always led to fully reliable inspection results independently of the characteristic of the corroded surface. This, however, was quite often connected with a large inspection effort measured in terms of the inspected coverage. On the other hand, in case of the regular scheme the total inspection coverage was always known in advance but simultaneously it was not always sufficient to obtain reliable information. The flexible character of the adaptive inspection model caused that this scheme appeared to be quite often the optimal solution. With this scheme, inspecting a relatively small coverage was likely to result in the detection of the critical defect and the correct surface classification.

All three schemes appeared to work well on the surfaces with a clustered (non-homogeneous) defect distribution. Therefore, when one is interested in the inspection of corroded surfaces, the choice between sampling plans should be based on a cost-criterion. However, in general, it is rather difficult to state the superiority of one of these schemes. If the priority is given to the reliability of inspection results, one can be advised to use the sequential random scheme. On the other hand, if the consequences of possible failure are not severe, a cost analysis should be involved to derive the optimal inspection strategy. Due to time constraints, a cost analysis was not performed in this project and is left for future research.

As the next steps improving the models we would recommend the following:

- Employ economical constraints for the inspection planning.

- Include possible dependency between adjacent corrosion defects within the sequential random scheme in order to better extrapolate and estimate the probability distribution of the corrosion defects in the non-inspected part of the surface. As a consequence, one would expect a smaller inspection coverage that is necessary to examine. This further would result in a more reliable and less expensive sampling inspection scheme. As it was suggested in the report, the dependency could be incorporated by the 'extremal index'.

- When fitting probability distributions in the sequential random scheme, take into account the statistical uncertainty inherent in the parameters estimated from a small number of data points.

- Perform the estimation of the parameters that are used in the models to simulate corrosion. To do this, the elicitation of experts can be advised.
- Extend the adaptive sampling scheme by including an option that gives the possibility of applying different values of the initial coverage parameter. This would be especially useful when the setting costs of additional inspection are high.

- Check the performance of the sampling schemes when applied to real corrosion data.

- Combine the Poisson and the gamma model for generating corrosion surfaces. This would give the possibility of obtaining more variable corroded structures. For example, the increments of the corrosion in the Poisson model can be generated by the gamma process.

APPENDIX A

1) Sensitivity analysis of the number of simulations for the regular inspection scheme using the gamma technique with coefficient parameter d = 1.

a) Overall analysis

In general, when some results are obtained based on simulation experiments, the number of performed simulations is a crucial parameter. Depending on its value one can obtain information of different quality and reliability. Since the performance of the sampling inspection plans is investigated in simulation experiments, their number has to be appropriately chosen.

Below we present an extended sensitivity analysis of the number of simulations for the regular sampling scheme model with the inspection coverage equal to 0.3 and 0.6. This analysis is made based on derivation of the distribution of the scheme reliability. More precisely, the standard deviations of the latter distributions, obtained for different numbers of simulations, will be compared.

When determining the distribution of the unreliability scheme, the central limit theorem [17] was applied as a driving tool. Based on this theorem, we can argue that when repeating the same experiment (consisting of a fixed number of simulations) sufficiently often, the distribution of its mean can be estimated and has the Gaussian (normal) shape. We are looking for the optimal number of simulations that gives us reliable results or, in different words, for which the results will not differ significantly when running the experiment several times. Such a property can be nicely verified using the standard deviation as a distribution's spread measure. In our study the experiments were performed (run) 100 times each consisting of 100, 300 or 500 of simulations.

It appeared that the obtained distributions of the scheme unreliability when 300 and 500 of simulations were performed have small (compared with the mean) and quite similar values of the standard deviations- see Tables A1-1 and A1-2 and Figures A1-2 and A1-3. On the other hand, the same figures indicate that when only 100 simulations were made the distribution of the unreliability scheme has bigger standard deviation, and as a consequence the obtained results may differ from experiment to experiment. Further taking into account the time required for performing one experiment with a different number of simulations (see Table A1-6), the 300 simulations seems to be the reasonable and reliable choice.

Additionally presented histograms of the regular inspection scheme unreliability distributions (Figure A1-1) show that for higher values of the inspection coverage parameter, these distributions are more concentrated and shifted to the left. One could obviously expect such trend because the more we inspect the more reliable (corresponding to the reality) information we get and as a result it is unlikely to make a wrong surface classification.

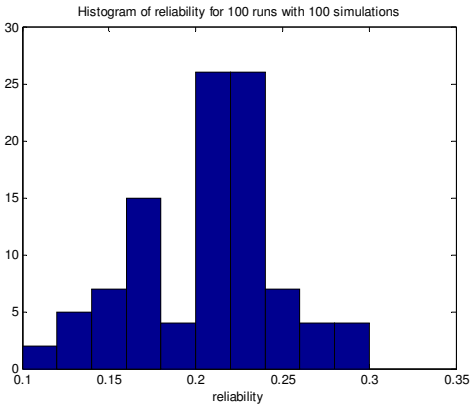

100 simulations, the inspection coverage = 0.3

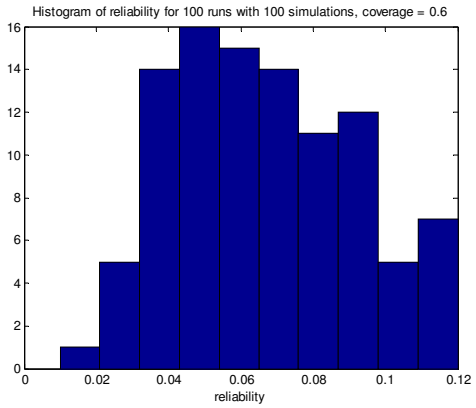

100 simulations, the inspection coverage = 0.6

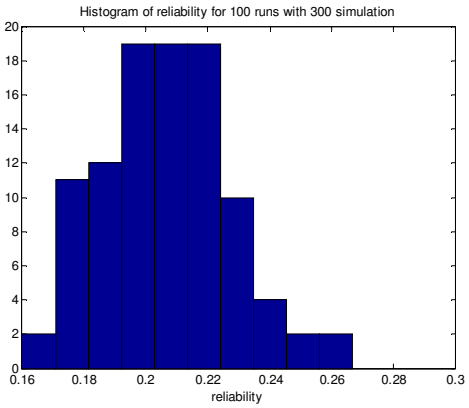

300 simulations, the inspection coverage = 0.3

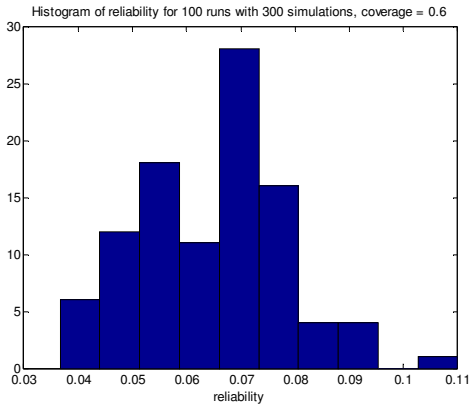

300 simulations, the inspection coverage = 0.6

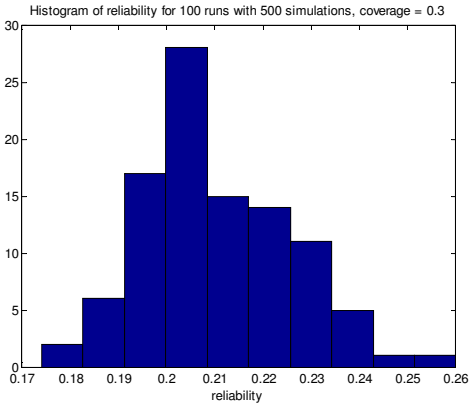

500 simulations, the inspection coverage = 0.3

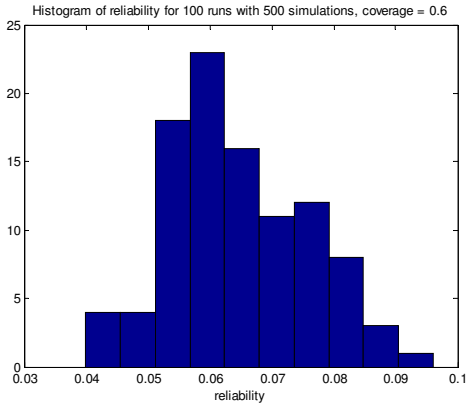

500 simulations, the inspection coverage = 0.6

Figure A1-1 *The histograms of the regular inspection scheme unreliability for different numbers of simulations.*

Number of simulations	Coverage = 0.3			Coverage = 0.6		
	Standard deviation	Lower 95% conf bound	Upper 95% conf bound	Standard deviation	Lower 95% conf bound	Upper 95% conf bound
100	0.0384	0.0337	0.0446	0.0236	0.0207	0.0274
300	0.0214	0.0188	0.0248	0.0138	0.0121	0.0160
500	0.0159	0.0139	0.0184	0.0112	0.0098	0.0130

Table A1-1 *The standard deviations of the regular inspection scheme unreliability for different numbers of simulations.*

Number of simulations	Coverage = 0.3			Coverage = 0.6		
	Mean	Lower 95% conf bound	Upper 95% conf bound	Mean	Lower 95% conf bound	Upper 95% conf bound
100	0.2026	0.1950	0.2102	0.0666	0.0619	0.0713
300	0.2058	0.2016	0.2100	0.0652	0.0625	0.0679
500	0.2103	0.2072	0.2135	0.0649	0.0626	0.0671

Table A1-2 *The means of the regular inspection scheme unreliability for different numbers of simulations.*

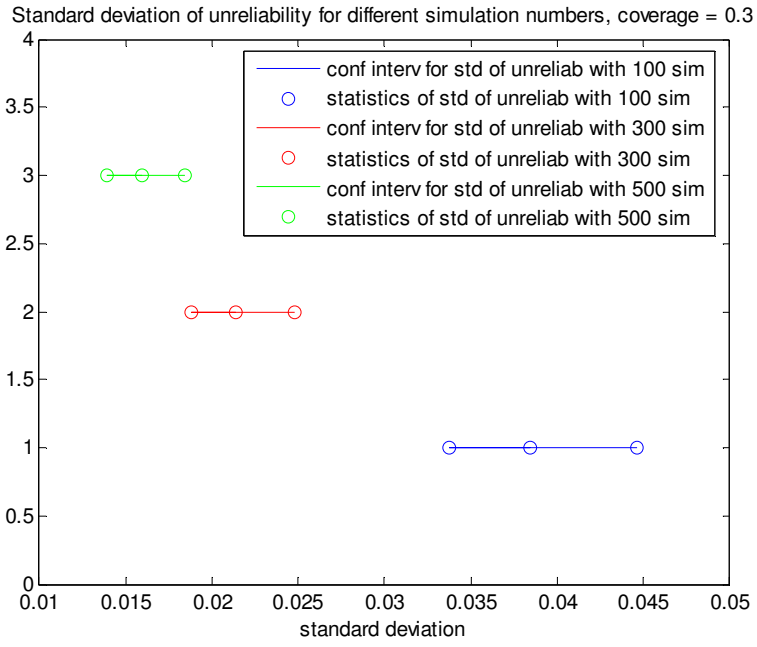

Figure A1-2 *The 95% confidence intervals for the standard deviation of the regular inspection scheme unreliability with different numbers of simulations and the inspection coverage = 0.3.*

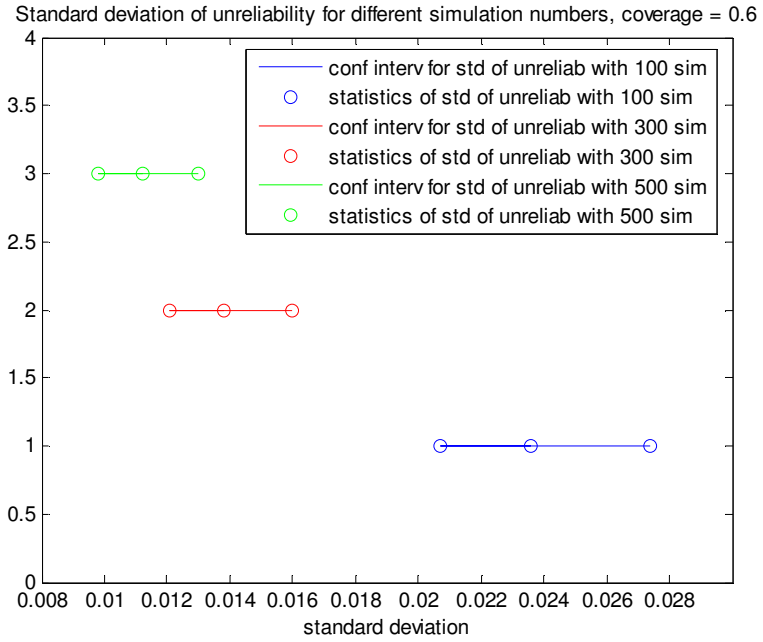

Figure A1-3 *The 95% confidence intervals for the standard deviation of the regular inspection scheme unreliability with different numbers of simulations and the inspection coverage = 0.6.*

b) Illustrating example (based on two runs experiment)

- 100 simulations

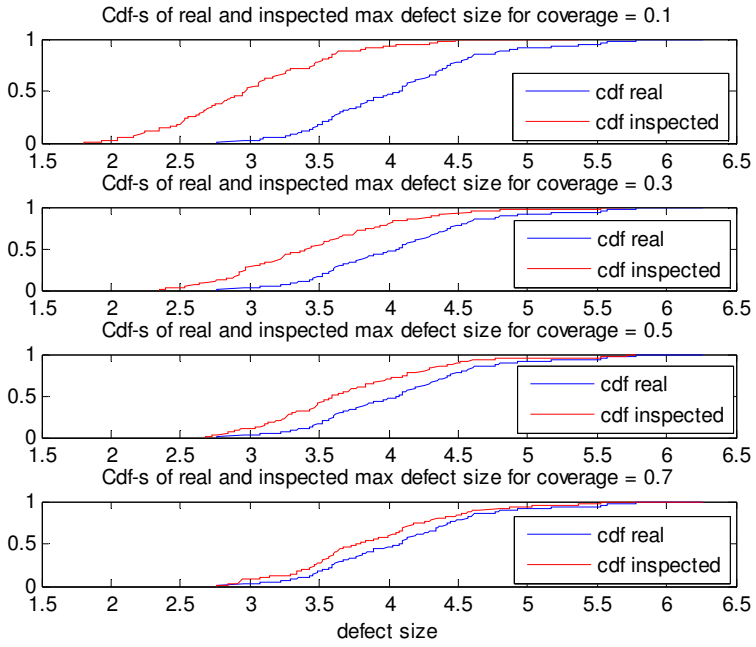

Figure A1-4 *The cumulative distribution functions of the real maximum defects and the maximum defects recorded during RIS for different inspection coverage and 100 simulations.*

Correlation parameter d = **1**, number of simulations = 100								
Inspected coverage	0.1	0.2	0.3	0.4	0.5	0.6	0.7	0.8
Number of wrong decisions first run	50	27	25	14	8	14	6	2
Number of wrong decisions second run	61	37	20	14	9	11	4	1

Table A1-3 *The number of wrong acceptance decisions against the inspection coverage within the regular scheme with 100 simulations.*

- 300 simulations

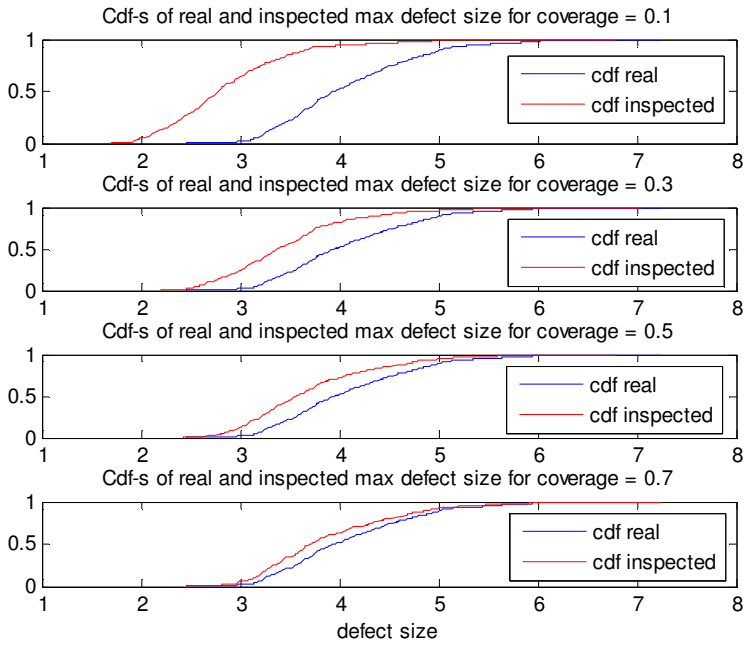

Figure A1-5 *The cumulative distribution functions of the real maximum defects and the maximum defects recorded during RIS for different inspection coverage and 300 simulations.*

Correlation parameter d = **1**, number of simulations = 300								
Inspected coverage	0.1	0.2	0.3	0.4	0.5	0.6	0.7	0.8
Number of wrong decisions first run	183	109	64	49	30	20	10	7
Number of wrong decisions second run	182	117	53	55	34	25	15	8

Table A1-4 *The number of wrong acceptance decisions against the inspection coverage within the regular scheme with 100 simulations.*

- 500 simulations

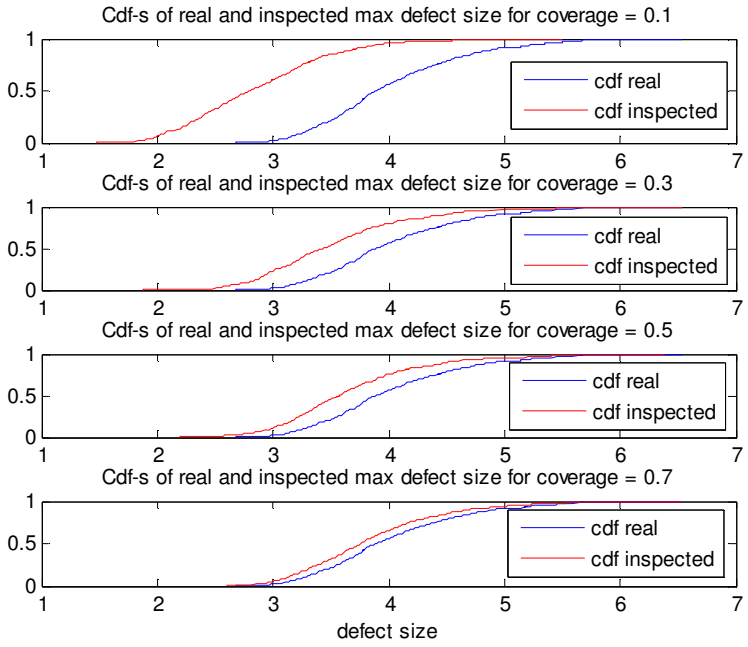

Figure A1-6 *The cumulative distribution functions of the real maximum defects and the maximum defects recorded during RIS for different inspection coverage and 500 simulations.*

Correlation parameter d = **1**, number of simulations = 500								
Inspected coverage	0.1	0.2	0.3	0.4	0.5	0.6	0.7	0.8
Number of wrong decisions first run	294	190	101	74	43	36	15	15
Number of wrong decisions second run	292	185	112	85	42	33	20	16

Table A1-5 *The number of wrong acceptance decisions against the inspection coverage within the regular scheme with 500 simulations.*

Number of simulations	100	300	500
Total simulation time in minutes	2.99	7.31	11.93

Table A1-6 *Simulation times for the regular sampling scheme (computer type: Pentium 4, 2.20 GHz).*

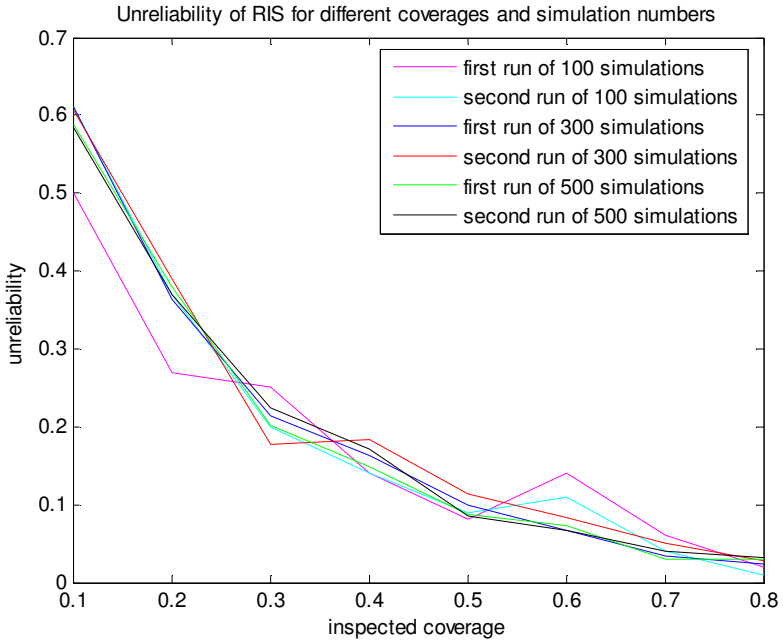

Figure A1-7 *Unreliability plots of RIS for different numbers of simulations.*

Number of simulations	100	300	500
Max difference between the reliability in first and second run	0.11	0.037	0.022

Table A1-7 *Maximum differences between the regular inspection scheme unreliability obtained in two runs of the simulation experiment.*

From tables and figures presented above one can conclude that with bigger number of simulations this parameter does not have a big influence on the inspection results. It is especially seen when looking at the plots obtained when simulations were repeated 300 and 500 times. As a result it seems to be redundant and to be connected with bigger computational effort (see Table A1-6 with simulation times) to perform simulations 500 times instead of 300 times. On the other hand, 100 simulations may bring not reliable results since repeating similar experiments (i.e. running 100 simulations several times) may cause quite different results (see pink and sky-blue plots in Figure A1-7 above). The latter situation, however, is rather unlikely to be observed when generating a surface 300 or 500 hundred times (see corresponding plots in the same figure). It is also worth to note that the cumulative distribution curves corresponding to the real maximum defects and maximum defects recorded during inspection are very similar and sufficiently smooth when performing 300 and 500 simulations. Therefore, the choice of performing simulations 300 times seems to be justified.

2) Sensitivity analysis of the number of simulations parameter for the adaptive inspection scheme using the gamma technique with correlation parameter d = 1.

a) Overall analysis

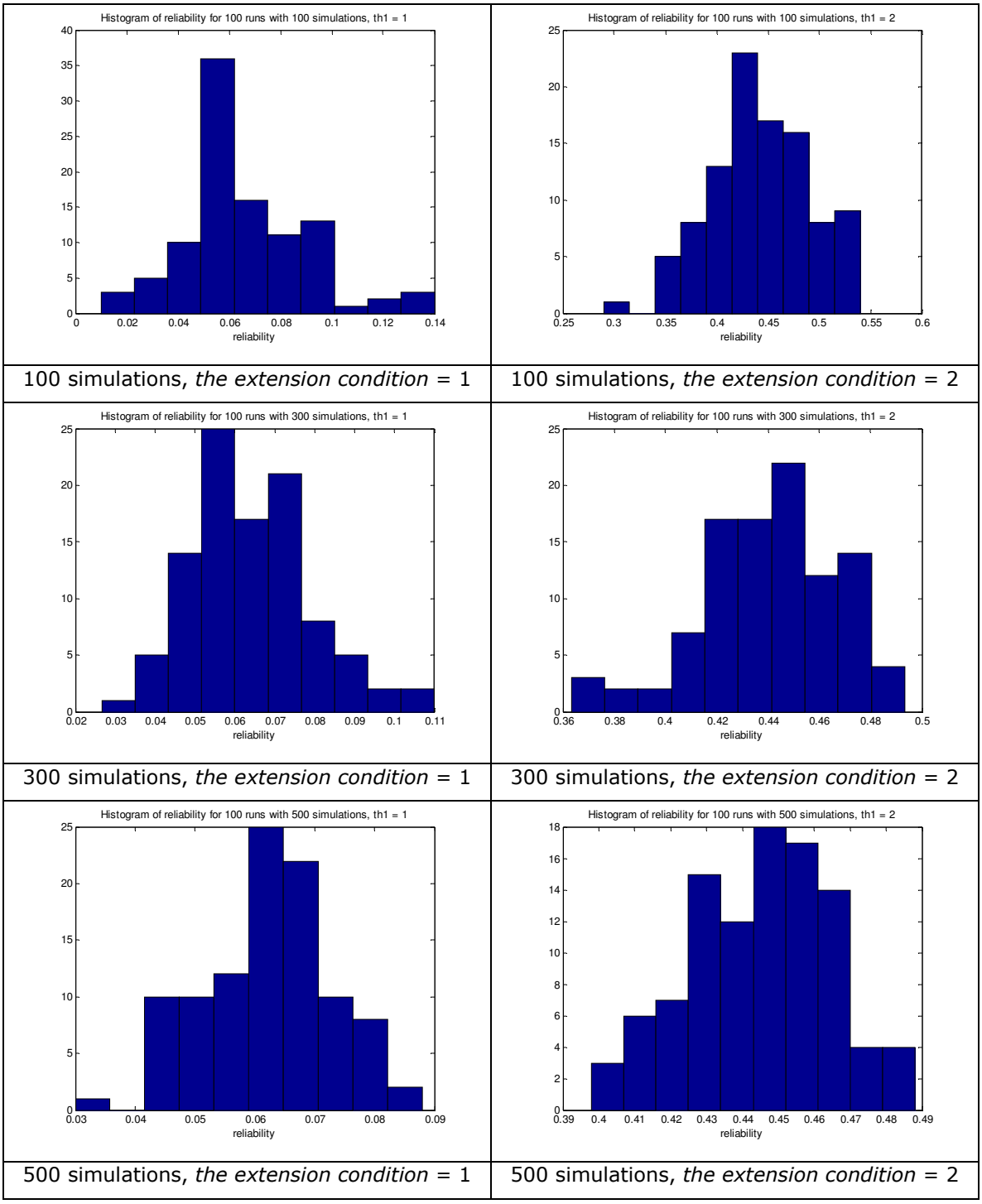

100 simulations, *the extension condition* = 1 | 100 simulations, *the extension condition* = 2

300 simulations, *the extension condition* = 1 | 300 simulations, *the extension condition* = 2

500 simulations, *the extension condition* = 1 | 500 simulations, *the extension condition* = 2

Figure A2-1 *The histograms of the adaptive inspection scheme unreliability for different numbers of simulations.*

Number of simulations	the extension condition = 1			the extension condition = 2		
	Standard deviation	Lower 95% conf bound	Upper 95% conf bound	Standard deviation	Lower 95% conf bound	Upper 95% conf bound
100	0.0251	0.0221	0.0292	0.0484	0.0425	0.0562
300	0.0151	0.0133	0.0176	0.0274	0.0240	0.0318
500	0.0111	0.0098	0.0129	0.0196	0.0172	0.0228

Table A2-1 *The standard deviations of the adaptive inspection scheme unreliability for different numbers of simulations.*

Number of simulations	the extension condition = 1			the extension condition = 2		
	Mean	Lower 95% conf bound	Upper 95% conf bound	Mean	Lower 95% conf bound	Upper 95% conf bound
100	0.0651	0.0601	0.0701	0.4448	0.4352	0.4544
300	0.0644	0.0614	0.0674	0.4408	0.4353	0.4462
500	0.0626	0.0604	0.0648	0.4452	0.4413	0.4491

Table A2-2 *The means of the adaptive inspection scheme unreliability for different numbers of simulations.*

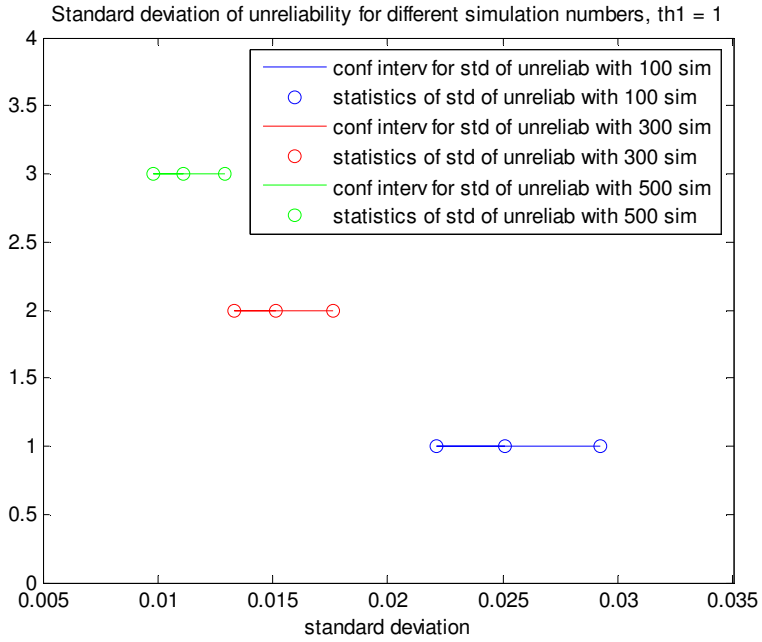

Figure A2-2 *The 95% confidence intervals for the standard deviation of the adaptive inspection scheme unreliability with different numbers of simulations and th1 = 1.*

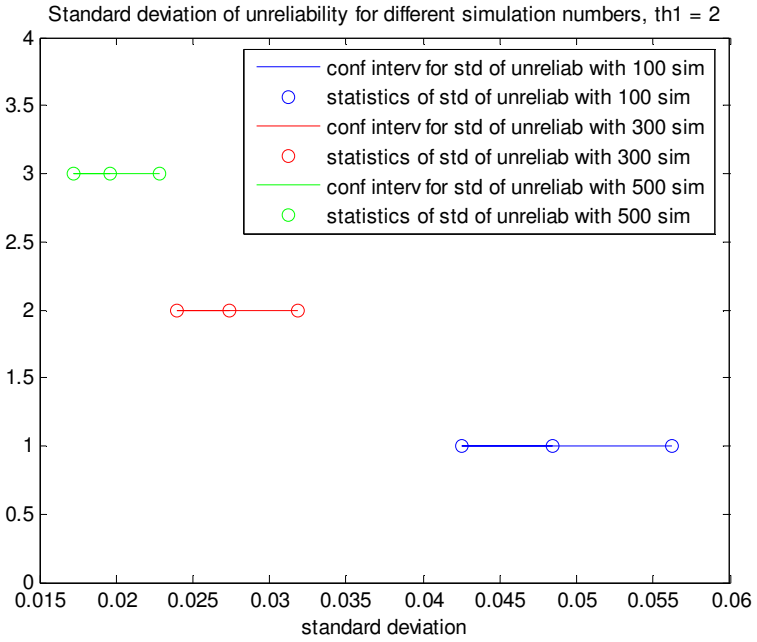

Figure A2-3 *The 95% confidence intervals for the standard deviation of the adaptive inspection scheme unreliability with different numbers of simulations and th1 = 2.*

The sensitivity analysis with respect to the number of simulations for the adaptive inspection scheme was performed in the same way as for the regular scheme. The distribution functions of the unreliability function were estimated by performing 100 experiments consisting of 100, 300 and 500 simulations. Figure A2-1 shows obtained results (given in histograms' form) while Tables A2-1 and A2-2 and Figures A2-2 and A2-3 contain statistics of these distributions. One can observe that when applying 300 or 500 simulations the standard deviation of the unreliability function is very small. It means that with these numbers of simulations the inspection results are reliable and it is rather unlikely that they would significantly differ when repeating simulation experiment. On the other hand, when performing only 100 simulations one can expect bigger variability in inspection results from run to run. In this case the standard deviation of the unreliability function is about two times larger and is equal to 0.0251, than it was for 300 or 500 of simulations. Therefore, taking also into account time required for performing simulation experiments (see Table A2-7), the number of simulation equals to 300 was chosen for checking the performance of AIS.

In order to show what kind of differences between inspection results one could expect when running simulation experiments several times with 100, 300 and 500 of simulations, an example is presented. One can see that indeed for bigger numbers of simulations, i.e. 300 and 500, these differences are insignificant. On the other hand, when looking at the results obtained for 100 simulations, the difference between outcomes of the first and second run is more visible. For example, Table A2-3 shows that when applying AIS with the extension

condition (th1) equal to 1.5 the difference in the values of the unreliability function between two runs of experiment may be equal about 14%.

b) Illustrating example (based on two runs experiment)

- 100 simulations

Correlation parameter d = **1**, number of simulations = 100			
The extension condition	th1= 1	th1= 1.5	th1= 2
Mean inspected coverage first run	0.218	0.154	0.118
Mean inspected coverage second run	0.231	0.151	0.117
Reliability of scheme 2 first run	0.06	0.19	0.45
Reliability of scheme 2 second run	0.09	0.33	0.51

Table A2-3 *The characteristic results obtained for the adaptive inspection scheme with 100 simulations.*

- 300 simulations

Correlation parameter d = **1**, number of simulations = 300			
The extension condition	th1= 1	th1= 1.5	th1= 2
Mean inspected coverage first run	0.219	0.149	0.117
Mean inspected coverage second run	0.212	0.146	0.117
Reliability of scheme 2 first run	0.07	0.22	0.43
Reliability of scheme 2 second run	0.07	0.22	0.40

Table A2-4 *The characteristic results obtained for the adaptive inspection scheme with 300 simulations.*

- 500 simulations

Correlation parameter d = **1**, number of simulations = 500			
The extension condition	th1= 1	th1= 1.5	th1= 2
Mean inspected coverage first run	0.214	0.147	0.116
Mean inspected coverage second run	0.213	0.147	0.116
Reliability of scheme 2 first run	0.06	0.27	0.47
Reliability of scheme 2 second run	0.07	0.25	0.45

Table A2-5 *The characteristic results obtained for the adaptive inspection scheme with 500 simulations.*

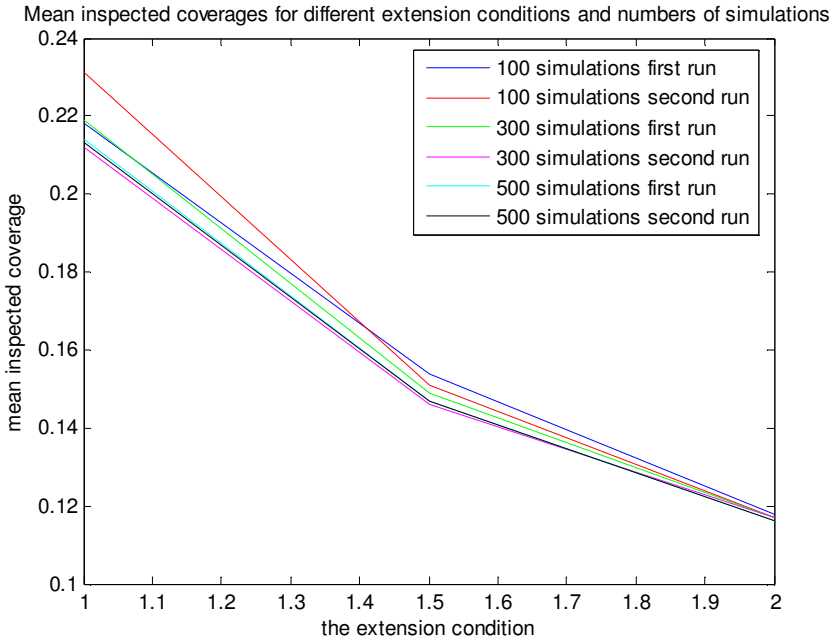

Figure A2-4 *Mean inspected coverages for different extension conditions and numbers of simulations.*

Number of simulations	100	300	500
Total simulation time in minutes	2.85	8.58	14.46

Table A2-6 *Simulation times for the adaptive inspection scheme (computer type: Pentium 4, 2.20 GHz).*

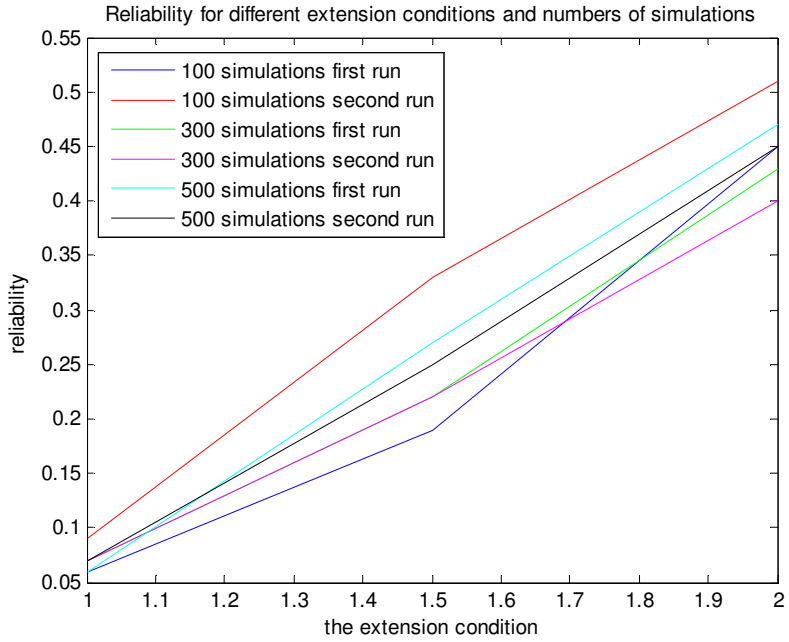

Figure A2-5 *Reliability plots for different extension conditions and numbers of simulations.*

3) Sensitivity analysis of the number of simulations parameter for the sequential random scheme with the generalized extreme value distribution.

Below we present the results that were obtained for the purpose of the sensitivity analysis of the simulation number for SRS. Since the standard deviation of the unreliability function with 300 simulations appeared to be very small and very close to this obtained with 500 simulations (see Table A3-1and Figure A3-2), we decided to apply 300 simulations when performing the experiments.

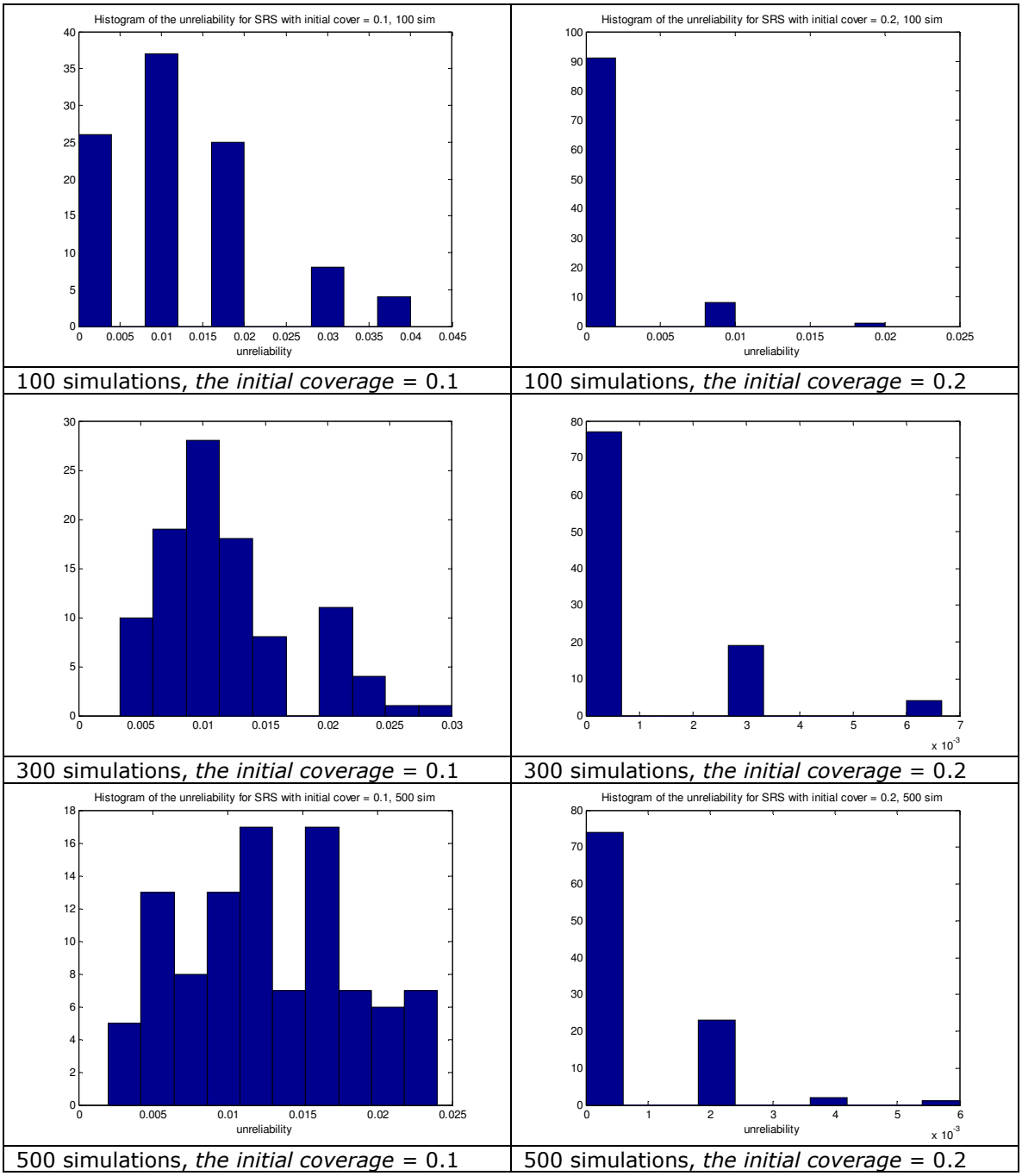

Figure A3-1 *The histograms of the sequential random scheme unreliability for different numbers of simulations.*

Number of simulations	the initial coverage = 0.1			the initial coverage = 0.2		
	Standard deviation	Lower 95% conf bound	Upper 95% conf bound	Standard deviation	Lower 95% conf bound	Upper 95% conf bound
100	0.0106	0.0093	0.0123	0.0033	0.0029	0.0039
300	0.0058	0.0051	0.0068	0.0018	0.0015	0.0020
500	0.0052	0.0046	0.0061	0.0011	0.0010	0.0013

Table A3-1 *The standard deviations of unreliability function within SRS for different numbers of simulations.*

Number of simulations	the initial coverage = 0.1			the initial coverage = 0.2		
	Mean	Lower 95% conf bound	Upper 95% conf bound	Mean	Lower 95% conf bound	Upper 95% conf bound
100	0.0127	0.0106	0.0148	0.001	0.0003	0.0017
300	0.0118	0.0107	0.0130	0.0009	0.0006	0.0012
500	0.0127	0.0116	0.0137	0.0006	0.0004	0.0008

Table A3-2 *The mean of unreliability function within SRS for different numbers of simulations.*

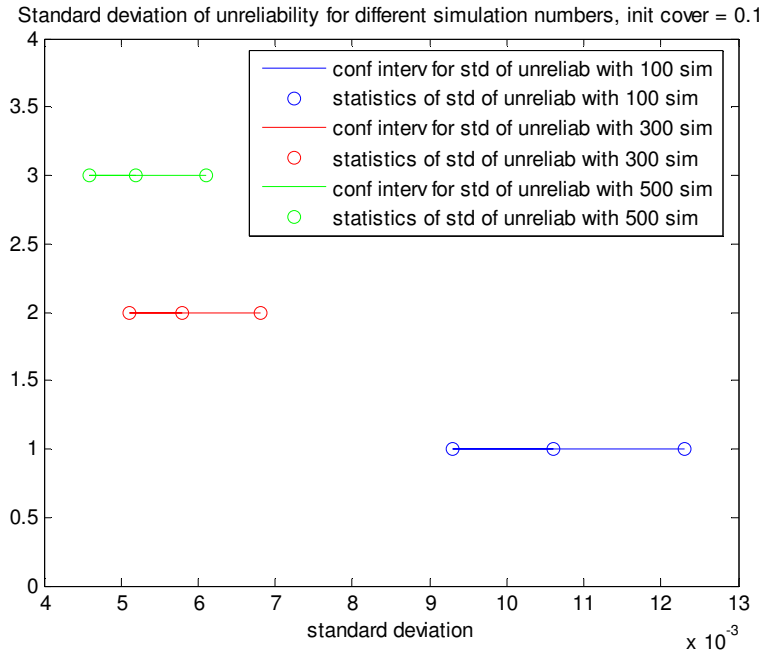

Figure A3-2 *The 95% confidence intervals for the standard deviation of SRS unreliability with different numbers of simulations and initial coverage = 0.1.*

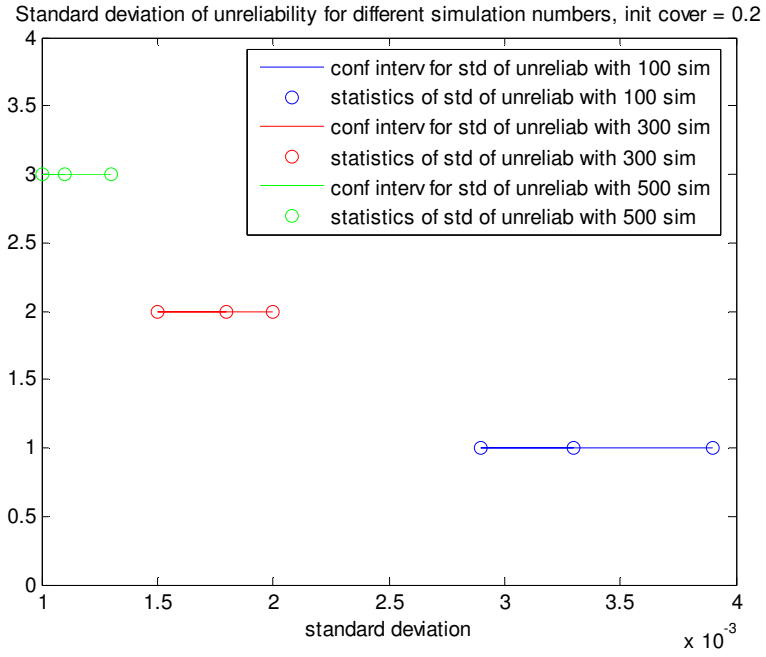

Figure A3-3 *The 95% confidence intervals for the standard deviation of SRS unreliability with different numbers of simulations and initial coverage = 0.2.*

4) Differences between the values of the product moment correlation matrices and the rank correlation matrices.

Due to the fact that the product moment correlation is not invariant under monotonic transformations, the product moment correlation matrices of the multivariate distributions obtained by the joint normal transform methods differs from the induced product moment correlation matrices given by the formula

$$\rho(X_k, X_l) = \exp\left\{-d\left(\sum_{i=1}^{2} |\, dist_i \,|^p\right)^q\right\}. \qquad (2.1)$$

In order to get some feeling how big these differences are, the actual product moment correlation matrices were estimated in the simulation experiments. As a deviation measure, the maximum difference between these matrices (i.e. the designed matrix Sigma of (2.1) form and the actual estimated correlation matrix RHO corresponding to the multivariate distribution), was used. During the experiment the 2000 samples (each of size kxk) from the obtained multivariate distribution were drawn. Based on these samples the product moment correlation matrix was estimated.

The estimated maximum differences obtained for the multivariate distributions considered in this report are presented below. These distributions were obtained by the join normal transform with the gamma margins with parameters a = 1.5 and b = 0.5 to assigned to the variables X_i and the dependence structure given by the formula (1.1). To be consistent, the norm parameters p and q were equal 2 and 0.5, respectively, while in case of the parameter d its three choices were examined, i.e. 1, 0.5 and 0.05. As in all performed simulations the surface size was equal k = 25, however other values were also examined for illustration purpose.

The product moment correlation matrices obtained for k = 2:

- d = 1

matrix (surface) size	*k* = 2	*k* = 3	*k* = 5	*k = 10*	*k* = 25	*k* = 35
maximum difference between correlations	0.0519	0.0921	0.0770	0.1083	0.1149	0.1117

$$\text{Sigma} = \begin{bmatrix} 1.0000 & 0.3679 & 0.3679 & 0.2431 \\ 0.3679 & 1.0000 & 0.2431 & 0.3679 \\ 0.3679 & 0.2431 & 1.0000 & 0.3679 \\ 0.2431 & 0.3679 & 0.3679 & 1.0000 \end{bmatrix} \quad \text{RHO} = \begin{bmatrix} 1.0000 & 0.3314 & 0.3360 & 0.1958 \\ 0.3314 & 1.0000 & 0.2385 & 0.3160 \\ 0.3360 & 0.2385 & 1.0000 & 0.3320 \\ 0.1958 & 0.3160 & 0.3320 & 1.0000 \end{bmatrix}$$

- d = 0.5

matrix (surface) size	*k* = 2	*k* = 3	*k* = 5	*k = 10*	*k* = 25	*k* = 35
maximum difference between correlations	0.0221	0.0905	0.0845	0.0863	0.1223	0.1244

$$\text{Sigma} = \begin{bmatrix} 1.0000 & 0.6065 & 0.6065 & 0.4931 \\ 0.6065 & 1.0000 & 0.4931 & 0.6065 \\ 0.6065 & 0.4931 & 1.0000 & 0.6065 \\ 0.4931 & 0.6065 & 0.6065 & 1.0000 \end{bmatrix} \quad \text{RHO} = \begin{bmatrix} 1.0000 & 0.5917 & 0.5881 & 0.4787 \\ 0.5917 & 1.0000 & 0.4738 & 0.5861 \\ 0.5881 & 0.4738 & 1.0000 & 0.5845 \\ 0.4787 & 0.5861 & 0.5845 & 1.0000 \end{bmatrix}$$

- d = 0.05

matrix (surface) size	*k* = 2	*k* = 3	*k* = 5	*k = 10*	*k* = 25	*k* = 35
maximum difference between correlations	0.0148	0.0231	0.0220	0.0768	0.1032	0.1111

$$\text{Sigma} = \begin{bmatrix} 1.0000 & 0.9512 & 0.9512 & 0.9317 \\ 0.9512 & 1.0000 & 0.9317 & 0.9512 \\ 0.9512 & 0.9317 & 1.0000 & 0.9512 \\ 0.9317 & 0.9512 & 0.9512 & 1.0000 \end{bmatrix} \quad \text{RHO} = \begin{bmatrix} 1.0000 & 0.9435 & 0.9425 & 0.9169 \\ 0.9435 & 1.0000 & 0.9226 & 0.9424 \\ 0.9425 & 0.9226 & 1.0000 & 0.9425 \\ 0.9169 & 0.9424 & 0.9425 & 1.0000 \end{bmatrix}$$

5) The performance analysis of the adaptive inspection scheme applied with characteristic defects' distribution

Let us check the performance of the adaptive inspection scheme when is applied to corroded surfaces when the domain of defects' depths is the same but their distribution is different. In different words, we will consider the surfaces on which the major part of locations is highly corroded- representing the general type of corrosion. On the other hand, we will consider the surfaces with few deep pits and remaining locations not at all or just slightly affected, illustrating the so-called pitting type of corrosion. Examples of such surfaces are presented in Figure A5-1.

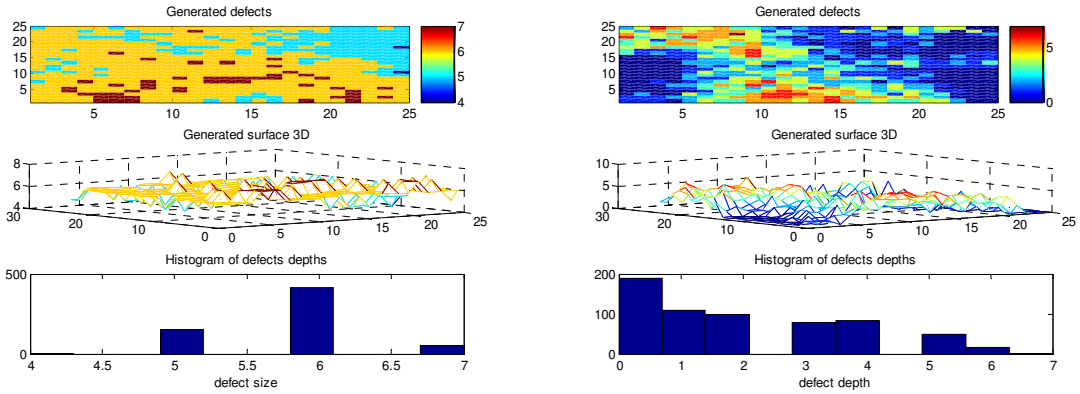

a) general corrosion b) pitting corrosion

Figure A5-1 *Characteristic plots of the corroded surfaces representing the general and pitting type of corrosion.*

When simulating the adaptive inspection scheme the extension condition equal to 3, 4 and 5 units was used. On the other hand, the critical defect size was fixed to be equal 6 units. The histograms of defects depths show that on the surfaces subject to the general corrosion process (see Figure A5-1a) a lot of locations could be classified as critical. On the other hand, the histogram corresponding to surfaces with localized corrosion (Figure A5-1 b) indicates that the defects of size bigger or equal to 6 units were less likely to being recorded.

The result obtained in the simulation experiments when surfaces were generated 300 times are presented below.

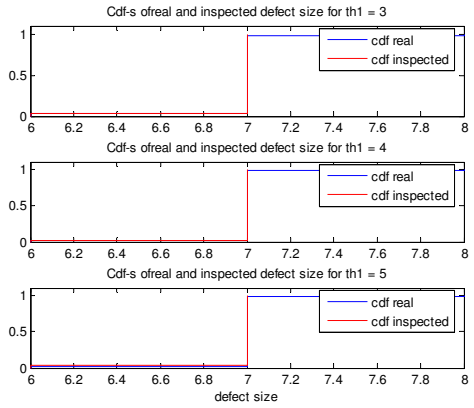

a) general corrosion

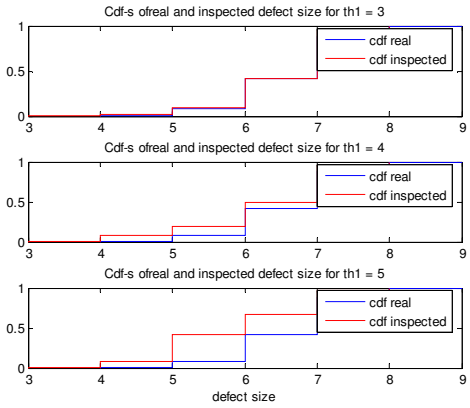

b) pitting corrosion

Figure A5 -2 *The cumulative distribution functions of the real maximum defects and the maximum defects recorded within AIS.*

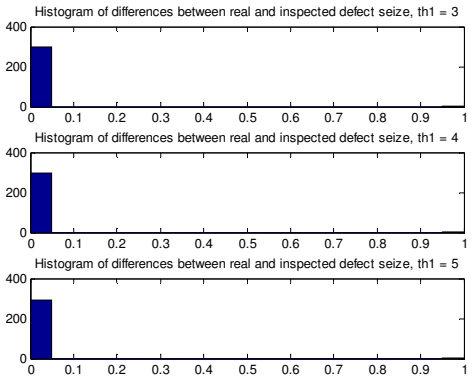

a) general corrosion

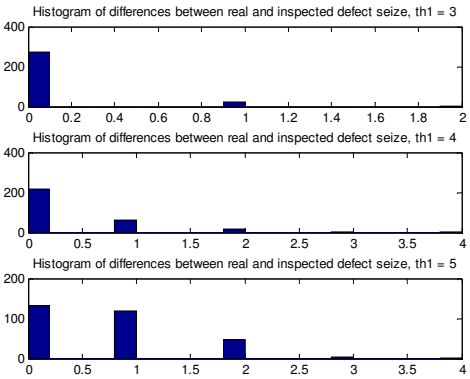

b) pitting corrosion

Figure A5-3 *The histograms of differences between the real maximum defects and the maximum defects recorded within AIS.*

general corrosion, *the critical defect size* = 6			
the extension condition	th1 = 3	th1 = 4	th1 = 5
Mean inspected coverage	0.2229	0.2218	0.1745
Mean number of additional inspections	0.4800	0.4867	0.5367
Mean inspected coverage when wrong acceptance	0	0	0.1792
Unreliability	0	0	0.0033
Number of wrong acceptances	0	0	1

Table A5-1 *The simulation results of AIS for surfaces with general type of corrosion.*

pitting corrosion, *the critical defect size* = 6			
the extension condition	th1 = 3	th1 = 4	th1 = 5
Mean inspected coverage	0.2644	0.1523	0.1106
Mean number of additional inspections	3.22	2.23	0.7167
Mean inspected coverage when wrong acceptance	0.2880	0.1685	0.1126
Unreliability	0.0033	0.0833	0.25
Number of wrong acceptances	1	25	75

Table A5-2 *The simulation results of AIS for surfaces with pitting type of corrosion.*

As one could expect, in case of surfaces where all locations are highly corroded, the critical defect size was detected in all cases, resulting in perfect reliability of the adaptive inspection scheme (see Table A5-1). Moreover, it is worth to point out that the applied value of the extension condition did not affect the performance of this scheme significantly. One can observe that for all choices of th1, the mean inspected coverage oscillates around 20 % and the mean number of additional inspections is equal to 0.5. It means that usually the critical defect size was found among initially inspected points, or only one additional inspection was necessary to detect it. The cumulative distribution functions in Figure A5-2a and histograms in Figure A5-3a confirm the inference that for surfaces with uniform defect distribution, the inspection results are independent of the choice of extension condition.

When analyzing results obtained for the surfaces corresponding to localized corrosion, completely opposite conclusions can be drawn. It can be seen that choosing smaller value of the extension parameter, the reliability of AIS is much better than when applying less demanding extension condition (bigger values of th1). Table A5-2 shows that with th1 = 3 only one wrong acceptance was made while with th1 = 5, in 25% of cases surface containing the critical defect was classified as good one. The same table indicates also, that the choice of the value of the extension parameter has an impact on the inspected coverage as well as on the number of additional inspections. Therefore, when dealing with surfaces having similar characteristics as the one shown in Figure A5-1a, the reliability of results obtained from the adaptive inspection will depend on proper choice of its driving parameter.

APPENDIX B

Proof B-1

We will show that the Gumbel distribution is a special case of the generalized extreme value distribution.

The cumulative distribution function of the generalized extreme value distribution with shape, location and scale parameters ξ, μ and ψ, respectively, is given by:

$$GEV(x) = \exp\left\{-\left[1+\xi\left(\frac{x-\mu}{\psi}\right)\right]_+^{-\frac{1}{\xi}}\right\}, \qquad (i)$$

where, $x_+ = \max\{x, 0\}$.

On the other hand, the cumulative distribution function of the Gumbel distribution with location parameter μ and scale parameter ψ is given by:

$$G(x) = \exp\left\{-\exp\left(-\frac{x-\mu}{\psi}\right)\right\}. \qquad (ii)$$

We will show that with $\xi \to 0$, the formula (i) reduces to (ii).

We can write the following transformation of the formula (i):

$$GEV(x) = \exp\left\{-\left[1+\xi\left(\frac{x-\mu}{\psi}\right)\right]_+^{-\frac{1}{\xi}}\right\} = \exp\left\{-\exp\left(\log\left[1+\xi\left(\frac{x-\mu}{\psi}\right)\right]_+^{-\frac{1}{\xi}}\right)\right\} =$$

$$= \exp\left\{-\exp\left(-\frac{1}{\xi}\cdot\log\left[1+\xi\left(\frac{x-\mu}{\psi}\right)\right]_+\right)\right\}$$

Now using the fact that $\log(1+h) \approx h$ for $h \downarrow 0$ and assuming that $\xi \to 0$ we obtain:

$$\exp\left\{-\exp\left[-\frac{1}{\xi}\cdot\xi\left(\frac{x-\mu}{\psi}\right)\right]\right\} = \exp\left\{-\exp\left[-\left(\frac{x-\mu}{\psi}\right)\right]\right\},$$

which proves the statement.

APPENDIX C

The software presented in this appendix is designed to provide an overview of the performance of the sampling inspection schemes developed during the study. Created applications allow seeing both how the inspection procedures are carried out step by step and show the effectiveness of these schemes. The software interfaces together with a short description are presented below, while a detailed description can be found in the help files attached to the *Matlab* applications.

C-1 Regular inspection scheme

In order to investigate the performance of the regular inspection scheme (see section 3.1.1) applied to the corroded surfaces generated by the gamma and Poisson model, two applications were developed. They allow comparing the effectiveness of this scheme for different values of its parameter- the inspection coverage. The gathered results are presented in forms of the cumulative distribution functions of the real maximum defects and the maximum defects recorded among inspected points. The histograms of differences between the real maximum defects and the maximum defects found during inspection are created additionally. The values and a plot of the unreliability function are presented for the purpose of the performance analysis. The next figure (Figure C-1) shows an example of the results obtained by running one of the mentioned programs, when the corroded surface was created using the gamma model.

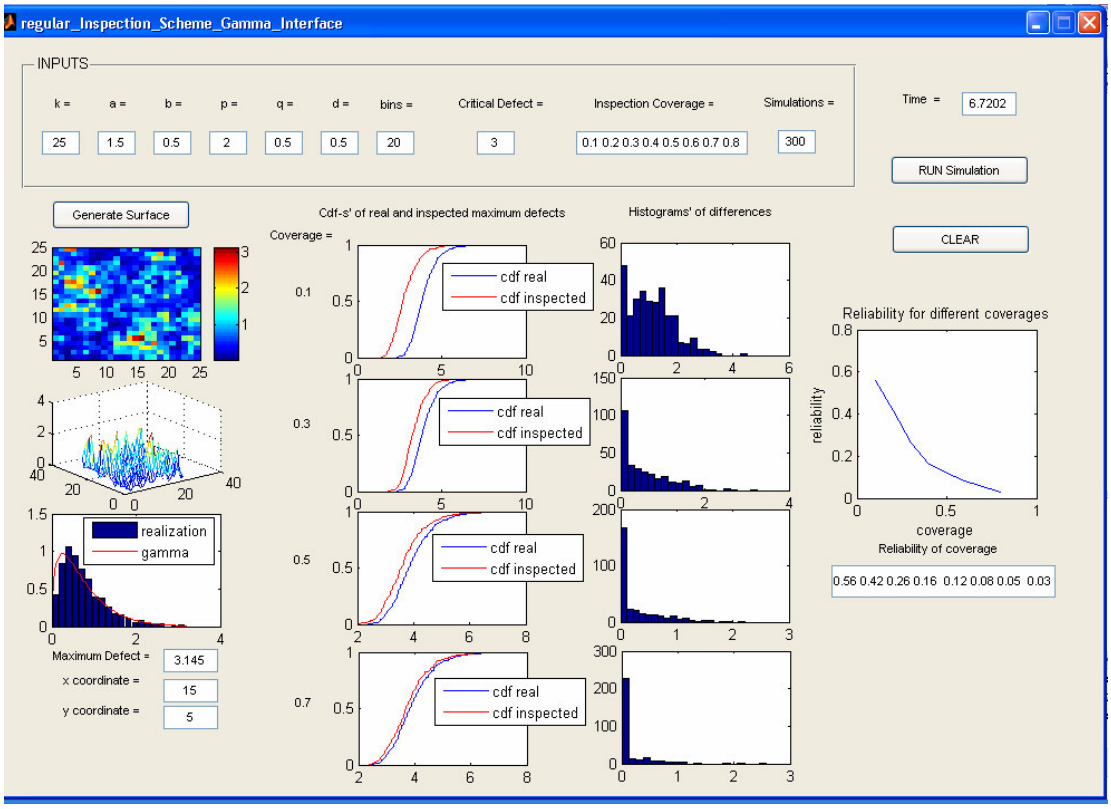

Figure C-1 *Example of the simulation results of the regular inspection scheme applied to the corrosion surface generated by the gamma model.*

C-2 Adaptive inspection scheme

For the adaptive inspection scheme application purposes (see section 3.2.1), two *Matlab* routines were created. These computer codes generate the corrosion surfaces using the gamma or Poisson model and implement the mentioned inspection scheme. In both cases two options are possible. First, it generates the designed surface (with parameters determined by the user) and performs the adaptive inspection scheme several times until one of the termination conditions (also specified by the user) is satisfied. As an output the last three inspection steps represented by the previous, the adaptive and the total inspection surfaces are shown (Inspection Total button). Moreover, the histograms of all defect depths and the inspected defect depths are created and plotted.

On the other hand, a second option (Inspection step button) allows seeing how the whole inspection procedure is carried out step by step. After each inspection stage (from its initial to termination level) three plots representing the previous, the additional and the overall (after current inspection step) surfaces are created. In addition, the percentage of the coverage so far inspected and a maximum depth among the new inspected points are

displayed. The latter gives the eventual indication of a necessity of further inspection or confirms its termination. This routine option returns also histograms of all defect sizes and defect sizes inspected so far (in terms of their depths). Of course, reaching one of the termination conditions the final inspection results are presented and a message about its termination is displayed.

Two figures below contain results created by the mentioned routines for the gamma and Poisson surfaces (Figure C-2a and Figure C-2b, respectively).

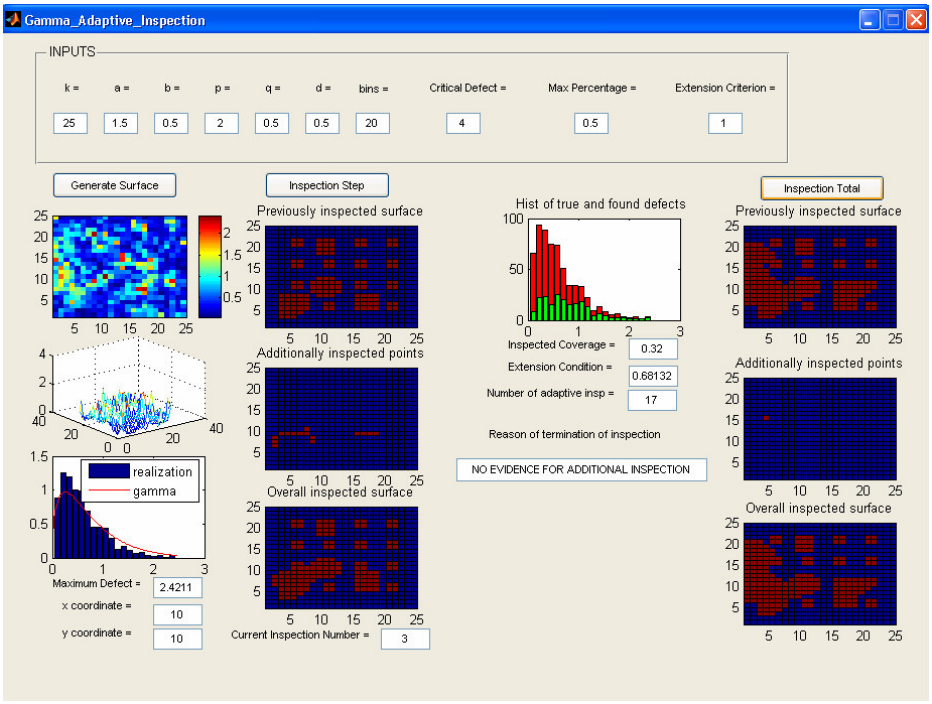

Figure C-2 a) *Example of the adaptive inspection procedure performed using Matlab application for the gamma corrosion surface.*

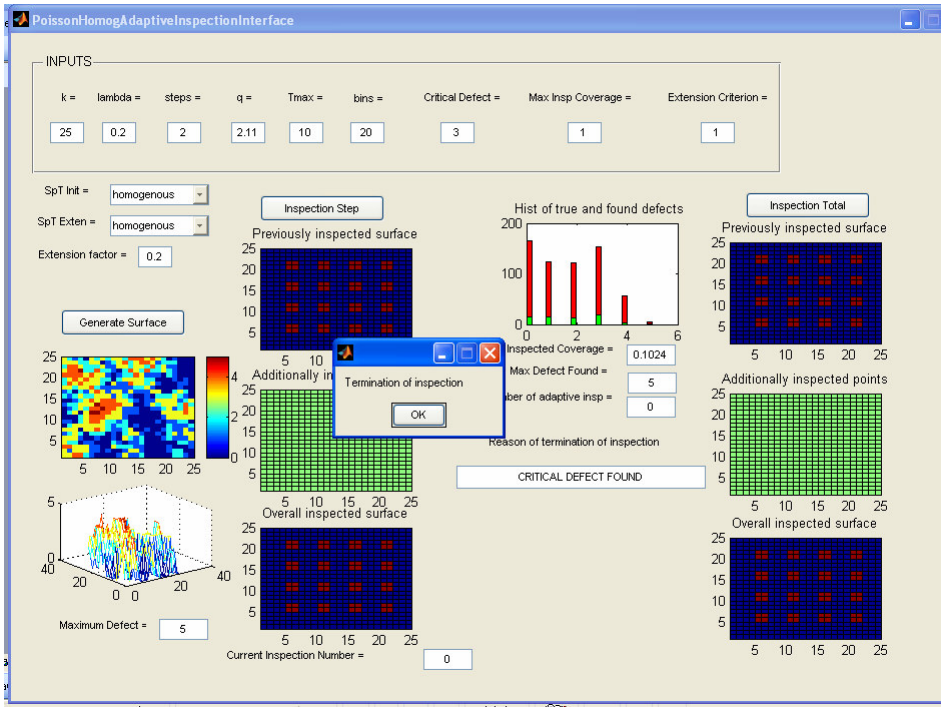

Figure C-2 b) *Example of the adaptive inspection procedure performed using Matlab application for the Poisson corrosion surface.*

The performance of the adaptive inspection scheme was investigated with respect to the extension condition parameter. The simulation experiments were performed with help of two applications: one designed for the corroded surfaces generated by the gamma model and one for the surfaces generated by the Poisson model. Both of them create the histograms of the number of additional inspections and the histograms of the inspected coverages for the applied values of the extension condition. Moreover, the probability of undetected defects of this scheme is calculated for the latter values. The unreliability function of the regular inspection scheme (for determined values of the inspection coverage) allows the comparison of performance of these two sampling inspection methods.

Figure C-2c illustrates an example of simulation results that are created by the *Matlab* program designed for the performance analysis of adaptive inspection scheme with surfaces generated by the Poisson model.

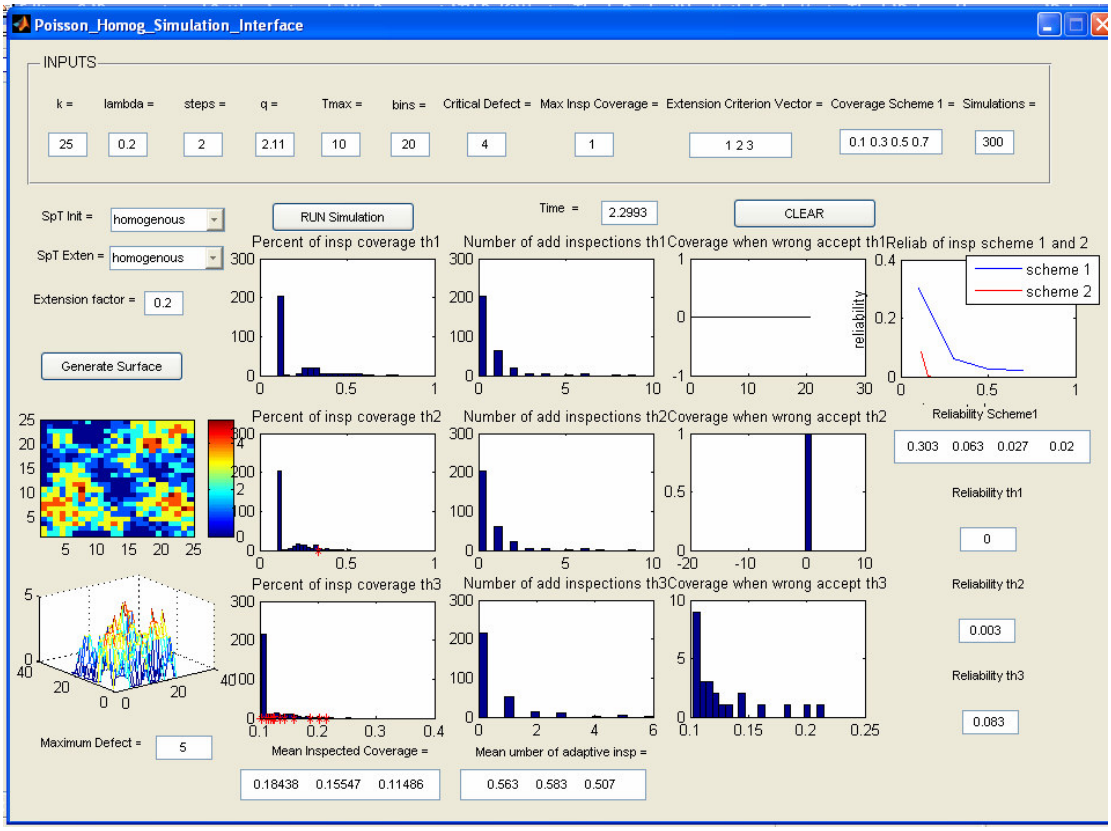

Figure C-2 c) *Example of the simulation results for AIS performed using Matlab application for the Poisson corrosion surface.*

C-3 Sequential random scheme

The simulation experiments of the sequential random scheme (see section 3.3.1) were performed with help of two *Matlab* applications (one for the gamma fitting method and one for the GEV fitting approach). Both of them create the histograms of the total inspection coverages and histograms of the number of inspection steps for given values of the initial inspection coverage parameter. These programs calculate also the un-detection probability of the critical defect (the so-called unreliability function) and plot this value as a function of the mean inspection coverage. Moreover, the unreliability function of the regular inspection scheme allows comparing the performance of both inspection schemes.

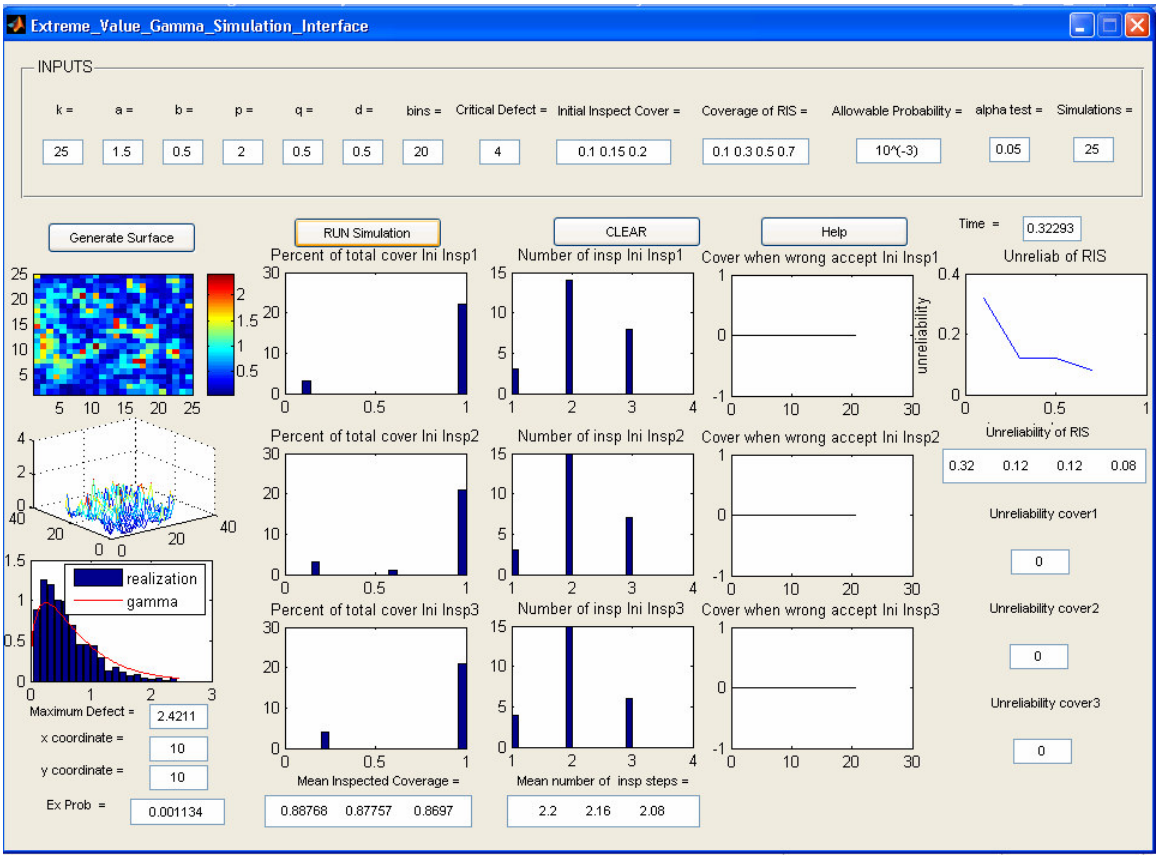

Figure C-3 a) *Example of the simulation results for SRS performed using Matlab application for the corrosion surface generated by the Poisson model.*

To illustrate how the sequential random scheme procedure is performed step by step two additional programs were designed. They give the graphical representation of the inspected surface points, create the histograms of all and inspected defects, and plot the fitted and extrapolated distributions, what can give some indication about the appropriateness of the assumptions (independence and homogeneity) used within this sampling scheme. The goodness of fit of mentioned distributions can be verified by the displayed value of the Kolmogorov-Smirnov test and the p – value.

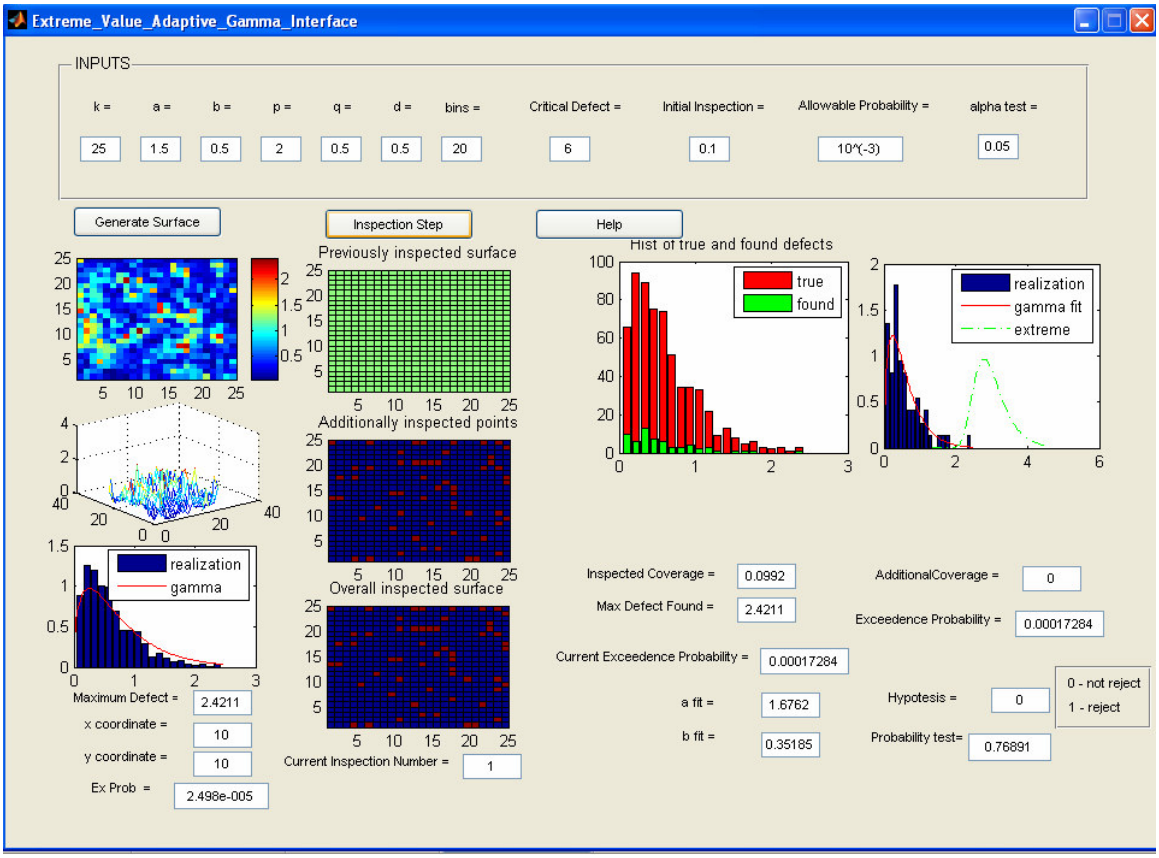

Figure C-3 b) *Example of the sequential inspection procedure with the gamma fit distribution.*

APPENDIX D

List of informal definitions and abbreviations used in the thesis

steps - a parameter of the Poisson model for generating corroded surfaces. It expresses the maximum allowable difference in corrosion level between neighboring locations.

the critical defect size - is a defect size defined in advance by the inspector and depends on the considered surface. Existence of a pit depth of this size is equivalent with component failure and the surface is judged as a defective one.

the extension condition – a parameter of the adaptive inspection scheme that forces the inspection extension. A defect with depth smaller than this value is considered as not dangerous for the considered component, for example, it can be regarded as inherited unevenness of surface. On the other hand, finding the pit bigger than the extension parameter results in additional inspection. This parameter (also denoted by th1) is specified by the inspector before the inspection process is carried out.

the number of wrong decisions – counts the number of situations when among the inspected points *the critical defect* (defined below) was not recorded (found) while it was present on the simulated surface. In other words, it counts the number of bad acceptance decisions when after the inspection procedure the considered surface is judged as a good one (without evidence of the critical defect) while it does not reflect the reality. This quantity shows when the applied inspection scheme performs well, whether it results in a small number of wrong decisions or possibly leads to severe consequences.

the unreliability function - a function of the mean inspected coverage that expresses the non-detection probability of the critical defect. In different words, it gives a proportion of the number of wrong decisions among performed simulations.

the SpT function – a function that is used for modeling the preferential locations for the occurrences of the initial corrosion spots This function is defined on the surface S takes values on the interval [0, 1] and expresses a probability that a particular location will be affected by the corrosion initiation process.

the ν function – a extension intensity function defined on the surface S . This function, $\nu(i, j)$, takes values on [0, ∞) and determines the corrosion extension at the particular location.

RIS – the regular inspection scheme

AIS – the adaptive inspection scheme

SRS – the sequential random scheme

REFERENCES

[1] S. Ghosh, S.G. Henderson, 2002, *Properties of the notra method in higher dimensions*, Proc of the 2002 Winter Simulation Conference, pages 263-269

[2] R. Iman, J. Helton, 1985, *A comparison of uncertainty and sensitivity analysis techniques for computer models*, Technical report, NUREG/CR-3904 SAND84-1461 RG, Albuquerque

[3] D. Kurowicka, R. M. Cooke, 2006, *Uncertainty Analysis with High Dimensional Dependence Modelling*, Chichester: John Wiley & Sons, Ltd

[4] J. M. van Noortwijk, H.E. Klatter, 1999, *Optimal inspection decisions for the block mats of the Eastern-Scheldt barrier*, Reliability Engineering and Safety 65 (3), pages 203-211

[5] J. M. van Noortwijk, *Deterioration and Maintenance Modelling*

[6] M.J. Kallen and J.M. van Noortwijk, 2003, *Inspection and Maintenance Decisions based on Imperfect* Inspections, Proceedings of the European Safety and Reliability Conference (ESREL), Maastricht, the Netherlands, June 15-18, 2003. Bedford and van Gelder (eds.), Balkema 2003

[7] Z. Brzezniak, T. Zastawniak, 1999, *Basic Stochastic Processes*, Springer

[8] S. M. Ross, 1997, *Introduction to probability models*, 6th edition, Boston: Academic Press

[9] P. A. Scarf, P. J. Laycock, 1996, *Estimation of extremes in corrosion engineering*, Journal of Applied Statistics, Vol. 23, No. 6, pages 621-643

[10] S. Kotz, S. Nadarajah, 2002, *Extreme Value Distributions. Theory and Applications*, London: Imperial College Press

[11] S. Coles, 2001, *An Introduction to Statistical Modeling of Extreme Values*, London: Springer-Verlag

[12] F.I. Khan, M.M. Haddara, S.K. Bhattachary, 2006, *Risk-Based Integrity and Inspection Modeling (RBIIM) of Process Components/System*, Risk Analysis, Vol. 26, No. 1, pages 203-221

[13] D. Straub, M.H. Faber, October 2005, *Risk based inspection planning for structural systems*, Structural Safety, Vol. 27, Issue 4, pages 335-355

[14] M.J. Kallen and J.M. van Noortwijk, November-December 2005, *Optimal maintenance decisions under imperfect inspection*, Reliability Engineering & System Safety, Vol. 90, Issues 2-3, pages 177-185

[15] D.C. Montgomery, G.C. Runger, 1999, *Applied statistics and probability for engineers*, second edition, New York: Wiley

[16] S.M. Ross, 2003, *Introduction to Probability Models*, 8th ed., California: Barkley,

[17] L. Wasserman, 2004, *All of Statistics. A Concise Course in Statistical Inference*, New York: Springer-Verlag,

[18] R.P. Nicolai, G. Budai, R. Dekker, M. Vreijling, 2004, *Modeling the deterioration of the coating on steel structures*, IEEE International Conference on Systems, Man and Cybernetics

[19] J.M. van Noortwijk, J.A.M. van der Weide, M.J. Kallen, M.D. Pandey, *Gamma Processes and Peaks-Over-Threshold Distributions for Time-dependent Reliability*, TU Delft

[20] D. Lord, S.P. Washington, J.N. Ivan, *January 2005*, *Poisson, Poisson-gamma and zero inflated regression models of motor vehicle crashes: balancing statistical fit and theory, Accident Analysis & Prevention, Vol. 37, Issue 1, pages 35-46*

[21] S.E. Rigdon, A.P. Basu, 2000, *Statistical methods for the reliability of repairable systems*, New York: Wiley

[22] S. Kotz, S. Nadarajah, 2002, *Extreme value distribution: theory and applications*, London: Imperial College Press

[23] A. Ramachandra Rao, K.H. Hamed, 2000, *Flood frequency analysis*, CRC Press LLC

[24] R.A. Cottis, P.J. Laycock, D. Holt, S.A. Morris, P.A. Scarf, 1987, *The statistics of pitting of austenitic stainless steels in chloride solutions,* H. ISSACS & U. BERTOCCI (Eds), *Advances in Localized Corrosion*, pages 117 – 121

[25] R.A. Cottis, P.J. Laycock, P.A. Scarf, 1993, Statistics of Pitting, *Final Report NIST Contract 60NANB5D0519* (Gaithersburg, MD, National Institute of Standards and Technology)

[26] B. Castanier, M. Rausand**,** April 2006, *Maintenance optimization for subsea oil pipelines*, International Journal of Pressure Vessels and Piping, Vol. 83, Issue 4, , pages 236-243

[27] G.B. Wetherill, 1977, *Sampling Inspection and Quality Control,* 2nd ed., Chapman and Hall, London

[28] A.A. Bartolucci, A.D. Bartolucci, S.Bae, K.P. Singh, September 2006, *A Bayesian method for computing sample size and cost requirements for stratified random sampling of pond water*, Environmental Modelling & Software, Vol. 21, Issue 9, , pages 1319-1323

[29] M.E. Robinson, J.A. Tawn, 1997, *Statistics for Extreme Sea Currents*, Journal of the Royal Statistical Society: Series C (Applied Statistics), Vol. 46, Number 2, pages 183-205

[30] P. Embrechts, C. Klüppelberg, T. Mikosch, 1997, *Modeling extremal events for Insurance and Finance*, Springer-Verlag

[31] F. Dufresne, H.U. Gerber, E.S.W. Shiu, 1991, *Risk theory with the gamma process*, ASTIN Bulletin, 21(2), pages 177-192